



University of Kentucky  
UKnowledge

---

University of Kentucky Doctoral Dissertations

Graduate School

---

2006

## STRUCTURAL AND FUNCTIONAL STUDIES OF SYNAPTIC ENZYMES

Eun Jeong Lim  
*University of Kentucky, elim0@uky.edu*

[Right click to open a feedback form in a new tab to let us know how this document benefits you.](#)

---

### Recommended Citation

Lim, Eun Jeong, "STRUCTURAL AND FUNCTIONAL STUDIES OF SYNAPTIC ENZYMES" (2006). *University of Kentucky Doctoral Dissertations*. 259.  
[https://uknowledge.uky.edu/gradschool\\_diss/259](https://uknowledge.uky.edu/gradschool_diss/259)

This Dissertation is brought to you for free and open access by the Graduate School at UKnowledge. It has been accepted for inclusion in University of Kentucky Doctoral Dissertations by an authorized administrator of UKnowledge. For more information, please contact [UKnowledge@lsv.uky.edu](mailto:UKnowledge@lsv.uky.edu).

ABSTRACT OF DISSERTATION

Eun Jeong Lim

Department of Molecular and Cellular Biochemistry

College of Medicine

University of Kentucky

2006

STRUCTURAL AND FUNCTIONAL STUDIES OF SYNAPTIC ENZYMES

---

ABSTRACT OF DISSERTATION

---

A dissertation submitted in partial fulfillment of the requirements for the degree of Doctor of Philosophy in the Department of Molecular and Cellular Biochemistry and College of Medicine at the University of Kentucky

By

Eun Jeong Lim

Lexington, Kentucky

Director: Dr. David W. Rodgers  
Associate Professor of Molecular and Cellular Biochemistry

Lexington, Kentucky

2006

Copyright © Eun Jeong Lim, 2006

## ABSTRACT OF DISSERTATION

### STRUCTURAL AND FUNCTIONAL STUDIES OF SYNAPTIC ENZYMES

Thimet oligopeptidase (TOP, EC 3.4.24.15) and neurolysin (EC 3.4.24.16) are zinc dependent metallopeptidases that metabolize small bioactive peptides. The two enzymes share 60 % sequence identity and their crystal structures demonstrate that they adopt nearly identical folds. They generally cleave at the same sites, but they recognize different positions on some peptides, including neurotensin, a 13-residue peptide involved in modulation of dopaminergic circuits, pain perception, and thermoregulation.

On the basis of crystal structures and previous mapping studies, four residues (E469/R470, M490/R491, H495/N496, and R498/T499, TOP residues listed first) in the substrate-binding channel appear positioned to account for differences in specificity. TOP mutated to the neurolysin residues at all four position cleaves neurotensin at the neurolysin site and neurolysin mutated to the TOP residues at all four sites cleaves at the TOP position. Using a series of constructs mutated at only three sites, it was determined that only two of the mutations, E469/R470 and R498/T499, are required to swap the specificity of TOP and neurolysin. These results were confirmed by testing the two mutation constructs, and either single mutant of TOP shown an intermediate specificity, cleaving at both sites.

Crystal structures of the two mutation constructs of TOP and neurolysin unliganded forms, the mutations do not perturb local structure, but side chain conformations at the R498/T499 position differ from those of the mimicked enzyme. A model for differential recognition of neurotensin based on differences in surface charge distribution in the substrate binding sites is proposed. The model is supported by finding that reducing the positive charge on the peptide results in cleavage at both hydrolysis sites.

This dissertation also includes a description of the production and crystallization trials of human neprilysin (E.C. 3.4.24.11), which will be used as another model system for studying specificity in metallopeptidases. In addition, the production and crystallization, and crystal characterization of human choline acetyltransferase (EC 2.3.1.6) is described.

KEYWORDS: Thimet oligopeptidase, neurolysin, crystallography, neurotensin, specificity



STRUCTURAL AND FUNCTIONAL STUDIES OF SYNAPTIC ENZYMES

By

Eun Jeong Lim

---

Director of Dissertation

---

Director of Graduate Studies

---

Date

## RULES FOR THE USE OF DISSERTATIONS

Unpublished dissertations submitted for the Doctor's degree and deposited in the University of Kentucky Library are as a rule open for inspection, but are to be used only with due regard to the rights of the authors. Bibliographical references may be noted, but quotations or summaries of parts may be published only with the permission of the author, and with the usual scholarly acknowledgements.

Extensive copying or publication of the dissertation in whole or in part also requires the consent of the Dean of the Graduate School of the University of Kentucky.

A library that borrows this dissertation for use by its patrons is expected to secure the signature of each user.

DISSERTATION

Eun Jeong Lim

The Graduate School  
University of Kentucky  
2006



STRUCTURAL AND FUNCTIONAL STUDIES OF SYNAPTIC ENZYMES

---

DISSERTATION

---

A dissertation submitted in partial fulfillment of the  
requirements for the degree of Doctor of Philosophy in the  
Department of Molecular and Cellular Biochemistry  
and College of Medicine at the University of Kentucky

By

Eun Jeong Lim

Lexington, Kentucky

Director: Dr. David W. Rodgers  
Associate Professor of Molecular and Cellular Biochemistry

Lexington, Kentucky

2006

Copyright © Eun Jeong Lim, 2006

*Dedicated to my parents, Jong Man Lim and Won Ja Hong – who are my role models. Their enthusiastic life, hard working, and moral characters always inspire me.*

## ACKNOWLEDGEMENTS

I would like to express my gratitude to my research mentor and dissertation advisor, Associate Professor David Rodgers, for his guidance, patience, and encouragement throughout my graduate studies. Dr. Rodgers provided me theoretical aspects of x-ray crystallography and taught me how to determine the crystal structures of macromolecules. And he always finds the time for listening to the little problems and roadblocks that unavoidably crop up in the course of performing research. His technical and theoretical advice was necessary for the completion of this dissertation and has taught me valuable lessons and insights on the workings of academic research in general.

I am also grateful to my dissertation committee members, Dr. Thomas Vanaman, Dr. Rebecca Dutch, Dr. Charles Snow, and Dr. Robert Houtz for reading previous drafts of this dissertation and providing many valuable comments that improved the presentation and contents of this dissertation.

I am also indebted to my former advisor, Dr. Young Gyu Chai. He always listened to my concerns and gave a lot of good advice even when I was preparing to study abroad and when I was determining the lab. And I am also thankful to Dr. Myung Hee Kim for her friendship, support, and encouragement.

I would also like to thank present members of the Dr. Rodgers' lab: Dr. Jack Schmidt for helping to determine kinetics of my proteins, Sowmya Sampath, Nick Noinaj for helping me how to use a lot of software, and Jerry Coll-Rodriguez for helping to prepare proteins. And I also thankful to former lab members, Dr. Christina Hines, Dr. Yiyang Cai, Dr. Kallol Ray, and Dr. Chad Haynes, for their friendship and support.

Finally, and most importantly, I would like to thank my husband Jun Ho Roh for his love and understanding during the past few years. I could not finish this dissertation without his support, patience, and encouragement. I also thank my parents, Jong Man Lim and Won Ja Hong, my sisters, Eun Suk and Eun Hee, and my brother, Jeong Hun, for their faith in me and providing me with unending encouragement and support.

## TABLE OF CONTENTS

Acknowledgements.....	iii
List of Tables.....	vi
List of Figures.....	vii
List of Files.....	ix
Chapter One: Introduction.....	1
Neuropeptides and neuropeptidases.....	1
Substrate specificity in neuropeptidases (fuzzy specificity).....	2
Thimet oligopeptidase (TOP) and neurolysin.....	4
Neurotensin.....	8
The present study.....	9
Significance.....	10
Neprilysin.....	11
Human choline acetyltransferase (hChAT).....	13
Chapter Two: Materials and methods.....	22
Preparation of TOP and neurolysin mutant constructs.....	22
Expression and purification of wild type TOP and mutants.....	23
Expression and purification of wild type neurolysin and mutants.....	24
Assay for cleavage position on NT.....	25
Kinetic assay of TOP and neurolysin.....	25
Swap experiment between TOP E469R mutant and NT(R9E).....	26
Crystallization of TOP 2 and neurolysin 2 mutants.....	26
Data collection and structure determination of TOP 2 and neurolysin 2 mutants.....	27
Preparation of human neprilysin (hNEP) constructs.....	27
Expression and purification of hNEP.....	28
Enzyme activity assay for hNEP.....	30
Preparation of human choline acetyltransferase (hChAT) constructs.....	30
Expression and purification of hChAT.....	31
Assay for hChAT activity.....	32

Crystallization of hChAT.....	32
Chapter Three: Reengineering of substrate specificity in thimet oligopeptidase and neurolysin.	41
Cleavage pattern of NT by TOP 4 and neurolysin 4 mutants.....	42
Cleavage pattern of NT by TOP 3 mutants.....	43
Cleavage pattern of NT by TOP 2 and neurolysin 2 mutants.....	43
Comparison of kinetic parameters for wild type TOP and neurolysin with the two mutant constructs.....	44
Cleavage pattern of NT(R9E) by TOP E469R mutant.....	44
Chapter Four: Crystal structures of TOP 2 and neurolysin 2 mutants.....	56
Introduction.....	56
Crystal structures of the TOP 2 and neurolysin 2 mutants.....	57
Chapter Five: Human neprilysin (hNEP).....	67
Introduction.....	67
Production of recombinant human neprilysin.....	68
Crystallization of neprilysin.....	68
Chapter Six: Human choline acetyltransferase.....	70
Introduction.....	70
Data collection and structure determination of hChAT.....	71
Chapter Seven: Discussion and Conclusions.....	73
Specificity in TOP and neurolysin.....	73
Neprilysin.....	77
Human ChAT.....	78
Bibliography:.....	83
Vita.....	100

## LIST OF TABLES

Table 2. 1:	Sequences of primers for TOP mutagenesis.....	33
Table 2. 2:	Sequences of mutation primers for neurolysin mutagenesis .....	34
Table 2. 3:	Sequences of primers for human choline acetyltransferase cloning.....	35
Table 3. 1:	Molecular masses of NT fragments produced by wild type TOP, wild type neurolysin, and TOP 4 mutant .....	46
Table 3. 2:	Summary of mutation sites and NT hydrolysis by the TOP 3 mutants .....	47
Table 3. 3:	Kinetics parameters for hydrolysis of fluorogenic NT by wild type TOP, TOP 2 mutant, wild type neurolysin, and neurolysin 2 mutant.....	48
Table 3. 4:	Molecular masses of NT(R9E) fragments and full length of NT(R9E) by TOP E469R mutant .....	49
Table 4. 1:	Summary of crystallographic data and refinement for TOP 2 and neurolysin 2 mutants.....	59
Table 4. 2:	The main chain and side chain torsion angles (in degrees) for the wild type TOP , wild type neurolysin, TOP 2 mutant and neurolysin 2 mutant residues at the mutated positions .....	60

## LIST OF FIGURES

Figure 1. 1.	Neuropeptide metabolism.....	15
Figure 1. 2.	Cleavage specificity of neuropeptidases .....	16
Figure 1. 3.	The overview of crystal structures of TOP and neurolysin.....	17
Figure 1. 4.	The active site of TOP.....	18
Figure 1. 5.	Key residue differences in the substrate binding channels of TOP and neurolysin .....	19
Figure 1. 6.	Overview of crystal structures of human neprilysin (hNEP) .....	20
Figure 1. 7.	Overview of the rat choline acetyltransferase (rChAT) crystal structure.....	21
Figure 2. 1.	Overview of mutation positions in the TOP 3 mutants .....	36
Figure 2. 2.	Overview of mutation positions in the TOP 2 mutant and neurolysin 2 mutant...	37
Figure 2. 3.	Residue swap to test a direct interaction between Glu469 of TOP and Arg9 of NT .....	38
Figure 2. 4.	Overexpression of hNEP 3 mutant in <i>Pichia pastoris</i> yeast cells .....	39
Figure 2. 5.	Overexpression and crystals of hChAT.....	40
Figure 3. 1.	Cleavage of NT by the TOP 4 and neurolysin 4 mutants.....	50
Figure 3. 2.	The cleavage pattern of NT by the TOP 3 mutants.....	51
Figure 3. 3.	Cleavage of NT by the TOP 2 and neurolysin 2 mutants.....	52
Figure 3. 4.	Kinetics of fluorogenic NT hydrolysis by TOP, TOP 2 mutant, wild type neurolysin and neurolysin 2 mutant.....	53
Figure 3. 5.	Cleavage of NT(R9E) by the TOP E469R mutant.....	55
Figure 4. 1.	The TOP 2 mutant crystal structure.....	61

## LIST OF FIGURES (CONTINUED)

Figure 4. 2.	Electron density for side chains of Arg469 and Thr498 in the TOP 2 mutant crystal structure.....	62
Figure 4. 3.	Superposition of Arg469 and Thr498 in TOP 2 mutant with the corresponding residues in wild type neurolysin .....	63
Figure 4. 4.	Crystal structure of the neurolysin 2 mutant .....	64
Figure 4. 5.	Electron density for the side chains of Glu470 and Arg499 in the neurolysin 2 mutant crystal structure.....	65
Figure 4. 6.	The superposition of Glu470 and Arg499 in the neurolysin 2 mutant with the corresponding residues in wild type TOP.....	66
Figure 6. 1.	Diffraction pattern from a hChAT crystal.....	72
Figure 7. 1.	Model for differential specificity of TOP and neurolysin with respect to primary NT cleavage sites.....	79
Figure 7. 2.	Surface electrostatic potential in the substrate binding channels of TOP and neurolysin.....	80
Figure 7. 3.	Initial binding sites of substrates and mutation residues in TOP .....	81
Figure 7. 4.	Model for NT binding in TOP and neurolysin .....	82



## **LIST OF FILES**

EJLDisse.pdf

## **Chapter 1: Introduction**

### **Neuropeptides and neuropeptidases**

Neuropeptides play important roles in cell communication by regulating signal pathways in the nervous and endocrine systems. To date, more than 100 biologically active neuropeptides have been identified. Neuropeptides are generally 2-40 residues in length and are involved in regulating a number of processes, including blood pressure, analgesia, and thermoregulation (Konkoy and Davis, 1996; Brown *et al.*, 2001). Changes in their levels in vivo are associated with various diseases such as hypertension, schizophrenia, and neurodegenerative diseases (Nemeroff *et al.*, 1982; Bauer, 1990; Genden and Molineaux, 1991; Koike *et al.*, 1999; Yamin *et al.*, 1999; Shrimpton *et al.*, 2000; Smith *et al.*, 2000; Shrimpton *et al.*, 2002).

Neuropeptides are usually synthesized as inactive precursor pro-peptides which are processed into active forms by peptidases known as pro-protein convertases that are present in the secretory system (Czyzyk *et al.*, 2003). The processed active neuropeptides are transported to the synaptic terminal via secretory vesicles (Zhou *et al.*, 1999) and released into the synaptic cleft (Figure 1.1). After release from a presynaptic neuron, they bind to cell surface receptors on a postsynaptic neuron and modulate cellular signaling pathways (Checler, 1993; Csuhai *et al.*, 1998; Brown *et al.*, 2001). The surface receptors are mostly G protein-coupled receptors, and activation of the receptors can affect a variety of pathways (Endoh, 2004). Released peptides are metabolized by hydrolytic enzymes known as neuropeptidases, which are almost exclusively metallopeptidases containing a zinc ion cofactor (Rawlings and Barrett, 1995). Many neuropeptidases exist in soluble form (Shrimpton *et al.*, 2002), so they inactivate neuropeptides in the extracellular medium or neuropeptides internalized by surface receptors (Konkoy and Davis, 1996). The remainder of the enzymes are associated with the plasma membrane and hydrolyze peptides present in the extracellular medium (Checler *et al.*, 1985; Molineaux and Ayala, 1990; Barnes *et al.*, 1992; Checler *et al.*, 1993; Konkoy *et al.*, 1996).

Neuropeptidases are restricted to peptide substrates generally less than 30 residues in length, and the restriction on size can be even more severe for particular enzymes (Camargo *et al.*, 1994; Barrett *et al.*, 1995; Jacchieri *et al.*, 1998). The crystal structures of a number of

neuropeptidases, including TOP (Ray *et al.*, 2004), neurolysin (Brown *et al.*, 2001), and neprilysin (Oefner *et al.*, 2000), have been determined and their overall folds explain why they hydrolyze the only short peptides. Their active sites are located in a deep substrate binding channel, which limits the access to only unstructured peptides (Oefner *et al.*, 2000; Brown *et al.*, 2001; Ray *et al.*, 2004). Inhibition of neuropeptidases has been shown to increase the levels of the neuropeptides they metabolize (Lasdun *et al.*, 1989; Lasdun and Orłowski, 1990; Wu *et al.*, 1997), making them attractive targets for therapeutic intervention in many diseases. Since nearly all the neuropeptidases have very similar active site regions, often with the same fold as the well-characterized bacterial protease thermolysin (Matthews *et al.*, 1974; Juers *et al.*, 2005), it is a challenge to design inhibitors with sufficient specificity that also have appropriate drug-like properties. Recent difficulties in developing specific inhibitors of matrix metalloproteinases illustrate this point (Peterson, 2006).

### **Substrate specificity in neuropeptidases (fuzzy specificity)**

Most neuropeptidases can hydrolyze a broad range of neuropeptides *in vitro*. Neprilysin (NEP, E.C. 3.4.24.11), for example, is an ectoenzyme capable of hydrolyzing many different peptides, including enkephalins, substance P, endothelin, bradykinin, and atrial natriuretic factor (Ishimaru *et al.*, 1997). Aminopeptidase N (APN), another neuropeptidase that functions as an exopeptidase, can cleave most N-terminal residues from peptides. Substrates of APN include vasoactive peptides such as somatostatin and angiotensin as well as opioid peptides such as enkephalins, bradykinin, and endorphins (Konkoy and Davis, 1995; Konkoy and Davis, 1996; Konkoy *et al.*, 1996). A key aspect of many neuropeptidases is, therefore, their ability to recognize a wide variety of peptide substrates.

Importantly, the sequences near known cleavage sites (which typically determine substrate preferences) vary widely and are not highly enriched for particular residues or residue types at any position. In the case of neprilysin, the only mild preference that has been established is for a hydrophobic residue at the P1' position (By convention, residue positions in peptidase substrates are indicated by position relative to the scissile bond (Schechter and Berger, 1967). Positions N terminal to the cleavage site are named, beginning at the adjacent residue, P1-Pn,

and positions C terminal to the cleavage site are named P1'-Pn'). But even at this position, many other residue types can be found in known cleavage sequences. Yet despite their ability to recognize seemingly unrelated sequences, these peptidases are not completely nonspecific. They show a high degree of selectivity for one or a small number of cleavage sites on any given peptide, hydrolyzing these positions much more rapidly than other possible sites. We refer to this ability to recognize specifically a variety of sequences as fuzzy specificity (Moodie *et al.*, 1996), and it is a property shared by a number of neuropeptidases. This broad level of recognition allows neuropeptidases to be used for different purposes in different tissues and subcellular locations, where the main substrates hydrolyzed depends on availability.

While many neuropeptidases show fuzzy specificity, some have a much higher degree of specificity, with easily defined preferences at particular positions. For example pyroglutamyl aminopeptidase II has a strong preference for the pyroglutamate residue at the P1 position (Charli *et al.*, 1989; Charli *et al.*, 1998). This enzyme is thought to be relatively specific for thyrotropin-releasing hormone (pGlu-His-ProNH<sub>2</sub>). Other neuropeptidases with high levels of specificity include aminopeptidase P (Orawski *et al.*, 1987), carboxypeptidase M (Skidgel *et al.*, 1989), and prolyl oligopeptidase (Barrett and Rawlings, 1992; Fülöp *et al.*, 1998).

## Thimet oligopeptidase (TOP) and neurolysin

Thimet oligopeptidase (TOP, EC 3.4.24.15) and neurolysin (EC 3.4.24.16), are closely related neuropeptidases that share 60% sequences identity, and their crystal structures demonstrate that they adopt nearly identical folds (Brown *et al.*, 2001; Ray *et al.*, 2002; Ray *et al.*, 2004) (Figure 1.3). They hydrolyze several bioactive or synthetic peptides such as gonadotrophin-releasing hormone (GnRH), opioid peptides, bradykinin, angiotensin I, somatostatin, and neurotensin (NT) (Orlowski *et al.*, 1983; Chu and Orlowski, 1985; Orlowski *et al.*, 1989; Barrett and Brown, 1990; Dahms and Mentlein, 1992; Dando *et al.*, 1993; Mentlein and Dahms, 1994; Yang *et al.*, 1994; Dendorfer *et al.*, 1997; Lew *et al.*, 1997; Wu *et al.*, 1997; Vincent *et al.*, 1997b) (Figure 1.2A). These two enzymes exemplify the fuzzy specificity exhibited by some neuropeptidases. They recognize a wide variety of cleavage sites, but it has not been possible to define strong sequence preferences at any particular position relative to the scissile bond (Dahms and Mentlein, 1992; Checler, 1993; Mentlein and Dahms, 1994; Barrett *et al.*, 1995; Checler *et al.*, 1995) (Figure 1.2B and C). Our group is using these two enzymes as model systems to investigate substrate recognition in neuropeptidases.

Not surprisingly, given the high level of sequence identity and structural similarity of TOP and neurolysin (Figure 1.3), they hydrolyze most bioactive peptides at the same cleavage site (Rioli *et al.*, 1998) (Figure 1.2A). Sometimes, however, they recognize different sites (Dahms and Mentlein, 1992; Mentlein and Dahms, 1994; Barrett *et al.*, 1995; Checler *et al.*, 1995). For example, TOP cleaves NT between Arg8 and Arg9, pELYENKPR↓RPYIL, whereas neurolysin cleaves the peptide between Pro10 and Tyr11, pELYENKPRRP↓YIL (Figure 1.2A). In addition, studies with synthetic peptides show that the weak sequence preferences that do exist at some positions differ for the two enzymes (Oliveira *et al.*, 2001; Oliveira *et al.*, 2001). The differences in cleavage site positions between TOP and neurolysin represent an opportunity to begin understanding substrate targeting in these enzymes. Defining what mediates the differences between the two in cleavage site selection will be a first step in understanding and being able to manipulate substrate specificity.

Thimet oligopeptidase was first isolated from the soluble form of rat brain homogenates (Orlowski *et al.*, 1983). TOP is highly expressed in brain, pituitary gland, and testis, but is expressed at lower levels in many cell types (Chu and Orlowski, 1985; Acker *et al.*, 1987; Pierotti *et al.*, 1990; Healy and Orlowski, 1992). TOP exists mainly as a soluble, cytosolic form (Orlowski *et al.*, 1983; Chu and Orlowski, 1985; Acker *et al.*, 1987; Pierotti *et al.*, 1990; Healy and Orlowski, 1992; Ferro *et al.*, 1995; Wu *et al.*, 1997; Ferro *et al.*, 1999; Garrido *et al.*, 1999; Massarelli *et al.*, 1999; Oliveira *et al.*, 2000; Fontenele-Neto *et al.*, 2001), but over 20% of TOP activity associates with membranes (Chu and Orlowski, 1985; Acker *et al.*, 1987; Healy and Orlowski, 1992) and nuclei in rat brain homogenates (Healy and Orlowski, 1992; Massarelli *et al.*, 1999; Fontenele-Neto *et al.*, 2001).

Neurolysin was first detected and purified from rat brain synaptic membranes (Checler *et al.*, 1983; Checler *et al.*, 1986) and initially called neurotensin-degrading enzyme for its ability to inactivate the 13 residue peptide NT. Like TOP, neurolysin is also distributed widely in mammalian tissues (Checler *et al.*, 1995; Shrimpton *et al.*, 2002) and exists in both soluble and membrane-associated forms (Vincent *et al.*, 1996). The soluble form is predominant. In addition to a cytosolic and plasma membrane location, neurolysin is also present in the mitochondrial compartment (Serizawa *et al.*, 1995; Vincent *et al.*, 1996). The gene for the enzyme contains a mitochondrial targeting sequence at an alternate initiation site for transcription (Kato *et al.*, 1997). It has been estimated that approximately 17 % of the transcripts contain this targeting sequence based on alternative usage of promoters, initiation sites and untranslated exons.

In the brain, TOP predominates in the striatum and the hypothalamus, both of which contain high levels of opioid peptides (Healy and Orlowski, 1992; Massarelli *et al.*, 1999), and neurolysin is highly expressed in NT rich areas of the brain including the ventral midbrain, the olfactory bulb and tubercle, the cingulate cortex, the neostriatum and the globus pallidus (Woulfe *et al.*, 1992; Checler *et al.*, 1995). TOP and neurolysin are present in both neurons and glia (Healy and Orlowski, 1992; Woulfe *et al.*, 1992; Vincent *et al.*, 1996; Massarelli *et al.*, 1999; Fontenele-Neto *et al.*, 2001). In rat brain neurons, a significant proportion of TOP is found in the nucleus (Massarelli *et al.*, 1999; Fontenele-Neto *et al.*, 2001), which has been ascribed to the putative nuclear localization sequences (<sup>234</sup> PETRRKV<sup>240</sup>) found in the enzyme (Pierotti *et*

*al.*, 1990), whereas neurolysin is not present in nucleus. Outside the nucleus, TOP and neurolysin are comparably distributed in the nerve cell bodies and dendrites as well as within axons and axon terminals (Fontenele-Neto *et al.*, 2001). They are also associated with vesicular membranes but are differently distributed with respect to the surface (Fontenele-Neto *et al.*, 2001). TOP is present only on the cytoplasmic side of Golgi and vesicular membranes, whereas neurolysin exists on both luminal and cytoplasmic sides of Golgi and vesicular membranes. Both TOP and neurolysin are thought to be secreted to some extent in certain cell types. Both lack classical signal sequences, however, and the mechanisms of secretion are currently under investigation (Pierotti *et al.*, 1990; Dauch *et al.*, 1995; McCool and Pierotti, 2000).

TOP and neurolysin are zinc metallopeptidases belonging to the M3 family. Members of this family, like those of a number of other metallopeptidase families, contain a His-Glu-Xaa-Xaa-His active site sequence motif (HEXXH) (Dando *et al.*, 1993; Barrett *et al.*, 1995; Rawlings and Barrett, 1995; Shrimpton *et al.*, 2002) (Figure 1.4A). The zinc ion cofactor is coordinated by the side chains of the two histidines. A glutamate residue, located 25 residues carboxyl terminal to the second active site histidine, serves as the third zinc ligand (Cummins *et al.*, 1999; Brown *et al.*, 2001; Ray *et al.*, 2004). The glutamate residue from the active site sequence motif makes hydrogen bonds with a zinc-coordinating water molecule that acts as the attacking nucleophile (Vallee and Auld, 1990) (Figure 1.4B).

Like other metallopeptidases, TOP and neurolysin are inhibited by metal ion chelators and can be reactivated by divalent cations such as zinc ion or manganese ions (Orlowski *et al.*, 1983). Both enzymes are inactivated by thiol reactive agents, and TOP, in particular, has been shown to be unusually sensitive to the level of reducing agent present. It is actually activated by low levels of reducing agents such as dithiothreitol (< 0.5 mM), and this process involves conversion from inactive multimers to active monomer (Orlowski *et al.*, 1983; Orlowski *et al.*, 1989; Lew *et al.*, 1995; Shrimpton *et al.*, 1997; Shrimpton *et al.*, 2003). The multimeric form may be inactive because substrate is blocked from the active site or conformational changes associated with catalysis are inhibited. At least three cysteine residues (Cys246, Cys248, and Cys253) are involved in the formation of the multimers (Shrimpton *et al.*, 1997; Shrimpton *et al.*, 2003). On the other hand, high levels of reducing compounds (>5 mM DTT, for example) inhibit

TOP (Orlowski *et al.*, 1983; Orlowski *et al.*, 1989; Lew *et al.*, 1995; Shrimpton *et al.*, 1997), presumably because they promote loss of the catalytic metal ion. TOP, but not neurolysin, has been shown to be phosphorylated *in vivo*, a possible regulatory mechanism (Tullai *et al.*, 2000). TOP is phosphorylated at Ser644 by cAMP-dependent protein kinase (PKA), producing effects on activity for certain substrates, such as gonadotrophin-releasing hormone (GnRH) (Tullai *et al.*, 2000; Portaro *et al.*, 2001).

As noted above, TOP and neurolysin are distributed widely in mammalian tissues and cell types (Checler *et al.*, 1995; Shrimpton *et al.*, 2002), suggesting they are involved in various physiological roles. They have been implicated in the inactivation of neuropeptides such as somatostatin, dynorphin, bradykinin, gonadotrophin-releasing hormone (GnRH), and luteinizing hormone-releasing hormone (LHRH) (Chu and Orlowski, 1985; Orlowski *et al.*, 1989; Barrett and Brown, 1990; Dahms and Mentlein, 1992; Dando *et al.*, 1993; Mentlein and Dahms, 1994; Yang *et al.*, 1994; Dendorfer *et al.*, 1997; Lew *et al.*, 1997; Wu *et al.*, 1997; Vincent *et al.*, 1997a; Kim *et al.*, 2003). The significance of their roles in metabolizing these peptides remains to be firmly established, however. The ability of TOP and neurolysin to process opioid precursors such as dynorphin A suggests a possible role for the enzymes in the modulation of pain perception (Molineaux and Ayala, 1990; Gomes *et al.*, 1993). There is some suggestion that TOP in particular may be at least partly responsible for the metabolism of bradykinin, which stimulates vascular smooth muscle contraction and increases vascular permeability (Orlowski *et al.*, 1983; Dendorfer *et al.*, 1997). In addition, TOP also converts angiotensin I to the biologically active angiotensin (1-7) fragment, which decreases blood pressure (Chappell *et al.*, 1998). Recent studies suggest that TOP participates in the metabolism of the A $\beta$  peptide associated with Alzheimer's disease (Koike *et al.*, 1999; Yamin *et al.*, 1999; Lew, 2004). In recent years, it has been suggested that TOP plays a role in processing potentially antigenic peptides. Peptides of 3-25 residues released into the cytosol by the proteasome are further hydrolyzed by TOP, in many cases preventing their transport to the endoplasmic reticulum and presentation on the cell surface by MHC class I molecules (Saric *et al.*, 2001; Kim *et al.*, 2003; York *et al.*, 2003).



Despite evidence for other roles of TOP and neurolysin, their most established role is in the metabolism of the 13 residue peptide NT (Figure 1.2A). Neurolysin specific inhibitors protected NT from degradation by primary cultured neuron from mouse embryos (Vincent *et al.*, 1997a). Hydrolysis of NT by neurolysin was completely and dose-dependently inhibited by a relatively specific phosphoramidate inhibitor. In addition, this inhibitor prevented the hydrolysis of NT by TOP with lower potency (Barelli *et al.*, 1992). Neurolysin inhibitors potentiated the recovery of intact NT and inhibited the formation of NT1-10 fragment, the product of NT hydrolysis by neurolysin, in the dog intestine (Barelli *et al.*, 1994). NT-induced antinociception of mice in a hot plate test was greatly potentiated when the animals were injected with neurolysin and TOP specific inhibitors (Vincent *et al.*, 1997a; Vincent *et al.*, 1997b). These results demonstrated that TOP and neurolysin are the main enzymes responsible for NT inactivation.

## **Neurotensin**

NT is an endogenous 13 amino acid bioactive peptide discovered initially in brain (Carraway and Leeman, 1973). It is found in many locations, including the central nervous system and gastrointestinal tract, and is believed to be involved in a number of effects, including modulation of central dopaminergic and cholinergic neurotransmission, thermoregulation, intestinal motility, antinociception, and blood pressure regulation (Tyler-McMahon *et al.*, 2000). It has also been suggested that NT plays a role in the growth of normal and cancerous cells (Moody *et al.*, 2003; St-Gelais *et al.*, 2006). NT mediates its effects through interaction with three cell surface receptors known as NTR1, 2, and 3 (Le *et al.*, 1996; Vincent *et al.*, 1999). NTR1 and NTR2 are seven transmembrane helix G-protein coupled receptors, and activation of these two receptors increases intracellular inositol phosphates and  $Ca^{2+}$  (Watson *et al.*, 1993; Chalon *et al.*, 1996). NTR3 has a single transmembrane domain and is identical with human gp95/sortilin (Mazella *et al.*, 1998), a protein that plays a role in cargo sorting in the secretory system. NTR3 at the plasma membrane seems to act in reinternalizing released NT, a possible mechanism for intracellular degradation or recycling, but it also is essential for proNGF mediated neuronal cell death (Nykjaer *et al.*, 2004).

It has been shown that CNS levels of NT are decreased in patients with schizophrenia (Boules *et al.*, 2005; Richelson *et al.*, 2005), and neuroleptic antipsychotics increase NT levels (Dobner *et al.*, 2003; Boules *et al.*, 2005; Fredrickson *et al.*, 2005). Levels of CNS NT are also lowered in Parkinson's disease (Boules *et al.*, 2005; St-Gelais *et al.*, 2006) and in patients with substance addictions (Hanson *et al.*, 1992). As noted above, levels of NT can be increased by inhibition of TOP and neurolysin, making them attractive targets for treatment of a number of CNS related disorders as well as acute and chronic pain.

### **The present study**

Prior work in our group showed that of the 224 residue differences between TOP and neurolysin, only a relatively small number map to the interior of the substrate binding channel (Ray *et al.*, 2002). A model of NT binding allowed four of these residue positions (E469/R470, M490/R491, H495/N496, and R498/T499, the TOP residues listed first) to be identified as the most likely to be affecting the relative substrate specificity of the two enzymes (Ray *et al.*, 2002; Ray *et al.*, 2004) (Figure 1.5). In the present study, I determine the role of these residues in mediating differential substrate specificity using site directed mutagenesis. Both the cleavage site position on NT and the steady state kinetic parameters were measured. I also determine the crystal structures of substituted residues in the TOP and neurolysin mutants to confirm that the mutations do not cause changes in the local structure of the altered enzymes that would complicate interpretation of the results.

In the model of the bound NT to TOP, the Glu469 of TOP (arginine in neurolysin) potentially could form a salt bridge with Arg9 of NT (Ray *et al.*, 2004). In order to determine whether there is a direct interaction between Arg9 of NT and Glu469 of TOP that might play a role in mediating differential substrate recognition, I performed a swap experiment, replacing Arg9 of NT with a glutamate and Glu469 of TOP with an arginine to see if the cleavage site position remains undisturbed.

## Significance

The major long term goal of our work is to understand how TOP and neurolysin, as model neuropeptidases, can recognize a variety of seemingly unrelated peptide sequences while still maintaining specificity for those sites. This is a basic question in molecular recognition and has implications for general protein-peptide interactions and even for protein-protein recognition. In addition, neuropeptidases are potential therapeutic targets, and all reported metallopeptidase inhibitors mimic substrates by binding at the active site (Vincent *et al.*, 1997a; Vincent *et al.*, 1997b; Kim *et al.*, 2003; Natesh *et al.*, 2003). Understanding how neuropeptidases recognize their substrates will undoubtedly help in the development of more specific and potent inhibitors of these enzymes. Neuropeptidases are also good candidates for gene therapy approaches to disease treatment. For example, neuropeptidases metabolize peptides that act as growth factors for lung cancer (Seufferlein and Rozengurt, 1996), and increasing the expression of one of the metabolizing enzymes would potentially slow the progression of the disease (Moody *et al.*, 1998). Neuropeptidases also metabolize the A $\beta$  peptide associated with Alzheimer's disease (Waters and Davis, 1997; Koike *et al.*, 1999; Yamin *et al.*, 1999; Saito *et al.*, 2003; Lew, 2004), and it has been proposed that adding additional metabolizing capacity may treat or prevent the disease. The problem with these approaches, however, is that the broad specificity of the enzymes will necessarily lead to metabolism of peptides other than the one or ones targeted, likely producing side effects. If we can reengineer the peptidases to be more specific for particular cleavage site sequences, they may make better therapeutics. The work reported here represents a first step in understanding the nature of substrate specificity in the neuropeptidases TOP and neurolysin. I establish that the basis for recognizing different sites in the NT peptide resides in just two residue positions that differ in the two enzymes. This result suggests that general retargeting of the enzymes may be possible with only a limited number of amino acid changes in the binding site region.

## Introduction to other studies included in this thesis

### Neprilysin

Neprilysin (NEP, EC 3.4.24.11) is type II integral membrane, zinc dependent metallopeptidase and a member of M13 subfamily. It was originally purified from the rabbit kidney and was initially implicated in the metabolism of insulin (Kerr and Kenny, 1974). But, further studies have demonstrated that NEP does not play a large role in insulin metabolism, with another zinc metallopeptidase, insulysin (insulin-degrading enzyme, IDE), being primarily responsible for initial insulin hydrolysis (Authier *et al.*, 1996). NEP is widely distributed in mammalian tissues (Sato *et al.*, 1996; Papandreou *et al.*, 1998; Takaki *et al.*, 2000), particularly kidneys and lungs (Kerr and Kenny, 1974; Cohen *et al.*, 1996). It consists of a short N-terminal cytoplasmic domain, a single transmembrane helix, and a large C-terminal extracellular domain containing the active site (Devault *et al.*, 1987; Barnes *et al.*, 1992). Hydrophobic sequences near the N-terminus function as a signal sequence to target the protein into the cisternae of the rough endoplasmic reticulum and as a membrane-spanning segment to anchor to the plasma membrane (Konkoy and Davis, 1996). The bulk of NEP is located at the cell surface where it functions as an ectoenzyme, degrading peptides at the extracellular face of the plasma membrane.

The crystal structure of extracellular domain (residues 52-749) of human NEP (hNEP) was determined complexed with phosphoramidon, a general metallopeptidase inhibitor, at 2.1 Å resolution (Oefner *et al.*, 2000) (Figure 1.6A). Like other zinc metallopeptidases, NEP contains the HEXXH zinc-binding motif. In addition, it has an EXA/GD sequence, in which the glutamate serves as the third zinc ligand (Figure 1.6B). The extracellular domain of NEP contains 12 cysteine residues, making six disulfide bonds, and the domain also has three established N-linked glycosylation sites (N144, N324, and N627). The extracellular domain of hNEP is composed of the larger N-terminal domain (domain 1) and a smaller domain (domain 2), which together embrace a large central cavity containing the active site (Figure 1.6A and B). Various natural substrates of hNEP are limited to about 25 residues since access to the active site is greatly restricted. Only a narrow opening leads to the bowl-shaped active site cavity. Several crystal structures of hNEP with various bound inhibitors, including the classic inhibitor phosphoramidon

(Figure 1.6C and D), are available, providing some information on likely substrate interactions (Robl *et al.*, 1997; Chen *et al.*, 1998; Robl *et al.*, 1999; Oefner *et al.*, 2004).

NEP has been implicated in the degradation of a variety of signalling peptides. First, it hydrolyzes the opioid peptides such as enkephalins, regulating opioid peptide action (Malfroy *et al.*, 1978; Matsas *et al.*, 1983). Second, NEP plays a role in control of blood pressure by hydrolyzing the peptides atrial natriuretic peptide (ANP), bradykinin, and endothelin (Kenny and Stephenson, 1988; Roques *et al.*, 1993; Turner and Tanzawa, 1997). Therefore, potent inhibitors of NEP have been pursued as novel analgesics or antihypertensive agents because they increase opioid or vasoactive peptide levels (Roques and Beaumont, 1990; Robl *et al.*, 1997; Chen *et al.*, 1998; Burnett, 1999; Robl *et al.*, 1999). More recently, significant elevations of amyloid  $\beta$  peptide (A $\beta$ 1-42), the primary pathogenic agent in Alzheimer's disease, has been observed in mice lacking NEP (Carson and Turner, 2002). This result suggests that NEP is involved in removal of A $\beta$  peptide and that selective re-expression of NEP in cells may provide a novel approach to the treatment of Alzheimer's disease (Marr *et al.*, 2004; Mohajeri *et al.*, 2004). NEP is dramatically down regulated in a number of cancer cells (Papandreou *et al.*, 1998), including forms of brain cancer (Harding, 2001), renal cancer (Gohring *et al.*, 1998), invasive bladder cancer (Koiso *et al.*, 1994), stomach cancer (Sato *et al.*, 1996), endometrial cancer (Suzuki *et al.*, 2001), and prostate cancer (Papandreou *et al.*, 1998; Shen *et al.*, 2000). Overall, then, manipulation of NEP levels, if attempted in therapies, must be done selectively, and it seems likely that inhibitors that can be targeted to specific tissues and cell types will be required. A better understanding of NEP substrate specificity will aid in developing novel inhibitors and reengineering the enzyme for therapeutic purposes.

Like TOP and neurolysin, NEP also recognizes a wide variety of sequences, but it does not have any strong sequence preference at any particular position relative to the cleaved peptide bond. Interestingly, NEP as well as TOP and neurolysin is involved in inactivation of the 13 residue neuropeptide NT even though it may be partially responsible for metabolism of the peptide *in vivo* (Oliveira *et al.*, 2001). TOP hydrolyzes NT between Arg8 and Arg9, while neurolysin cleaves the peptide between Pro10 and Tyr11. NEP also hydrolyzes NT at between Pro10 and Tyr11, cleavage site of neurolysin on NT. Therefore, as with TOP and neurolysin,

defining the determinants of recognition on the NT substrate will help understand the substrate specificity of NEP.

### **Human choline acetyltransferase (hChAT)**

Acetylcholine (ACh) was the first neurotransmitter to be identified (Loewi, 1921). It stimulates muscle contraction in the peripheral nervous system and helps formation of learning and short-term memory in the central nervous system (Karczmar, 1993). ACh is synthesized by choline acetyltransferase (ChAT, EC 2.3.1.6), which catalyzes the transfer of an acetyl group from the acetyl-coenzyme A (AcCoA) to choline (Nachmansohn and Machado, 1943). ChAT belongs to the choline/carnitine acyltransferase family and functions in the axon termini of cholinergic neurons, which are distributed throughout the central and peripheral nervous system (Karczmar, 1993). The single ChAT gene produces six different isoforms of ChAT mRNA (termed R, N1, N2, H, S and M) (Misawa *et al.*, 1992; Oda *et al.*, 1992; Misawa *et al.*, 1997; Robert and Quirin-Stricker, 2001). All transcripts translate into a 69 kDa form, but the M and S transcripts also can make 82 kDa and 74 kDa, respectively. The 69 kDa form exists in the cytoplasm, while the 82 kDa form is translocated to the nucleus because of the 118 amino acid extension on the N terminal of the enzyme containing a nuclear localization signal (Kong *et al.*, 1989; Oda *et al.*, 1995; Resendes *et al.*, 1999; Gill *et al.*, 2003). Most ChAT is present in a soluble form but a small portion of the total cellular enzyme is associated with membrane (Martinez-Murillo *et al.*, 1989; Carroll, 1994; Gabrielle *et al.*, 2003). The significance of the differential cellular localization and membrane binding of the isoforms of the enzyme is unknown. The 69 kDa ChAT is phosphorylated by protein kinase C (PKC), protein kinase CK2,  $\alpha$ -Ca<sup>2+</sup>/calmodulin-dependent protein kinase II (CaM kinase), whereas the 82 kDa form is phosphorylated by PKC and CaM kinase (Dobransky *et al.*, 2001; Dobransky *et al.*, 2003; Dobransky and Rylett, 2003; Dobransky *et al.*, 2004; Dobransky and Rylett, 2005). Recently, it has been demonstrated that phosphorylation of ChAT can alter its catalytic activity and membrane binding (Sha *et al.*, 2004).

The crystal structure of rat ChAT (rChAT) was determined at 2.5 Å resolution (Cai *et al.*, 2004) by molecular replacement with carnitine acetyltransferase (CrAT) (Jogl and Tong, 2003)

(Figure 1.7A). It showed the enzyme is divided into two domains with the active site located at the domain interface. The catalytic residue of the rChAT, histidine 334, extracts the proton from the hydroxyl group of choline or the thiol group of CoA, depending on the direction of the readily reversible reaction. Subsequent structural studies have shown that CoA substrate binds to ChAT in a long solvent accessible tunnel at the domain interface, placing its terminal thiol in a position to hydrogen bond with H334. ChAT uses choline reabsorbed from the synaptic cleft into the presynaptic nerve terminal by the high-affinity sodium-dependent choline transporter (Okuda *et al.*, 2000). Transport of choline may be rate-limiting in ACh synthesis (Guyenet *et al.*, 1973; Yamamura and Snyder, 1973). Newly synthesized ACh is accumulated in synaptic vesicles by a vesicular acetylcholine transporter (Parsons *et al.*, 1993; Erickson and Varoqui, 2000) for stimulated release into the synaptic cleft.

Decreases in ChAT activity and the number of cholinergic neurons are associated with Alzheimer's disease, Huntington's disease, amyotrophic lateral sclerosis, schizophrenia, sudden death syndrome, and Rett's syndrome (Oda, 1999; Dunn and MacLeod, 2001). Recessive loss of function mutations in ChAT are a cause of a motor disorder known as congenital myasthenic syndrome associated with episodic apnea (CMS-EA) (Figure 1.7B), resulting in severe muscular weakness and respiratory insufficiency (Ohno *et al.*, 2001; Kraner *et al.*, 2003; Maselli *et al.*, 2003; Schmidt *et al.*, 2003). Some of these mutations are close to the active site, but many of the mutations occur at considerable distances from the catalytic histidine. Despite their varied locations, nearly all the mutants substantially affect the  $K_m$  value for CoA/AcCoA (Ohno *et al.*, 2001). We need to understand why these mutations can affect ChAT activity in a similar way despite their varied locations. Thus far only the rat homolog has been determined, but the human form would be more relevant to the congenital disease caused by ChAT mutations. A detailed understanding of the structural effects of the mutations will help us design therapies for this disorder. Therefore, I overexpressed human ChAT and determined crystallization conditions. This work and subsequent characterization of the human ChAT crystals is described in this thesis.

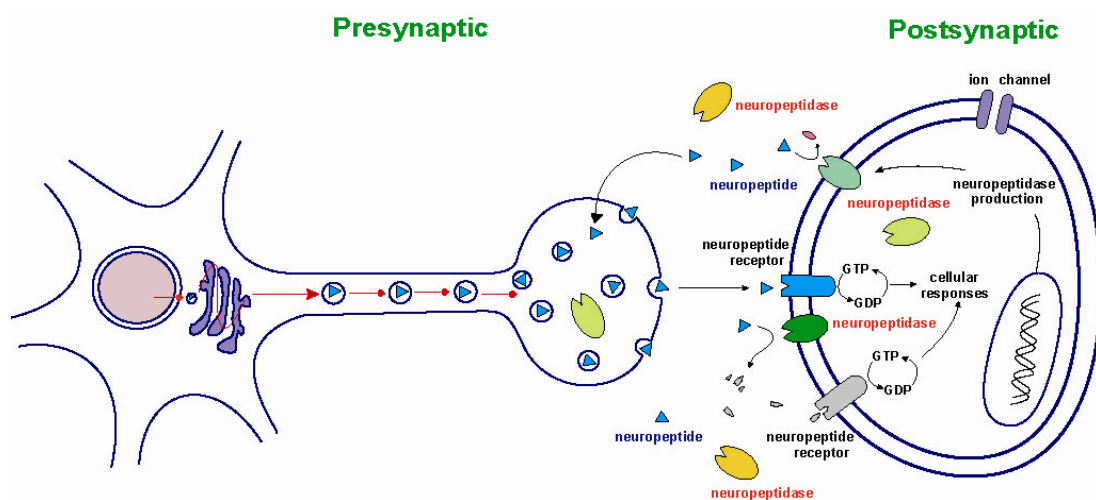
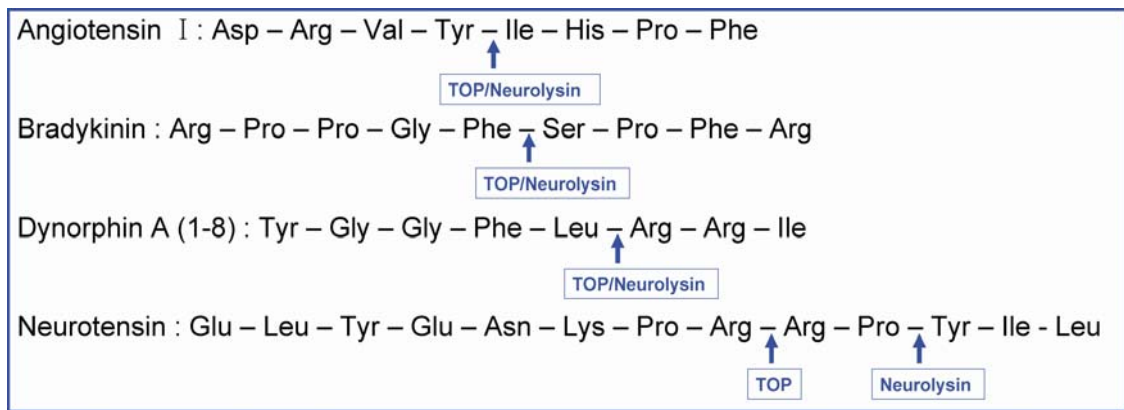


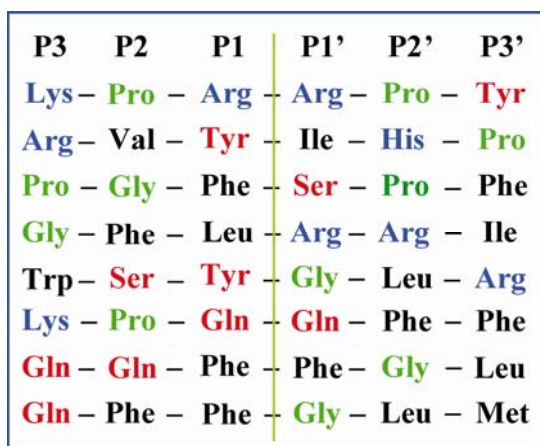
**Figure 1. 1. Neuropeptide metabolism.** Neuropeptides synthesized in a presynaptic neuron are transported to synaptic terminal via secretory vesicles and released into the synaptic cleft. After release from a presynaptic neuron, they bind to surface neuropeptide receptors on a postsynaptic neuron and modulate cellular signaling pathways. Neuropeptides released from presynaptic neurons or transported into postsynaptic neurons are metabolized by hydrolytic enzymes known as neuropeptidases.



A



B



C

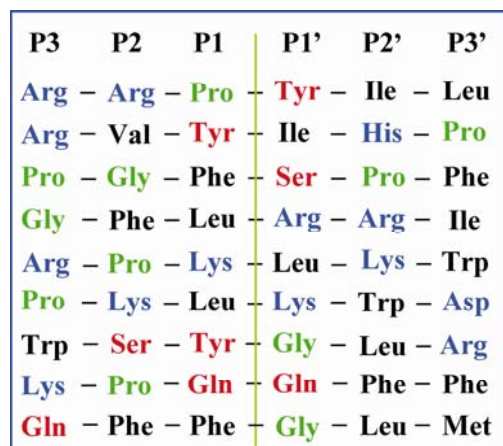
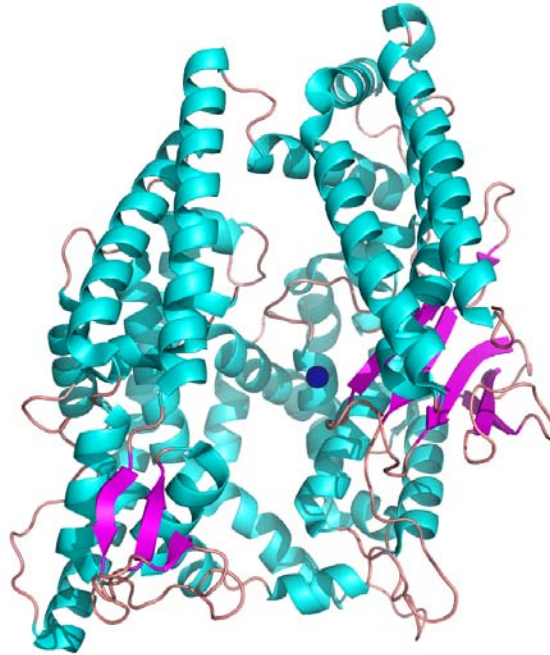


**Figure 1. 2. Cleavage specificity of neuropeptidases.** A, Cleavage sites in a few thimet oligopeptidase (TOP) and neurolysin substrates. Arrows indicate cleavage positions. B, Alignment of TOP cleavage site sequences. The green line indicates the position of the scissile bond, and amino acids N-terminal and C-terminal to the cleavage sites are labeled P1-3 and P1'-3', respectively. Colors indicate basic (blue), polar (red), gly and pro (green), and hydrophobic/aromatic amino acids (black). C, Alignment of neurolysin cleavage site sequences.

**A**



**B**

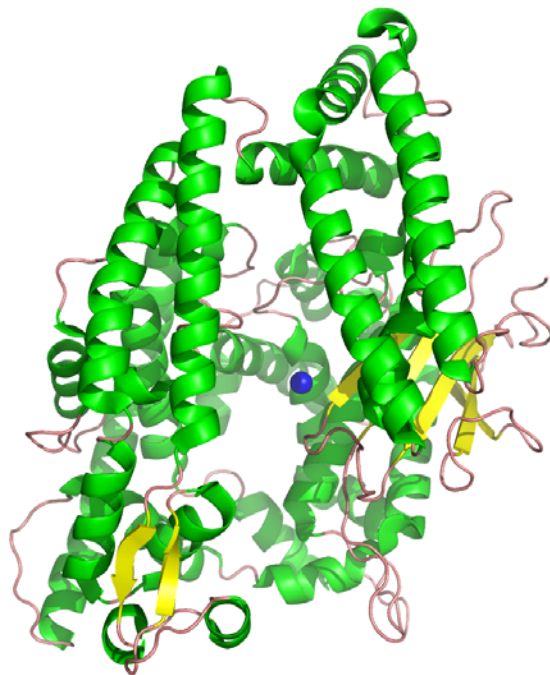
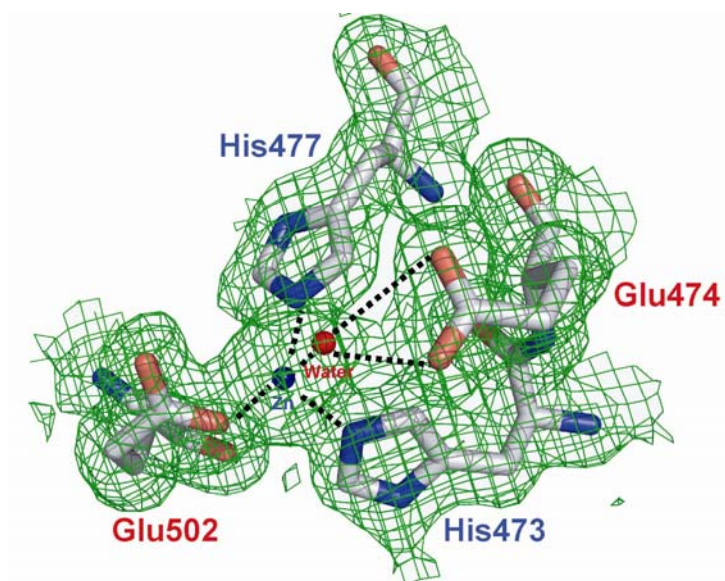


**Figure 1. 3. The overview of crystal structures of TOP and neurolysin.** Ribbons views of the human TOP (**A**) and rat neurolysin (**B**) crystal structures (Brown *et al.*, 2001; Ray *et al.*, 2004) are shown. The zinc ion cofactors, located deep in the substrate binding channel, are shown as blue spheres.

**A**



**B**

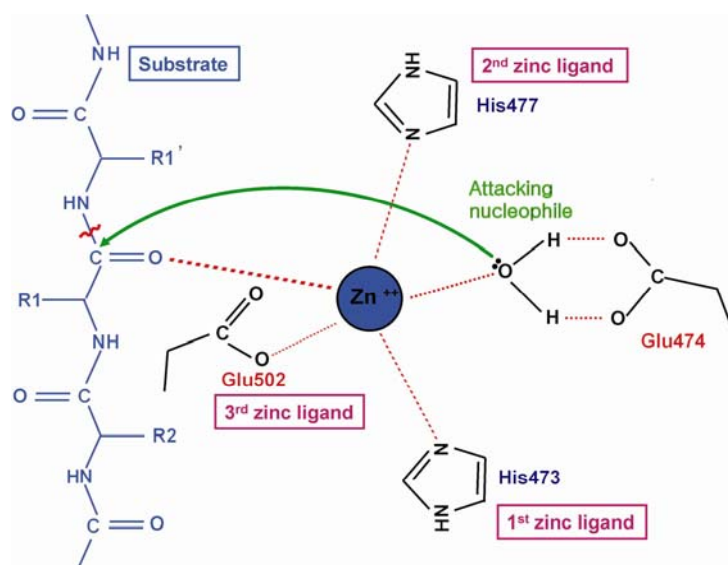
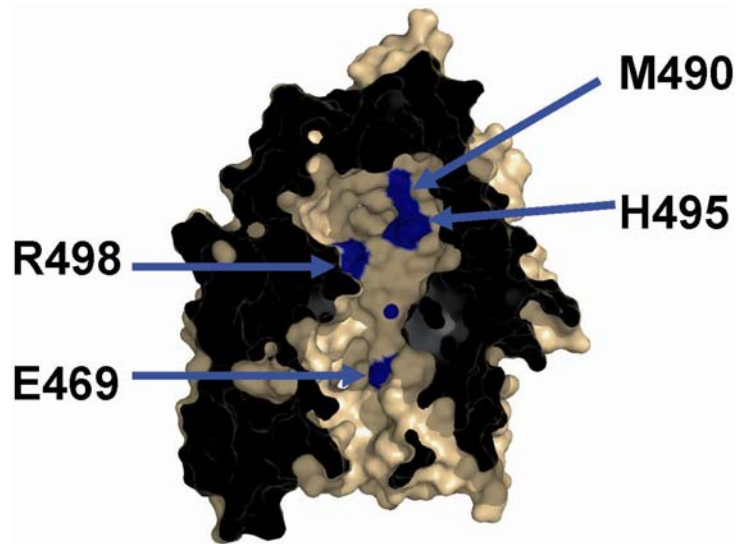


**Figure 1. 4. The active site of TOP.** **A**, The electron density of active site of TOP. Density ( $2F_o - F_c$ ) is shown in wire-frame representation (green) contoured at 1.0 times the r.m.s density of the map. The side chains of active residues are well defined by electron density. The zinc ion cofactor and the catalytic water are shown as spheres colored blue and red, respectively. **B**, A schematic representation of the active site showing the zinc cofactor and coordinating residues, the activating glutamate residue, the water that serves as the attacking nucleophile, and the peptide substrate. The hydrogen bonds and metal coordinating interactions are indicated by red dashed lines.

A



B

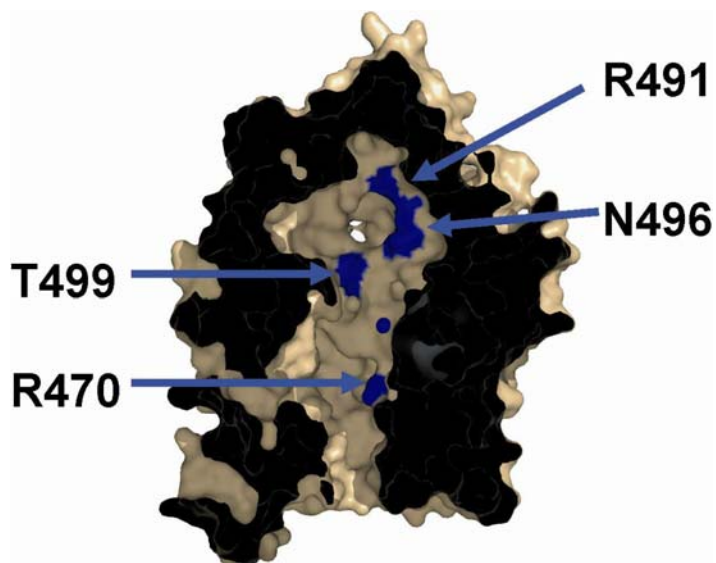


**Figure 1. 5. Key residue differences in the substrate binding channels of TOP and neurolysin.** Cutaway molecular surface views of TOP (A) and neurolysin (B) showing the positions of sequence differences that might affect cleavage site selection on NT. The one letter codes before the residue number represent wild type amino acids. All four positions are located near the floor of the substrate binding channel.

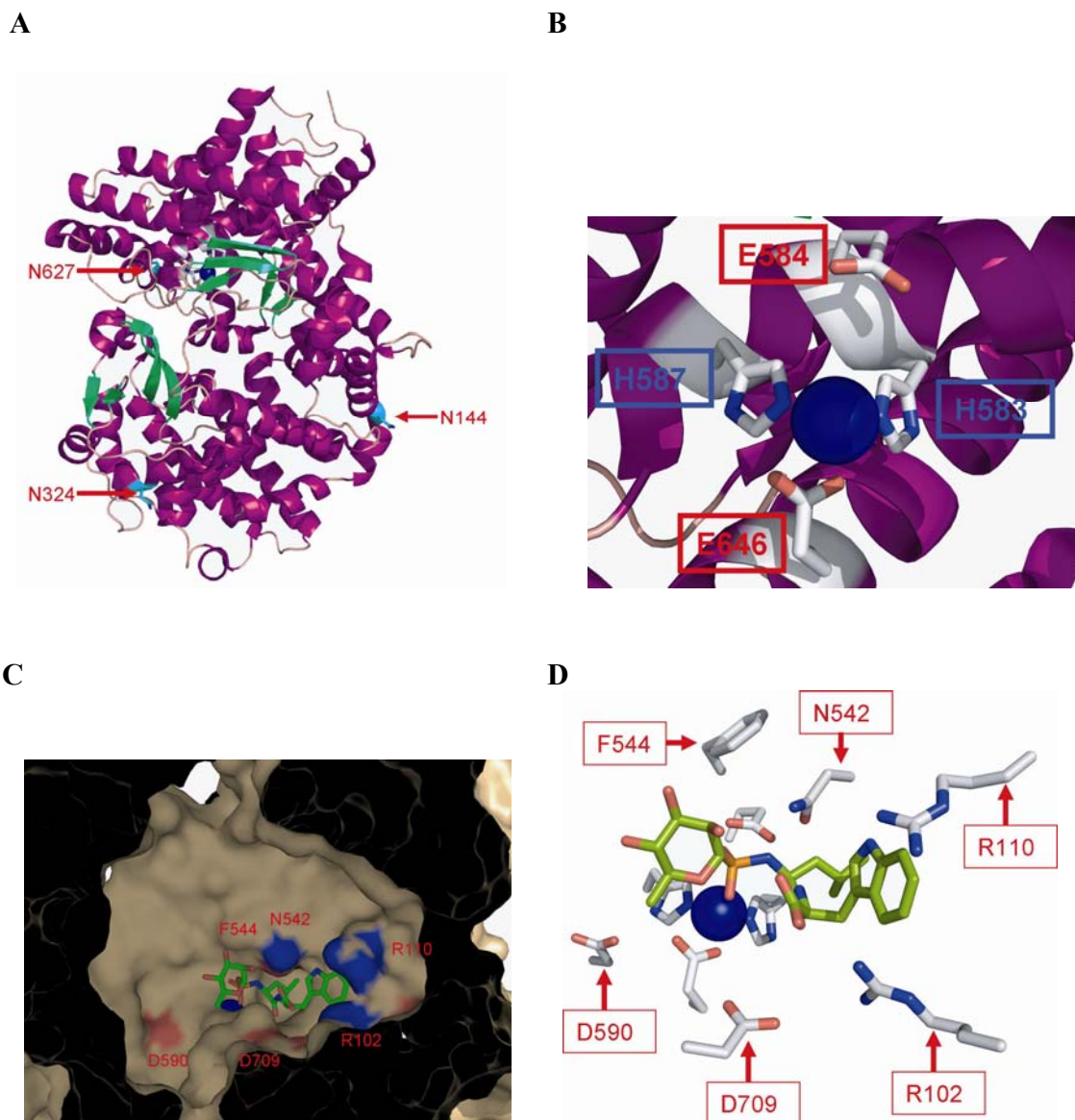
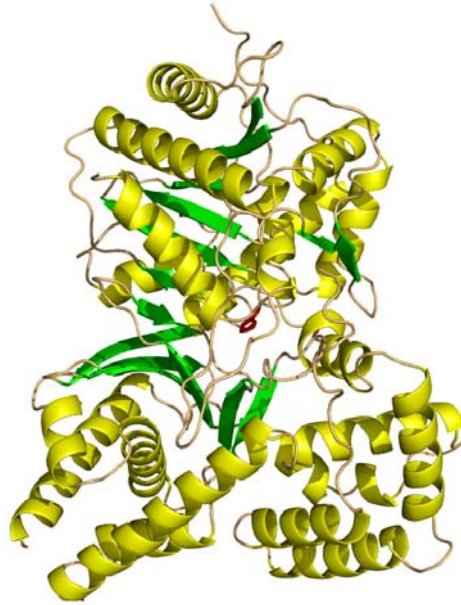


**Figure 1. 6. Overview of crystal structures of human neprilysin (hNEP).** A and B, Crystal structure of hNEP (Oefner *et al.*, 2000). The active site and zinc ion, shown in blue, are located in the central cavity and three glycosylation sites are indicated by red arrows. C and D, Phosphoramidon inhibitor binding to the active site. The recognition sites of phosphoramidon are labeled with red letters.

**A**



**B**

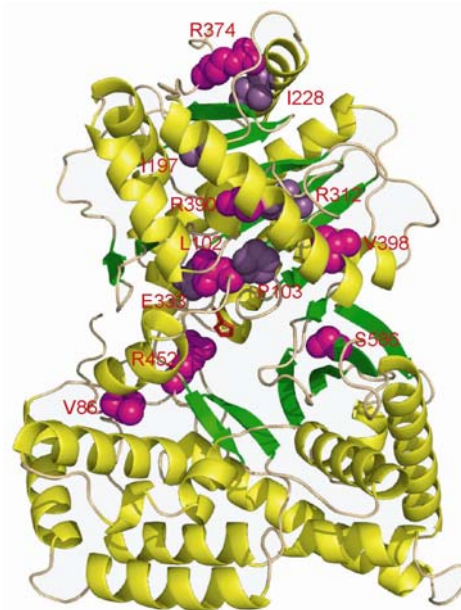


**Figure 1. 7. Overview of the rat choline acetyltransferase (rChAT) crystal structure. A,** Ribbons representation of rChAT (Cai *et al.*, 2004). The side chain of the of the catalytic histidine residue (His334) is shown in red. **B,** Side chains of residues mutated in patients with the motor disorder congenital myasthenic syndrome with episodic apnea (Engel *et al.*, 2003) are shown in a space filling representation.

Copyright © Eun Jeong Lim, 2006

## Chapter 2: Materials and methods

### Preparation of TOP and neurolysin mutant constructs

The modified human TOP sequence inserted into a pET32 vector (Invitrogen) was available in the lab (Ray *et al.*, 2004). The first mutant constructed, the TOP 4 mutant, had all four positions identified as likely mediating differential specificity (E469, M490, H495, and R498) changed to the corresponding residues in neurolysin (Figure 1.5A; Table 2.1). The TOP 4 mutant coding sequence was prepared by sequential site directed mutagenesis using the QuikChange site-directed mutagenesis system (Stratagene). The mutagenesis was performed with 5  $\mu$ l of 5 $\times$  reaction buffer, 1  $\mu$ l of 50 ng/ $\mu$ l of double strand DNA template, 1.25  $\mu$ l of 100 ng/ $\mu$ l of forward mutant primer, 1.25  $\mu$ l of 100 ng/ $\mu$ l of reverse mutant primer, 1  $\mu$ l of 100 mM dNTP mixture, 1  $\mu$ l of *Pfutura* DNA polymerase (2.5 U/ $\mu$ l), and 39.5  $\mu$ l of H<sub>2</sub>O to a final volume of 50  $\mu$ l. Each was cycled according to the parameters: 1 cycle at 95 °C for 30 seconds and 18 cycles at 95 °C for 30 seconds, 53 °C for 1 minute, and 68 °C for 16 minutes (Eppendorf personal master cycler). After 18 cycles of PCR, 1  $\mu$ l of the *Dpn* I restriction enzyme (10 U/ $\mu$ l) was added directly to each amplification reaction and the sample was immediately incubated at 37 °C for 1 hour to digest the parental DNA. After 1 hour of incubation, 1  $\mu$ l of the *Dpn* I treated DNA from sample reaction was transformed into 50  $\mu$ l of the XL1-Blue competent cells by heat shock at 42°C for 1 minute. The mutant and wild type sequences were confirmed by automated sequencing (Davis sequencing, [www.davissequencing.com](http://www.davissequencing.com)) using 8  $\mu$ l of 300 ng/ $\mu$ l plasmid DNA prepared with the Promega midiprep system. The plasmid was mixed with 3  $\mu$ M of 3 pmol/ $\mu$ l sequencing primer. TOP 3 mutants (Figure 2.1) and the TOP 2 mutant (Figure 2.2A), which had subsets of the four mutations, were prepared using the same protocol as used for the TOP 4 mutant.

The wild type neurolysin coding sequence in a pBAD (Invitrogen) vector was available in the laboratory (Brown *et al.*, 2001). The neurolysin 4 mutant was made by substitution of residues R470, R491, N496, and T499 to the corresponding ones in TOP using the QuikChange site-directed mutagenesis system as described for the TOP mutants (Figure 1.5B; Table 2.2). The

neurolysin 2 mutant was substituted at positions R470 and T499 using the same approach (Figure 2.2B).

### **Expression and purification of wild type TOP and mutants**

All wild type and mutant TOP constructs were expressed in *Escherichia coli* BL21(DE3)RP cells (Stratagene), which overproduce arginine and proline transfer RNAs that recognize codons for these amino acids common in mammals but rare in *E. coli*. Cells containing TOP constructs were cultured in Terrific Broth (TB) containing 50 mg/ml ampicillin and 34 mg/ml chloramphenicol at 37°C for overnight. Then 300 ml of cultured cells were inoculated into 7 L of TB media containing 7 ml of antifoam, 50 mg/ml ampicillin, and 34 mg/ml chloramphenicol and grown in a New Brunswick BioFlo 3000 cell culture device at 37°C until the  $A_{600}$  had reached 0.6. 1 mM of isopropyl- $\beta$ -D-thiogalactopyranoside (IPTG) was added to induce overexpression of the TOP proteins, and the cells were grown at 16°C for an additional 5 hours. Cells were collected by centrifugation at 8,000 rpm for 10 minutes, and the pellets were stored at -20°C.

Cell pellets were resuspended in cold lysis buffer (3 ml per gram of cells) containing 50 mM  $\text{NaH}_2\text{PO}_4$  (pH 8.0), 4% Glycerol, 5 mM 2-mercaptoethanol, 50 mM NaCl, and protease inhibitor cocktail III (Sigma; 100  $\mu\text{l}$ /1L of culture). Lysozyme (1 mg per ml of lysis buffer) was added and the cells incubated on ice for 30 minutes. Cells were lysed by passing them twice through a French press. The resulting mixture was centrifuged at 23,000 rpm for 60 minutes at 4°C to remove cell debris. The crude lysate was then mixed with the 50% Ni-NTA agarose resin (Qiagen; 1 ml of resin per 4 ml of crude lysate) equilibrated in 50 mM  $\text{NaH}_2\text{PO}_4$  (pH 8.0), 4% Glycerol, 5 mM 2-mercaptoethanol and incubated on a shaker for 2-3 hours at 4°C. The resin was washed with 40 ml cold wash buffer (50 mM  $\text{NaH}_2\text{PO}_4$  (pH 8.0), 4% Glycerol, 5 mM 2-mercaptoethanol, and 500 mM NaCl) on a shaker for 20 minutes and centrifuged at 4,000 rpm for 5 minutes at 4°C to pellet the resin. The resin was washed two times more with cold buffer containing 1 M NaCl and 1.5 M NaCl.



The resin was washed with 3 ml of digestion buffer containing 50 mM Tris-HCl (pH 8.0), 1 mM CaCl<sub>2</sub>, 0.1 % Tween-20, 2% glycerol, and 5 mM 2-mercaptoethanol before centrifuging at 4,000 rpm for 5 minutes. Then 20 units of enterokinase (EK; Invitrogen) were added and incubated for 2-3 days at 4°C to cleave the polyhistidine tag from the TOP protein, releasing it from the resin. To remove the EK from the digestion, prewashed EK-away resin (Invitrogen) was added and the sample and incubated for 15 minutes with gently rocking. TOP protein was dialyzed against 1 liter of buffer containing 20 mM Tris-HCl (pH 8.0), 10 mM NaCl, 5 % glycerol and 5 mM 2-mercaptoethanol overnight at 4°C, loaded onto an anion exchange column (Poros HQ resin, GE Healthcare), and eluted with salt gradient. Finally, the purified protein was dialyzed against 1 liter of buffer containing 20 mM Tris-HCl (pH 8.0), 5 % glycerol and 5 mM 2-mercaptoethanol overnight at 4°C and concentrated to 5-10 mg/ml using a Centricon-50 (Amicon, cutoff 50 kDa). The concentrated protein was stored at 4°C.

### **Expression and purification of wild type neurolysin and mutants**

Neurolysin variants were overexpressed in the *Escherichia coli* TOP10 cells (Invitrogen). Cells were transformed with neurolysin variants and grown at 37°C overnight. 300 ml of cultured cells were used to inoculate 7 L of Luria Bertani (LB) media containing 7 ml of antifoam and 50 mg/ml ampicillin in a New Brunswick BioFlo 3000 cell culture device, and the culture was grown at 37°C until the A<sub>600</sub> had reached 0.9-1.0. Then arabinose was added to a final concentration of 0.01 % to induce overexpression of neurolysin. Cells were further grown at 37°C for 4-5 hours and harvested by centrifugation at 8,000 rpm for 10 minutes. Cell pellets were stored at -20°C. The purification of neurolysin variants was similar to that of TOP as mentioned above. The purified protein was dialyzed against 1 liter of buffer containing 20 mM Tris-HCl (pH 7.4) and 100 mM NaCl overnight at 4°C and concentrated to 10-15 mg/ml in a Centricon-50 (Amicon; cutoff 50 kDa). The concentrated protein was stored at 4°C.

### **Assay for cleavage position on NT**

Cleavage positions were determined using 600  $\mu\text{M}$  of NT or NT(R9E), 0.5  $\mu\text{M}$  of purified enzyme (TOP or neurolysin), and 10 mM HEPES (pH 7.0). Reactions were incubated at 37  $^{\circ}\text{C}$  for 10 minutes and then stopped by 0.25% TFA. The hydrolyzed peptides were analyzed by HPLC using a Waters system with a C18 5  $\mu\text{M}$  4.6 x 150 mm column (Waters) and eluted with a linear gradient of 10 %-50 % acetonitrile in 0.1 % TFA for 40 min at a flow rate of 1 ml/min. Absorbance was monitored at a wavelength of 214 nm. The products were collected and dried on a centrifugal vacuum evaporator. The molecular weight of peptides was measured by using ESI-TOF mass spectrometry (Scripps Research Institute Center for Mass Spectrometry).

### **Kinetic assay of TOP and neurolysin**

Kinetic assays were performed with 5-6 nM enzyme (TOP or neurolysin), 1-6  $\mu\text{M}$  of fluorogenic substrate NT, the NT sequence flanked with N-terminal fluorescent 2-aminobenzoyl (Abz) and a C-terminal quencher ethylenediaminodinitrophenol (EDDnp) group (Peptides International), 25 mM HEPES (pH 7.5), 10 mM NaCl, and 2 mM 2-mercaptoethanol. The fluorescence of hydrolyzed NT was measured at  $\lambda_{\text{em}} = 420 \text{ nm}$  and  $\lambda_{\text{ex}} = 320 \text{ nm}$  in a luminescence spectrometer LS55 (Perkin Elmer). The change in fluorescence intensity over time was converted into rate of product formation at each substrate concentration. The conversion factor was 200 U /  $\mu\text{M}$ , which was determined by observation of the output level after the completed reaction, using sufficient enzyme concentration to reach completion within a short time. The kinetic parameters were calculated using a hyperbolic fit to the plot of substrate concentration versus rate of product formation. All the data were fit to the equation,  $V = V_{\text{max}} [S] / (K_m + [S])$ , using Prism version 4 from GraphPad.

### **Swap experiment between TOP E469R mutant and NT(R9E)**

The TOP E469R mutant was prepared using the QuikChange site-directed mutagenesis system (Stratagene) (Figure 2.3B; Table 2.1). The altered NT peptide, named NT(R9E), in which Arg9 was replaced by Glu9 was obtained from AnaSpec, Inc (Figure 2.3C). To determine the cleavage site on NT(R9E), a standard cleavage assay was performed using the TOP E469R mutant and NT(R9E). The samples were incubated at 37 °C for 10 min and hydrolyzed NT(R9E) fragments were analyzed on a C18 column using a Waters HPLC system. The masses of the isolated fragments were checked by ESI-TOF mass spectrometry (Scripps Research Institute Center for Mass Spectrometry). The details of the procedures are the same as noted above.

### **Crystallization of TOP 2 and neurolysin 2 mutants**

The TOP 2 mutant was crystallized by hanging drop vapor diffusion at 4°C. The crystals were grown by mixing 1 µl of 10 mg/ml protein with 1 µl of well solution containing 100 mM Na-Cacodylate (pH 6.5), 100 mM magnesium acetate, 2 mM 2-mercaptoethanol, and 12-14 % (w/v) polyethylene glycol 6000. For data collection, crystals were transferred briefly (a few seconds) into a solution containing 25 % glycerol, 100 mM Na-Cacodylate (pH 6.5), 100 mM magnesium acetate, 2 mM 2-mercaptoethanol, and 12-14 % (w/v) polyethylene glycol 6000, mounted in a nylon loop, and flash cooled by plunging into liquid nitrogen (Rodgers, 1997).

Neurolysin 2 mutant crystals were also obtained by hanging drop vapor diffusion at 4 °C. The well solution for neurolysin was 100 mM Na-Cacodylate (pH 6.5), 100 mM magnesium chloride, 0.1 mM zinc chloride, 1 mM 2-mercaptoethanol, and 10-12 % (w/v) polyethylene glycol 8000. The crystals were grown by mixing 1-2 µL of 15 mg/ml protein with an equal volume of well solution. In preparation for data collection, they were exposed briefly (a few seconds) to 20 % polyethylene glycol 400 in the crystallization well solution, mounted in a nylon loop, and plunged into liquid nitrogen (Rodgers, 1997).

## Data collection and structure determination of TOP 2 and neurolysin 2 mutants

X-ray data were collected at the Advanced Photon Source beamline 22-ID (Southeast Regional Collaborative Access Team), Argonne National Laboratory. Data were reduced with HKL2000 (Otwinowski and Minor, 1997), and initial structures of TOP 2 mutant and neurolysin 2 mutant were determined by molecular replacement with the CNS software package using wild type TOP and neurolysin coordinates, respectively (Protein Data Bank accession codes 1S4B and 111I). Model building and analysis were performed by using the program O and structures were refined by CNS. The space group of the TOP 2 mutant crystals was  $P2_12_12_1$  and cell dimensions were  $a=77.1 \text{ \AA}$ ,  $b=99.3 \text{ \AA}$ ,  $c=105.7 \text{ \AA}$ . The space group of the neurolysin 2 mutant crystals was  $P2_12_12$  with unit cell dimension of  $a=159.6 \text{ \AA}$ ,  $b=87.7 \text{ \AA}$ ,  $c=58.4 \text{ \AA}$ .

## Preparation of human neprilysin (hNEP) constructs

The gene for the extracellular domain of human neprilysin (hNEP, residues 52-749) was obtained from Dr. Hersh's laboratory and subcloned into pPICZ $\alpha$  vector (Invitrogen) for expression in the yeast *Pichia pastoris*. Recombinant hNEP protein was expressed as a fusion with the *Saccharomyces cerevisiae*  $\alpha$ -factor secretion signal to direct the protein into the secretory system and subsequently into the external media. A polyhistidine tag was also included at the N-terminus of the construct, and transcription was placed under control of the alcohol oxidase (*AOX1*) promoter, which allows for tight suppression until induced by the additional methanol to the medium. The construct was transformed into *Escherichia coli* TOP10 cells for amplification, and the sequence was confirmed (Davis sequencing, [www.davissequencing.com](http://www.davissequencing.com)). In later expression attempts, the hNEP construct in the pPICZ $\alpha$  vector was mutated at the three established N-linked glycosylation sites (N144, N324, and N627) (Figure 1.6) using the QuikChange site-directed mutagenesis system (Stratagene) in order to prevent glycosylation, which is known to inhibit formation of highly ordered crystals (Kalisz *et al.*, 1990; Kalisz *et al.*, 1991).

## Expression and purification of hNEP

The pPICZ $\alpha$ -hNEP construct was introduced into *Pichia pastoris* GS115 cells by electroporation. A yeast colony was used to inoculate a 5 mL culture of YPD media (EasySelect *Pichia* expression kit, version F from Invitrogen) and grown at 30°C on a rotating shaker. The cultured cells were used to inoculate 50 ml of additional media once they reached a density of  $5 \times 10^6$  cells/mL and then further cultured to an OD<sub>600</sub> of 0.6. The cells were harvested by spinning at 5,000 rpm for 5 min, resuspended in 50 ml of water, and spun down twice at 5,000 rpm for 5 min. Cells were resuspended in 2ml of 1M cold sorbitol and spun down at 5,000 rpm for 5 min. They were then treated with 2 mL LiTE made up to 25 mM DTT, and the cells were centrifuged at 5,000 rpm for 5 min. Cells were then resuspended in 2 ml of 1 M cold sorbitol and centrifuged at 5,000 rpm for 5 min. Finally, the cells were resuspended in 250  $\mu$ l of 1 M cold sorbitol. Approximately 30  $\mu$ g of hNEP DNA was linearized with *Sac* I . The linearized DNA was mixed with 50  $\mu$ l of competent cells, and mixtures were pulsed at 1.5 kV in the 0.2 mm cuvette with Bio-RAD Micropulser. Immediately after pulsing, 1 mL of cold 1 M sorbitol was added, and the sample was incubated at 30 °C without shaking for 1 hour. After 1 hour, 1 ml YPD medium was added to each tube and the culture grown at 30 °C for three more hours on a rotating shaker. The cells were centrifuged at 5,000 rpm, resuspended in 100  $\mu$ L 1M sorbitol, and plated on YPDS media plates (EasySelect *Pichia* expression kit, version F from Invitrogen) containing 100  $\mu$ g/ml, 200  $\mu$ g/ml, and 500  $\mu$ g/ml Zeocin (Invitrogen). Colonies formed in 2 to 4 days at 30 °C. A large number of colonies grown in small scale cultures and screened with an activity assay ((Li and Hersh, 1995); see below for a description) to identify the colony that produced the highest level activity. Stocks of cells were made from the colony having the highest activity and used for all future experiments.

For large scale culture, stock cells were inoculated into 500 ml of YPD medium containing 25  $\mu$ g/ml zeocin and cultured at 30 °C to OD<sub>600</sub> = 8-10. The cells were centrifuged at 9,000 rpm for 10 min at room temperature, resuspended with 0.5 liter YP medium and poured into 6.5 liters of YP medium containing 25  $\mu$ g/ml zeocin. 210 ml of 100 % methanol and 7 ml of 3 % antifoam were added to 7 liter of YP medium and the cells were grown at 30 °C for 4 days.

At the end of the expression period, the media was harvested and the cells spun down at 7,000 rpm for 15 minutes at 4 °C. The resulting supernatant was brought to 55 % (w/v) ammonium sulfate and stored at 4 °C for 30 minutes. Precipitated material was spun down at 7,000 rpm for 30-60 minutes and the resulting supernatant was transferred into new beakers while the pellets were resuspended in 20-30 ml of resuspension buffer (20 mM Tris-HCl (pH 7.4), 100 mM NaCl, 5 % glycerol, and 2 mM MgCl<sub>2</sub>). The supernatant was then brought to 75 % ammonium sulfate and stored at 4 °C for 30 minutes. Precipitated material was spun down at 7,000 rpm for 30-60 minutes and the pellet was resuspended in a total of 20-30 ml of resuspension buffer. The resuspended proteins were dialyzed against 4 liter of buffer containing 20 mM Tris-HCl (pH 7.4), 5 % glycerol, and 2 mM MgCl<sub>2</sub> at 4 °C for approximately 16 hours. The proteins were mixed with 10 ml of the equilibrated Ni-NTA agarose resin (Qiagen) by inverting at 4 °C for 3-5 hours, and the resin was pelleted by centrifuging at 4,000 rpm for 5 minutes. The resin was washed with 50 ml of 20 mM Tris-HCl (pH 7.4) and pelleted at 4,000 rpm for 5 minutes. The protein was eluted in 10 ml of elution buffer (150 mM imidazole, 20 mM Tris-HCl (pH 7.0), 150 mM NaCl, 5 % glycerol, and 2 mM MgCl<sub>2</sub>) at 4 °C for 1 hour and dialyzed overnight against 1 liter of buffer containing 20 mM Tris-HCl (pH 8.5), 5 % glycerol, and 2 mM MgCl<sub>2</sub>. The protein was loaded onto an anion exchange column (Poros HQ resin, GE Healthcare) and eluted with a linear salt gradient from 0 to 1 M NaCl. The protein was further purified by passing it over a Superdex 200 column (GE Healthcare) using buffer containing 20 mM Tris-HCl (pH 7.0), 150 mM NaCl, 5 % glycerol, and 2 mM MgCl<sub>2</sub>. The protein was concentrated in a Centricon-50 (Amicon) to 7-10 mg/ml and stored at 4 °C for crystallization (Figure 2.4).

### **Enzyme activity assay for hNEP**

Enzyme activity was determined with a coupled assay (Li and Hersh, 1995) by monitoring the cleavage of a fluorogenic substrate at  $\lambda_{\text{ex}} = 340 \text{ nm}$  and  $\lambda_{\text{em}} = 425 \text{ nm}$  in a 96-well ELISA fluorescence plate reader (SpectraMAX Genomics, Molecular Devices). Reactions were performed with 50  $\mu\text{M}$  of glutaryl-Ala-Ala-Phe-4-4-methoxy-2-naphthylamide, 1-10  $\mu\text{l}$  of secreted or purified hNEP proteins, 1  $\mu\text{g}$  of puromycin sensitive aminopeptidase (PSA), and 20 mM MES (pH 6.5) in the 200  $\mu\text{l}$  of total volume. The substrate is first hydrolyzed by hNEP to Phe-4-4-methoxy-2-naphthylamide which is converted to the fluorescent 4-methoxy-2-naphthylamide by PSA.

### **Preparation of human choline acetyltransferase (hChAT) constructs**

The full length gene of ChAT (hChAT) in a pCRT7 vector was obtained from the laboratory of Dr. Louis Hersh at the University of Kentucky (Kong *et al.*, 1989) and inserted into a pTrcHis2A vector (Invitrogen) by PCR. The reaction was performed with 5  $\mu\text{l}$  of 5 $\times$  reaction buffer, 1  $\mu\text{l}$  of 100 ng/ $\mu\text{l}$  of double strand DNA template, 1  $\mu\text{l}$  of 100 pmol/ $\mu\text{l}$  of forward primer, 1  $\mu\text{l}$  of 100 pmol/ $\mu\text{l}$  of reverse primer, 1  $\mu\text{l}$  of 100 mM dNTP mixture, 1  $\mu\text{l}$  of *Pfutura* DNA polymerase (2.5 U/ $\mu\text{l}$ ), and 40  $\mu\text{l}$  of H<sub>2</sub>O to a final volume of 50  $\mu\text{l}$ . Each was cycled according to the parameters: 1 cycle at 95 °C for 45 seconds and 35 cycles at 95 °C for 30 seconds, 53 °C for 1 minute, and 72 °C for 2 minutes (Eppendorf personal master cycler). A stop codon was added to the 3' end of the gene to prevent expression of a C-terminal hexahistidine sequence present in the vector (Table 2.3). Both the full length hChAT and a truncated construct were expressed. The truncated hChAT lacked the N-terminal 10 residues and the C-terminal 23 residues, which are disordered in the crystal structure of the rat enzyme and therefore might inhibit crystallization. The constructs were transformed into *Escherichia coli* TOP cells by electroporation and the sequences of full length and truncated hChAT inserts were confirmed by sequencing (Davis sequencing, [www.davissequencing.com](http://www.davissequencing.com)).

## Expression and purification of hChAT

Constructs of hChAT were expressed in *Escherichia coli* BL21(DE3)RP cells (Stratagene). Cells containing the hChAT constructs were cultured overnight at 37°C in Luria Bertani (LB) media containing 50 mg/ml ampicillin and 34 mg/ml chloramphenicol. 300 ml of overnight culture were used to inoculate 7 L of LB media containing 7 ml of antifoam, 50 mg/ml ampicillin, and 34 mg/ml chloramphenicol. The cells were cultured at 37°C until the  $A_{600}$  of the culture had reached 0.7-0.9. Isopropyl- $\beta$ -D-thiogalactopyranoside (IPTG) was added to a final concentration of 1 mM to induce overexpression of the protein, and the cells were grown at 16°C for an additional 5 hours. Cells were centrifuged at 8,000 rpm for 10 minutes and the pellets stored at -20°C.

Cell pellets were resuspended in cold lysis buffer (3 ml per gram of cells) containing 20 mM Tris-HCl (pH 8.0), 5% Glycerol, 5 mM 2-mercaptoethanol, 100 mM NaCl, and protease inhibitor cocktail III (100  $\mu$ l/1L of culture). Cells were lysed by twice passing them through a French press, and the insoluble material was removed by centrifugation at 23,000 rpm for 60 minutes at 4°C. The crude lysate was mixed with 50% Ni-NTA agarose resin (Qiagen) that had been equilibrated with 20 mM Tris-HCl (pH 8.0), 5% Glycerol, 5 mM 2-mercaptoethanol on a shaker for 2-3 hours at 4°C. The resin was washed with 40 ml cold wash buffer (20 mM Tris-HCl (pH 8.0), 5% Glycerol, 5 mM 2-mercaptoethanol, and 500 mM NaCl) on a shaker for 20 minutes and centrifuged at 4,000 rpm for 5 minutes at 4 °C. The resin was washed with cold buffer containing 1 M NaCl and then again with cold buffer containing 1.5 M NaCl. The protein was eluted with 10 ml of elution buffer (150 mM imidazole, 20 mM Tris-HCl (pH 8.0), 5% Glycerol, 5 mM 2-mercaptoethanol, and 500 mM NaCl) on a shaker for 30 minutes.

The hChAT protein was dialyzed against 1 liter of buffer containing 20 mM MES (pH 6.0), 10 mM NaCl, 5 % glycerol and 5 mM 2-mercaptoethanol overnight at 4°C prior to loading onto a cation exchange column (HS resin, GE Healthcare). The protein was eluted with a salt gradient (0 M to 1 M). The eluted hChAT protein was loaded into a Superdex200 column (GE Healthcare) using buffer containing Tris-HCl (pH 7.4) and 50 mM NaCl. The eluted protein was



pooled and dialyzed against 1 liter of buffer containing 20 mM Tris-HCl (pH 8.0), 20 mM NaCl, 5 % glycerol and 5 mM 2-mercaptoethanol overnight at 4°C and concentrated to 5-10 mg/ml in a Centricon-50 (Amicon). The concentrated protein was stored at 4°C for crystallization trials and assays (Figure 2.5A).

### **Assay for hChAT activity**

The activity of hChAT samples was determined by monitoring the reverse ChAT reaction in which an acetyl group is transferred from acetylcholine to CoA (Hersh *et al.*, 1978; Wu *et al.*, 1995; Wu and Hersh, 1995). The reaction is coupled to the production of NADH, which was monitored  $\lambda_{em} = 450$  nm and  $\lambda_{ex} = 340$  nm in an Optical Technologies fluorometer, by the sequential action of citrate synthase and malate dehydrogenase. The assay was performed in a buffer containing 10 mM potassium phosphate (pH 7.4), 250 mM NaCl, 0.125 mM NAD<sup>+</sup>, 0.5 mM L-malate, 0.1 mM DL-dithiothreitol, 25 mM acetylcholine chloride, 0.1 mM CoA, 1.5 U of pig heart citrate synthase (Sigma), and 4 U of pig heart malate dehydrogenase (Sigma). The reaction was initiated by the addition of acetylcholine chloride (Sigma).

### **Crystallization of hChAT**

Full length and truncated hChAT was crystallized by hanging drop vapor diffusion at 4°C. The crystals were grown by mixing 1  $\mu$ l of 10-15 mg/ml protein with 1  $\mu$ l of well solution containing 100 mM Tris-HCl (pH 8.5), 200 mM magnesium chloride, and 2-3 M 1, 6-hexanediol. Crystals typically grew to 0.15 x 0.3 x 0.01 mm (Figure 2.5B). For data collection, crystals were transferred briefly (a few seconds) into a solution containing 25 % glycerol, 100 mM Tris-HCl (pH 8.5), 200 mM magnesium chloride, and 2-3 M 1, 6-hexanediol, mounted in a nylon loop, and plunged in liquid nitrogen (Rodgers, 1997).

**Table 2. 1: Sequences of primers for TOP mutagenesis**

Primers	Sequences
TOP 4 mutant H495N F†	5'-GCCATGTTTCAGCGGGACCAACGTGGAGCGGGACTTTGTG-3'
TOP 4 mutant H495N R‡	5'-CACAAAGTCCCGCTCCACGTTGGTCCCGCTGAACATGGC-3'
TOP 4 mutant R498T F	5'-GCGGGACCAACGTGGAGACGGACTTTGTGGAGGCGCC-3'
TOP 4 mutant R498T R	5'-GGCGCCTCCACAAAGTCCGTCTCCACGTTGGTCCCGC-3'
TOP 4 mutant M490R F	5'-CCCAGGCGGAGTTCGCCAGGTTTCAGCGGGACCAACGTG-3'
TOP 4 mutant M490R R	5'-CACGTTGGTCCCGCTGAACCTGGCGAACTCCGCCTGGG-3'
TOP 4 mutant E469R F	5'-CTGCAGCATGACGAGGTGCGGACCTACTTCCATGAGTTTG-3'
TOP 4 mutant E469R R	5'-CAAACCTCATGGAAGTAGGTCCGCACCTCGTCATGCTGCAG-3'
TOP 3 mutant N495H F	5'-CAGGTTTCAGCGGGACCCACGTGGAGACGGACTTTG-3'
TOP 3 mutant N495H R	5'-CAAAGTCCGTCTCCACGTGGGTCCCGCTGAACCTG-3'
TOP 3 mutant T498R F	5'-GGGACCAACGTGGAGCGGGACTTTGTGGAGGCG-3'
TOP 3 mutant T498R R	5'-CGCCTCCACAAAGTCCCGCTCCACGTTGGTCCC-3'
TOP 2 mutant R498T F	5'-GGGACCCACGTGGAGACGGACTTTGTGGAGGCG-3'
TOP 2 mutant R498T R	5'-CGCCTCCACAAAGTCCGTCTCCACGTGGGTCCC-3'

† Forward

‡ Reverse

**Table 2. 2: Sequences of mutation primers for neurolysin mutagenesis**

Primers	Sequences
Neurolysin 4 mutant N496H F†	5'-CGATTCAGTGGAACACACGTGGAAACTGACTTTG-3'
Neurolysin 4 mutant N496H R‡	5'-CAAAGTCAGTTTCCACGTGTGTTCCACTGAATCG-3'
Neurolysin 4 mutant T499R F	5'-CAGTGGAACACACGTGGAAAGAGACTTTGTAGAGGTGCCATC-3'
Neurolysin 4 mutant T499R R	5'-GATGGCACCTCTACAAAGTCTCTTTCCACGTGTGTTCCACTG-3'
Neurolysin 4 mutant R491M F	5'-CTGTGCGCAGACTGACTTTGCAATGTTTCAGTGGAACACACGTGGAAAG-3'
Neurolysin 4 mutant R491M R	5'-CTTCCACGTGTGTTCCACTGAACATTGCAAAGTCAGTCTGCGCACAG-3'
Neurolysin 4 mutant R470E F	5'-CTGAGACATGATGAAGTGGAGACTTACTTCCACGAGTTC-3'
Neurolysin 4 mutant R470E R	5'-GAACTCGTGGAAGTAAGTCTCCACTTCATCATGTCTCAG-3'
Neurolysin 3 mutant H496N F	5'-CAATGTTTCAGTGGAACAAACGTGGAAAGAGACTTTG-3'
Neurolysin 3 mutant H496N R	5'-CAAAGTCTCTTTCCACGTTTGTTCCTGAACATTG-3'
Neurolysin 3 mutant R499T F	5'-GGAACACACGTGGAAACTGACTTTGTAGAGGTG-3'
Neurolysin 3 mutant R499T R	5'-CACCTCTACAAAGTCAGTTTCCACGTGTGTTCC-3'
Neurolysin 2 mutant T499R F	5'-GGAACAAACGTGGAAAGAGACTTTGTAGAGGTG-3'
Neurolysin 2 mutant T499R R	5'-CACCTCTACAAAGTCTCTTTCCACGTTTGTTC-3'

† Forward

‡ Reverse

**Table 2. 3: Sequences of primers for human choline acetyltransferase cloning**

<b>Primers</b>	<b>Sequences</b>
Full length ChAT BamH F†	5'- CGGGATCCAGCAGCAAAAACCTCCCAGCAG-3'
Full length ChAT EcoR R‡	5'- GGAATTCTTATCAAGGTTGGTGTCCTGGCTGG-3'
Truncated ChAT BamH F	5'- CGGGATCCACTGCCCAAACCTGCCCGTGCC-3'
Truncated ChAT EcoR R	5'- GGAATTCTTATCACAGCAGACTGCAGAGGTCTCTC-3'

† Forward

‡ Reverse

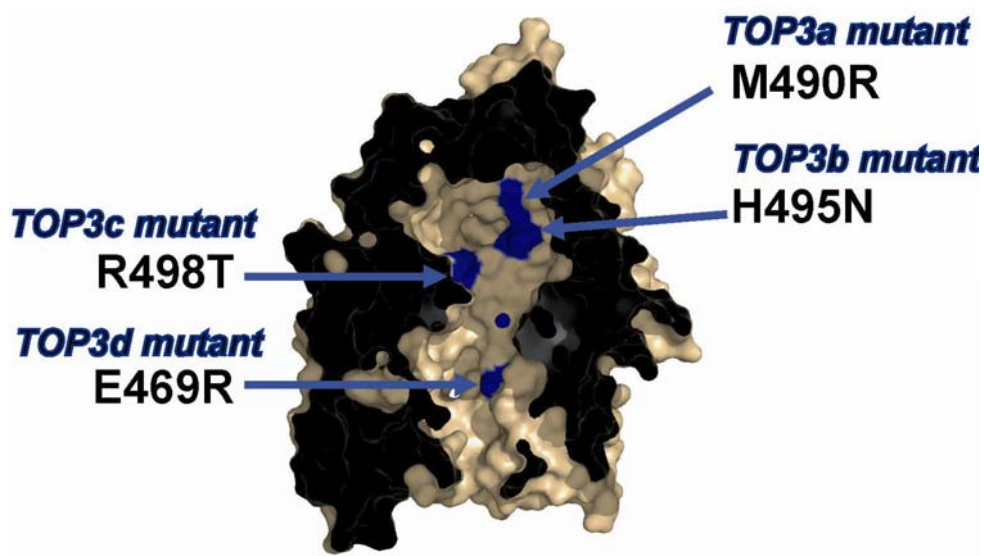


**Figure 2. 1. Overview of mutation positions in the TOP 3 mutants.** Blue labels indicate the residues that retained the wild type sequence in each of the TOP 3 mutants. The zinc ion cofactor is indicated by the blue sphere.

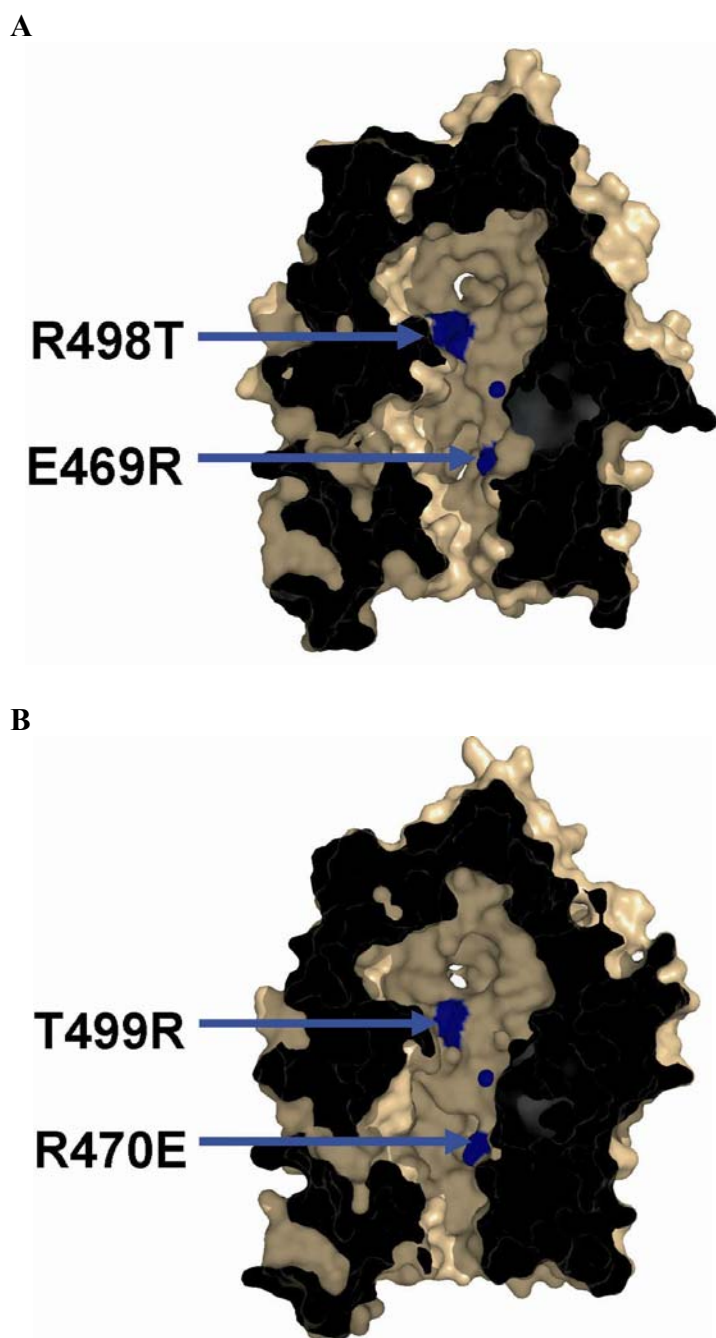


**Figure 2. 2. Overview of mutation positions in the TOP 2 mutant and neurolysin 2 mutant.** The mutation positions of TOP 2 mutant (**A**) and neurolysin 2 mutant (**B**). The substituted residues of TOP 2 mutant and neurolysin 2 mutant are indicated.

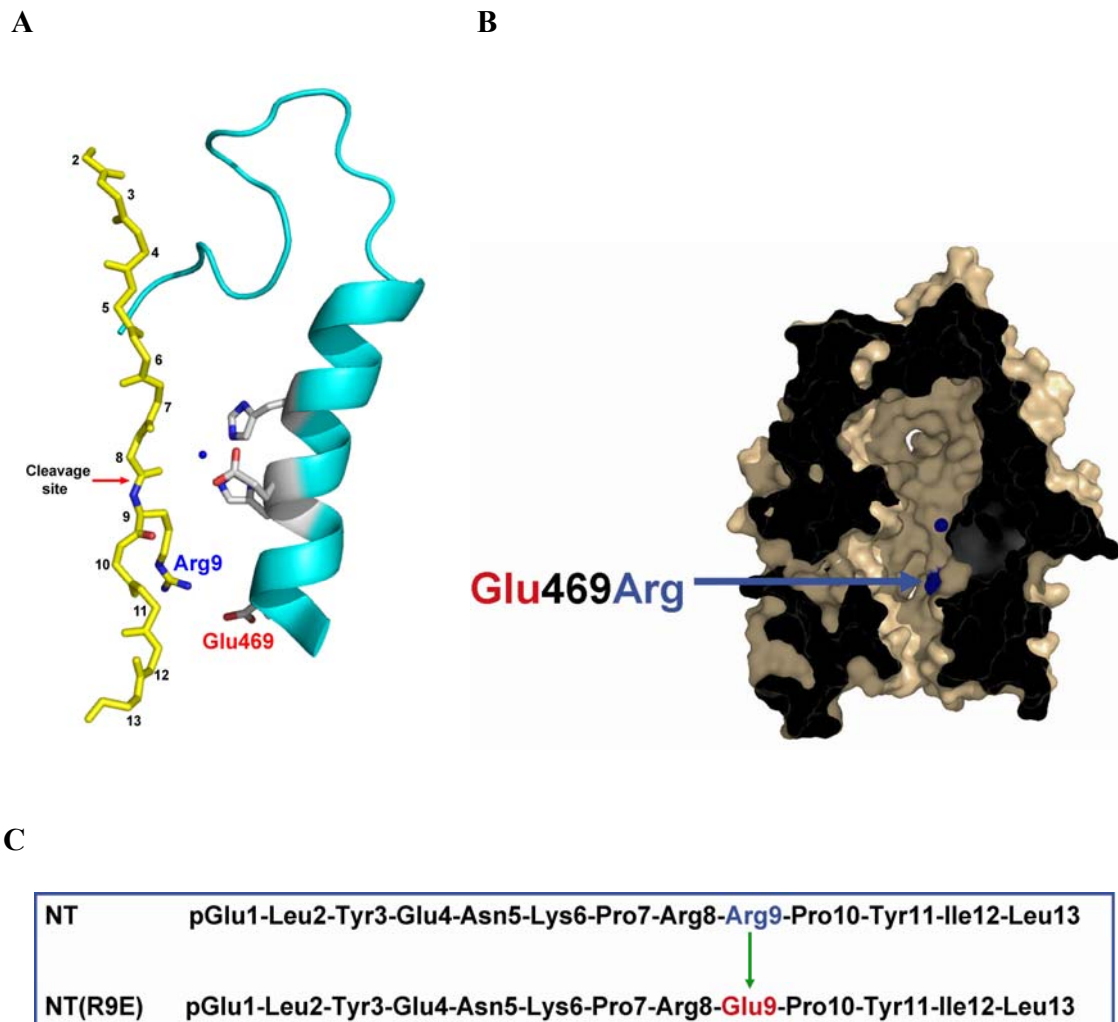


**Figure 2. 3. Residue swap to test a direct interaction between Glu469 of TOP and Arg9 of NT.** **A**, Salt interaction between Glu469 of TOP and Arg9 of NT in the model for NT binding to TOP. TOP (residues 468-498) is indicated by cyan and yellow represents NT. **B**, Site mutated in TOP to swap arginine for the wild type glutamate. **C**, Sequence change in NT for the swap experiment. The arginine of NT is replaced by glutamate giving the NT(R9E) peptide.

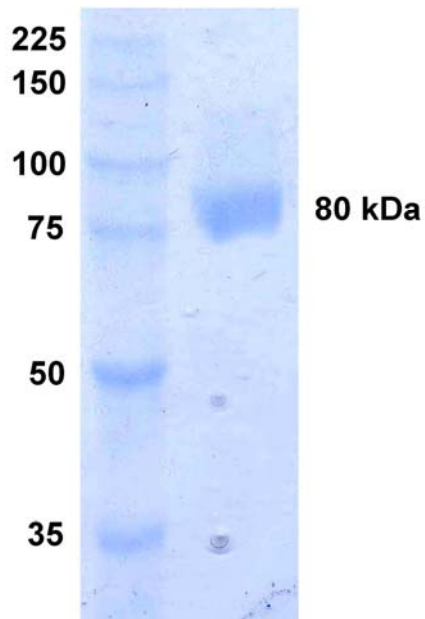


**Figure 2. 4. Overexpression of hNEP 3 mutant in *Pichia pastoris* yeast cells.** Coomassie stained SDS polyacrylamide gel showing purified recombinant hNEP. Molecular weight markers are in the left lane and hNEP is in the right lane. The molecular weight of hNEP 3 mutant is about 80 kDa.



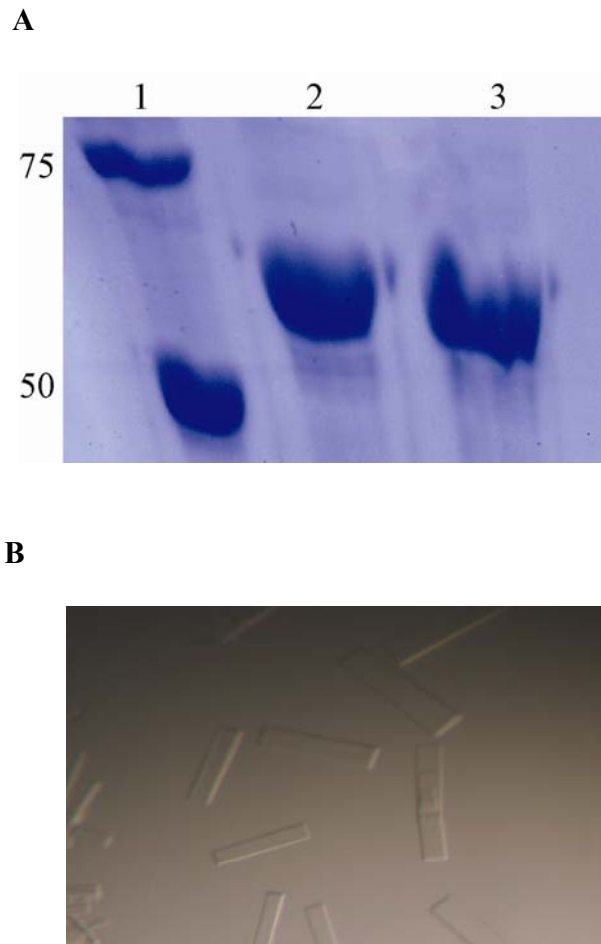


**Figure 2. 5. Overexpression and crystals of hChAT.** **A**, Coomassie stained SDS polyacrylamide gel. Molecular weight markers are in lane 1, purified full length hChAT in lane 2 and truncated hChAT in lane 3. **B**, Crystals of hChAT. The longest dimension of the crystals is approximately 0.2 mm.

### **Chapter 3: Reengineering of substrate specificity in thimet oligopeptidase (TOP) and neurolysin**

TOP and neurolysin are closely related neuropeptidases that hydrolyze most peptides at same cleavage site (Rioli *et al.*, 1998) (Figure 1.2A). One exception is the 13 residue peptide NT. TOP cleaves NT between Arg8 and Arg9 while neurolysin hydrolyzes the peptide between Pro10 and Tyr11 (Mentlein and Dahms, 1994) (Figure 1.2A). Very few of the 224 sequence differences between the two enzymes are located in the substrate binding channel (Ray *et al.*, 2002). On the basis of modeling studies, it was determined that four changes (E469/R470, M490/R491, H495/N496, and R498/T499, the TOP residues listed first) are likely to cause differences in substrate specificity (Figure 1.5). We have substituted these four residues in TOP and neurolysin with the corresponding ones the other enzyme in order to test the role of these residues in mediating differential substrate specificity.

One of the identified sequences changes, Glu469 in TOP to Arg470 in neurolysin, is responsible for a strong difference in surface electrostatic potential at one end of the substrate binding channel floor (Ray *et al.*, 2004). In previous studies, it was suggested that the Arg9 of NT may make a salt bridge with the Glu469 of TOP (Figure 2.3A), and that this interaction may help determine the difference in cleavage site compared with neurolysin. In order to determine whether a direct interaction between TOP and NT may be involved in differential substrate specificity, I swapped the two residues, placing the enzyme residue in the peptide and the peptide residue in the enzyme (Figure 2.3B and C). If there is a direct interaction, it should still be made when the altered peptide binds to the altered enzyme. If Glu469 plays another role, however, this swap will likely alter the substrate interaction. Arg9 of NT was replaced to Glu9, resulting in a peptide named NT(R9E) (Figure 2.3C), and TOP was substituted at Glu469 with an arginine (Figure 2.3B). The preferred cleavage site of this altered substrate and enzyme was then determined to see if the position was maintained relative to the corresponding wild type molecules.

### **Cleavage pattern of NT by TOP 4 and neurolysin 4 mutants**

To determine if substituting all four residues can convert the TOP cleavage site on NT to that of neurolysin, the cleavage site was determined using reverse phase HPLC separation of cleavage products and subsequent identification by mass spectrometry. Wild type TOP hydrolyzed NT between Arg8 and Arg9, producing NT1-8 and NT9-13 fragments (Figure 3.1C and E), while wild type neurolysin cleaved the peptide between Pro10 and Tyr11, producing NT1-10 and NT11-13 fragments (Figure 3.1A and E). These are the products expected based on the literature (Mentlein and Dahms, 1994). NT1-8 and NT1-10 fragments were separated well with specific retention times, but NT9-13 and NT11-13 fragments had similar retention times when using the C18 column. The molecular masses of NT fragments and full length of NT were determined by ESI-TOF to confirm the cleavage sites on NT by both enzymes. The masses of NT1-8 and NT9-13 fragments were  $1030 \pm 0.37$  and  $661 \pm 0.59$  Daltons, respectively, while those of NT1-10 and NT11-13 fragments were  $1283 \pm 0.21$  and  $408 \pm 0.73$  Daltons, respectively (Table 3.1). These values compare well with the calculated molecular masses of the expected NT fragments.

Like wild type neurolysin, products produced by the TOP 4 mutant (E469R, M490R, H495N, and R498T) showed the same retention times as those of NT1-10 and NT11-13 fragments produced by wild type neurolysin (Figure 3.1B and E). The masses of NT1-10 and NT11-13 fragments were  $1283 \pm 0.21$  and  $408 \pm 0.74$  Daltons, respectively (Table 3.1), same as those of wild type neurolysin. These results suggest that substitution of four residues in TOP can convert the TOP cleavage site on NT to that of neurolysin. In the opposite experiment, substitution of the corresponding four residues in neurolysin (R470E, R491M, N496H, and T499R) produced a similar exchange of cleavage sites. The neurolysin 4 mutant also showed the same retention times as those of NT1-8 and NT8-13 fragments produced by wild type TOP (Figure 3.1D and E), suggesting that neurolysin 4 mutant cleaved NT at the same cleavage site as wild type TOP. It is clear, then that these four residues or a subset of the four are responsible for the observed differences in NT cleavage site selection between TOP and neurolysin.

### **Cleavage pattern of NT by TOP 3 mutants**

In order to determine if all four changes are needed to swap cleavage sites, I examined a series of TOP mutants each carrying only three of the four mutations tested previously. Each of the four mutants retained the wild type amino acid at a different one of the four residue positions. The TOP 3a and 3b mutants, which retain the wild type residues Met490 and His495 (Figure 2.1), respectively, both produced peptide products of NT hydrolysis consistent with cleavage at the neurolysin site (Figure 3.2A, B, and C; Table 3.2). In contrast, the TOP 3c and 3d mutants, which retain the wild type residues Glu469 and Arg498 respectively (Figure 2.1), each cleaved NT at both the TOP and neurolysin sites, suggesting a mixed specificity (Figure 3.2A, D, E, and F; Table 3.2). These results, taken together, suggest that both the E469R and the R498T mutations are required for swapping the cleavage site position. The M490R and H495N mutations have no effect on differential specificity.

### **Cleavage pattern of NT by TOP 2 and neurolysin 2 mutants**

In order to further test the possibility that just the two mutations are sufficient to swap specificity, I made constructs of TOP and neurolysin that were mutated at only those two positions (Figure 2.2A and B). The TOP 2 mutant (E469R and R498T) and neurolysin two mutant (R470E and T499R) were produced and used in cleavage site assays. As expected, TOP 2 mutant hydrolyzed NT at the wild type neurolysin site (Pro10-Tyr11) (Figure 3.3A and B) and the neurolysin 2 mutant hydrolyzed the NT at the wild type TOP site (Arg8-Arg9) (Figure 3.3C and D). These studies therefore show that only two residue positions are responsible for differences in NT cleavage between TOP and neurolysin.

## **Comparison of kinetic parameters for wild type TOP and neurolysin with the two mutant constructs**

Results described so far demonstrate that it is possible to swap the cleavage sites on NT of TOP and neurolysin by mutating two residue positions. In order to determine if these mutations not only swap cleavage sites but also reproduce the kinetic parameters of the enzyme being mimicked, I determined the steady state kinetic parameters for the wild type and mutant constructs. These studies were carried out using a fluorogenic version of NT, in which cleavage can be monitored by the increase in fluorescence resulting from separating the N-terminal fluorescent and C-terminal quenching groups. The neurolysin 2 mutant has similar  $k_{cat}$  and  $K_m$  values to those of wild type TOP (Figure 3.4A and D; Table 3.3). The TOP 2 mutant also has a similar  $k_{cat}$  to that of wild type neurolysin, but the  $K_m$  of TOP 2 mutant is significantly higher than that of wild type neurolysin (Figure 3.4B and C; Table 3.3). Energetically, however, the effect on  $K_m$  is small, and overall the mutants show similar kinetics to the wild type enzyme being mimicked.

## **Cleavage pattern of NT(R9E) by TOP E469R mutant**

In the published model of NT binding to TOP, it was suggested that the Glu469 of TOP may form a salt bridge with the Arg9 of NT (Figure 2.1A) (Ray *et al.*, 2004). If such a direct interaction occurs, it seems likely that the interacting residues could be swapped between peptide and enzyme without affecting the salt bridge contact. Therefore, Arg9 of NT was changed to Glu9 to produce a peptide named NT(R9E) (Figure 2.3C), and TOP Glu469 was replaced with an arginine (Figure 2.3B). Cleavage site analysis was performed with the altered peptide and enzyme. Analysis of NT(R9E) cleavage by wild type TOP and neurolysin was also done for comparison.

Wild type TOP cleaved NT(R9E) at two positions that correspond to the TOP and neurolysin cleavage sites on NT (positions 8-9 and 10-11) (Figure 3.5B and E; Table 3.4). The probability of cleavage at the Pro10-Tyr11 site may have been slightly higher. On the basis of modeling studies and previous results, we expected that NT(R9E) would be cleaved by the TOP

E469R mutant at between Arg8 and Glu9, the wild type TOP cleavage site. But like the wild type enzyme, TOP E469R cleaved NT(R9E) at two sites, between Arg8 and Glu9 and between Pro10 and Tyr11 (Figure 3.5C and E; Table 3.4). This result suggests that Glu469 does not simply make a salt bridge with Arg9.

Somewhat unexpectedly, wild type neurolysin cleaved the NT(R9E) peptide exclusively between Arg8 and Glu9, the site equivalent to the TOP NT cleavage site (Figure 3.5D and E; Table 3.4). Since both wild type TOP and neurolysin show altered activity toward the modified peptide, it seems clear that Arg9 of NT does play some role recognition of NT by both enzymes.

**Table 3. 1: Molecular masses of NT fragments produced by wild type TOP, wild type neurolysin, and TOP 4 mutant**

Enzyme	Fragment masses				
	NT1-8 (expected mass)	NT1-10 (expected mass)	NT9-13 (expected mass)	NT11-13 (expected mass)	NT (expected mass)
Wild type TOP	1030.5306 (1030.16)	-	661.4042 (660.81)	-	1672 (1672.96)
Wild type Neurolysin	-	1283.6833 (1283.47)	-	408.2416 (407.51)	1672 (1672.96)
TOP 4 mutant	-	1283.6830 (1283.47)	-	408.2507 (407.51)	-

**Table 3. 2: Summary of mutation sites and NT hydrolysis by the TOP 3 mutants**

	<b>TOP 3a mutant</b>	<b>TOP 3b mutant</b>	<b>TOP 3c mutant</b>	<b>TOP 3d mutant</b>
M490R	-	✓	✓	✓
H495N	✓	-	✓	✓
R498T	✓	✓	-	✓
E469R	✓	✓	✓	-
Cleavage pattern of NT	Neurolysin site ¶	Neurolysin site	Neurolysin and TOP sites§	Neurolysin and TOP sites

¶ Pro10 and Tyr11

§ Arg8 and Arg9, Pro10 and Tyr11

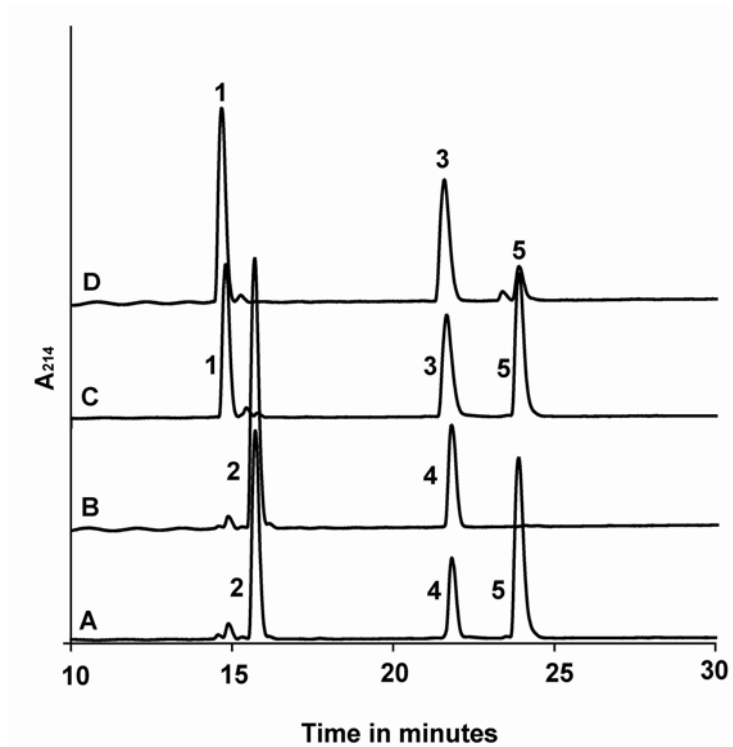


**Table 3. 3: Kinetics parameters for hydrolysis of fluorogenic NT by wild type TOP, TOP 2 mutant, wild type neurolysin, and neurolysin 2 mutant**

<b>Enzymes</b>	<b><math>k_{cat}</math> (sec<sup>-1</sup>)</b>	<b><math>K_m</math> (<math>\mu</math>M)</b>
Wild type TOP	$2.3 \pm 0.2$	$2.6 \pm 0.3$
Neurolysin 2 mutant	$2.79 \pm 0.42$	$2.95 \pm 0.45$
Wild type Neurolysin	$5.0 \pm 0.4$	$2.0 \pm 0.2$
TOP 2 mutant	$4.2 \pm 0.65$	$3.3 \pm 0.5$

**Table 3. 4: Molecular masses of NT(R9E) fragments and full length of NT(R9E) by TOP E469R mutant**

Enzyme	Fragment masses				
	NT(R9E) 1-8 (expected mass)	NT(R9E) 1-10 (expected mass)	NT(R9E) 9-13 (expected mass)	NT(R9E) 11-13 (expected mass)	NT(R9E) 1-13 (expected mass)
TOP E469R	1030.5311	1256.6256	408.2492	634.3452	1646
mutant	(1030.16)	(1256.4)	(407.51)	(633.74)	(1646.8)



**E**

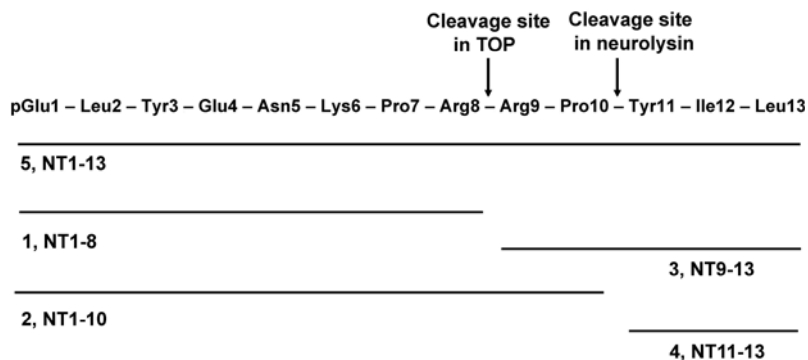


**Figure 3. 1. Cleavage of NT by the TOP 4 and neurolysin 4 mutants.** **A**, Reverse phase HPLC separation of cleavage products generated by wild type neurolysin. It hydrolyzes NT between Pro10 and Tyr11, producing a NT1-10 fragment (2) and a NT11-13 fragment (4). Full length NT is indicated by the number 5. **B**, Cleavage products generated by the TOP 4 mutant. It cleaves NT at the same cleavage site as wild type neurolysin. **C**, Cleavage products generated by wild type TOP. It cleaves NT between Arg8 and Arg9, producing the NT1-8 (1) and NT9-13 (3) fragments. **D**, Cleavage products generated by the neurolysin 4 mutant. NT is hydrolyzed by the neurolysin 4 mutant at the TOP cleavage site. The retention times of product peaks are normalized based on the migration of full length NT. **E**, Diagram indicating NT fragment sizes. NT1-8 and NT1-10 fragments are represented by numbers 1 and 2, respectively. Numbers 3, 4, and 5 indicate NT9-13, NT11-13, and NT1-13, respectively.

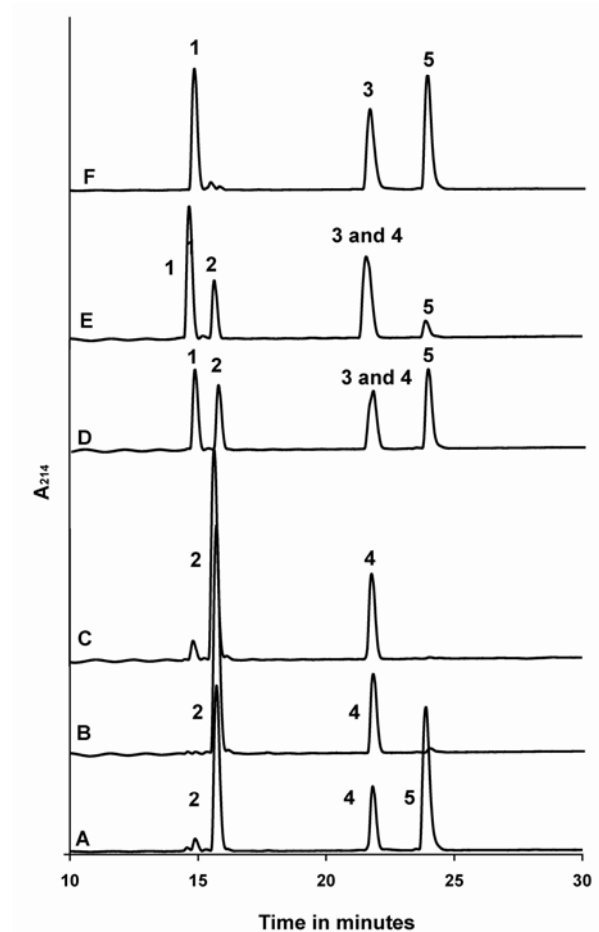


**Figure 3. 2. The cleavage pattern of NT by the TOP 3 mutants.** **A**, Cleavage pattern of NT by wild type neurolysin. It hydrolyzes the NT between Pro10 and Tyr11, producing NT1-10 fragment (2) and NT11-13 fragment (4). Number 5 indicates full length NT. **B and C**, Cleavage pattern of NT by the TOP 3a and 3b mutants. They cleave NT at the same cleavage site as wild type neurolysin. **D and E**, Cleavage pattern of NT by the TOP 3c and 3d mutants. NT is hydrolyzed by TOP 3c mutant and 3d mutant at both TOP cleavage site and neurolysin cleavage site. **F**, Cleavage fragments produced by wild type TOP. It cleaves the NT between Arg8 and Arg9, producing NT1-8 fragment (1) and NT9-13 fragment (3).

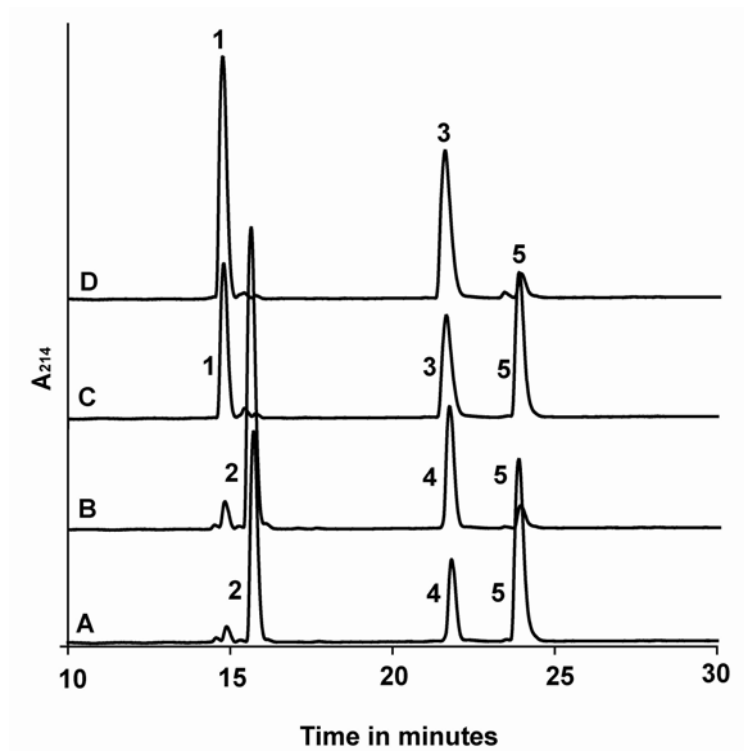


**Figure 3. 3. Cleavage of NT by the TOP 2 and neurolysin 2 mutants.** **A**, Reverse phase HPLC separation of products produced by wild type neurolysin. It hydrolyzes NT between Pro10 and Tyr11, producing the NT1-10 (2) and NT11-13 (4) fragments. Full length NT is indicated by the number 5. **B**, Cleavage products produced by the TOP 2 mutant. It hydrolyzes NT at the neurolysin cleavage site. **C**, Cleavage products produced by wild type TOP. Wild type TOP cleaves NT at between Arg8 and Arg9, producing the NT1-8 (1) and NT9-13 (3) fragments. **D**, Cleavage pattern of NT by the neurolysin 2 mutant. It hydrolyzes the peptide at the TOP cleavage site.

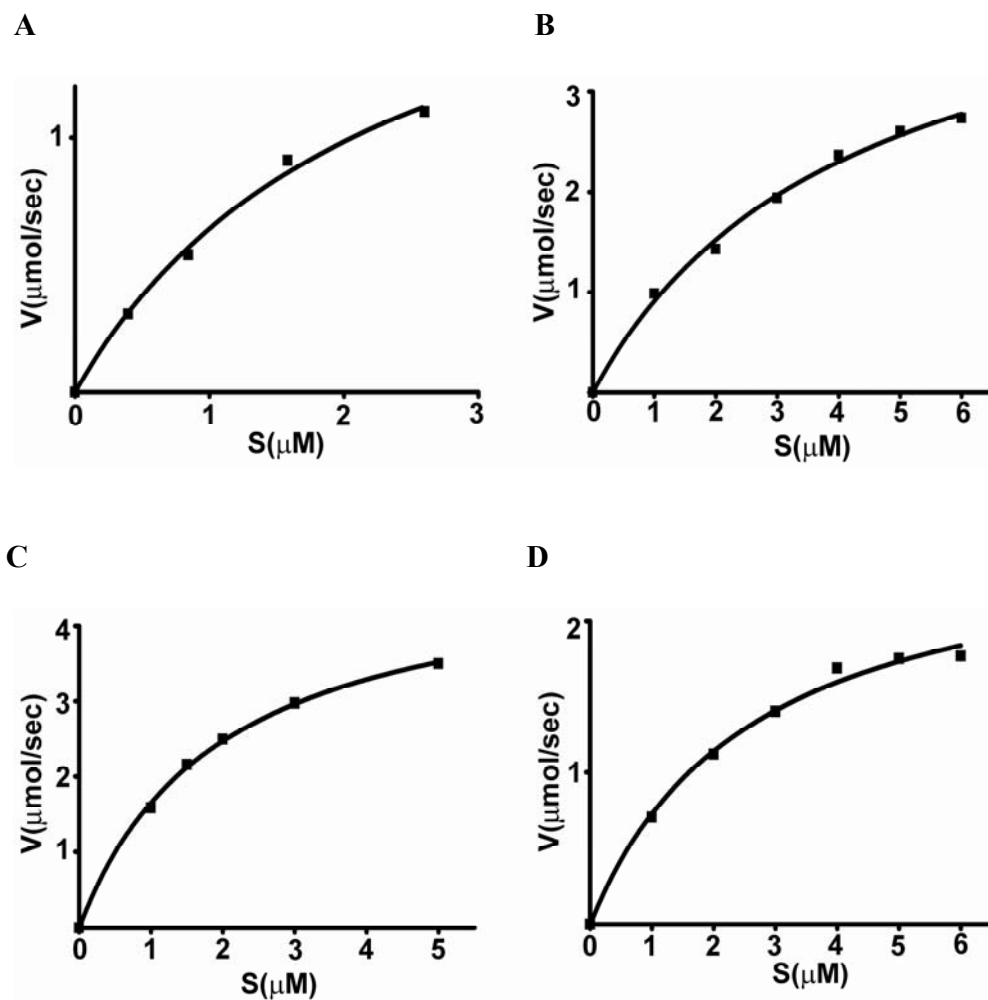
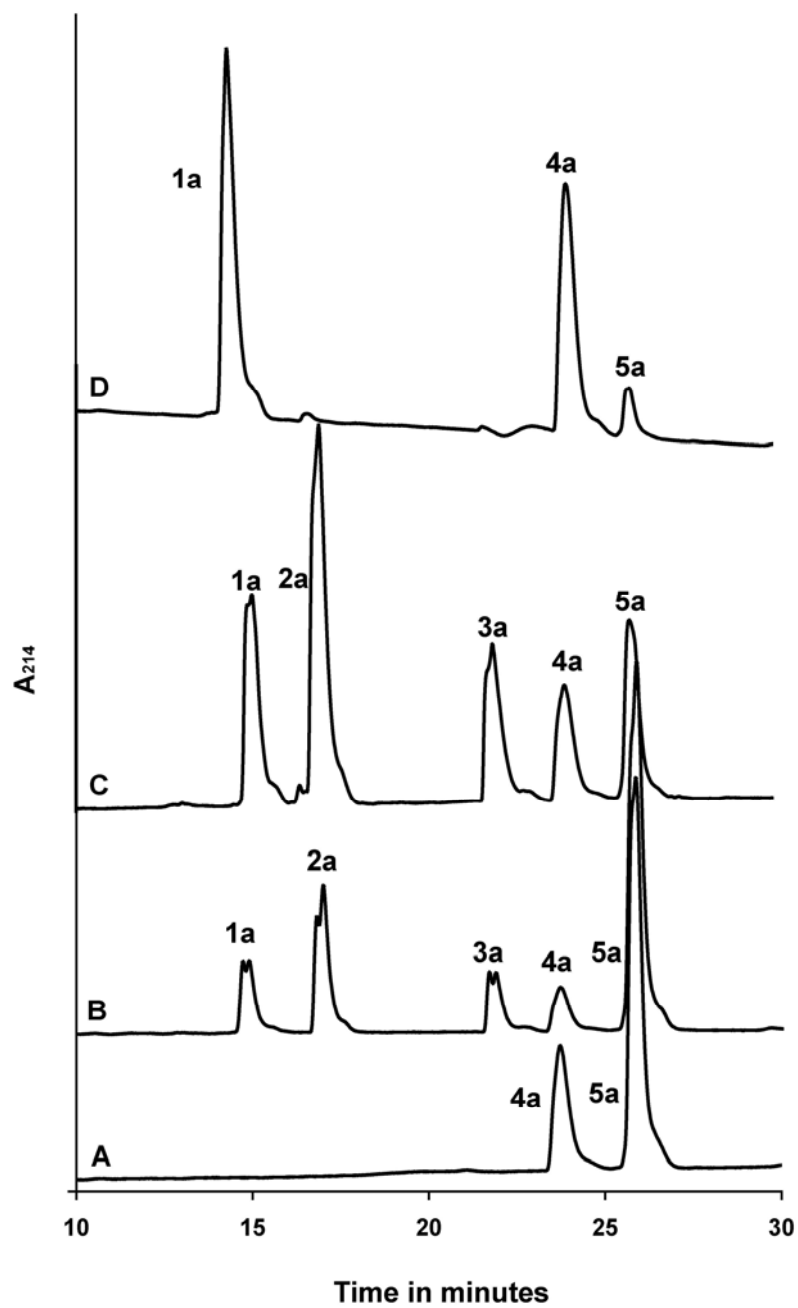


**Figure 3. 4. Kinetics of fluorogenic NT hydrolysis by TOP, TOP 2 mutant, wild type neurolysin and neurolysin 2 mutant.** Initial velocity versus substrate concentration plots for hydrolysis by: **A**, wild type TOP; **B**, the TOP 2 mutant; **C**, wild type neurolysin; and **D**, the neurolysin 2 mutant. Curves show the fit to the data using the equation  $V = V_{\text{max}} [S] / (K_m + [S])$  in Prism version 4 from GraphPad.



**E**

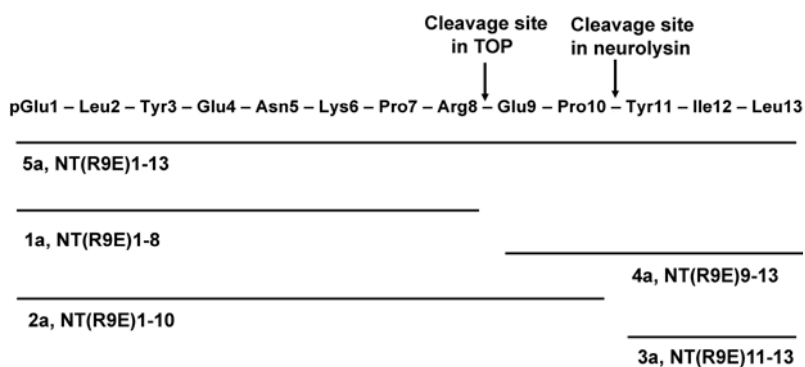


**Figure 3. 5. Cleavage of NT(R9E) by the TOP E469R mutant.** **A**, Reverse phase HPLC separation a synthetic NT(R9E) 9-13 fragment and full length of NT(R9E) to determine retention times of the peptides. **B**, Cleavage products produced by wild type TOP. **C**, Cleavage products produced by the TOP E469R mutant. **D**, Cleavage products produced by wild type neurolysin. **E**, Diagram showing the various cleavage products produced on hydrolysis of the NT(R9E) fragment.



## Chapter 4: Crystal structures of TOP 2 and neurolysin 2 mutants

### Introduction

The crystal structure of wild type neurolysin was determined by our group at 2.3 Å resolution (Brown *et al.*, 2001) (Figure 1.3B). The unit cell of the neurolysin crystals belongs to the P2<sub>1</sub>2<sub>1</sub>2 space group with dimensions of a=157.8 Å, b=88 Å, c=58.4 Å. The crystal structure revealed that neurolysin has a prolate ellipsoid shape with a high proportion (53 %) of α helix and only a small β sheet content (5.9 %). The molecule is divided by two distinct domains (I and II) by a deep narrow channel that runs its length, and the active site is located in domain I near the floor of the channel. In this position, the active site is accessible only to small, unstructured peptide substrates.

Our group also determined the crystal structure of human TOP at 2.0 Å resolution (Ray *et al.*, 2004) (Figure 1.3A). In order to crystallize TOP, the N terminal 15 residues were removed and two cysteine residues (Cys246 and Cys253) were mutated to serines to prevent covalent oligomerization of enzyme. The TOP structure is very similar to neurolysin, with an overall root mean square deviation on Cα positions of only 1.19 Å. Recently, another M3 family member, dipeptidyl carboxypeptidase (Comellas-Bigler *et al.*, 2005), has been shown to have a very similar structure to TOP and neurolysin.

Work of other groups has shown that the neurolysin/TOP fold is found in other families of metallopeptidases. Angiotensin-converting enzyme (ACE), a M2 family member targeted in antihypertensive therapy (Kim *et al.*, 2003; Natesh *et al.*, 2004), shares the fold as does the enzyme angiotensin converting enzyme related carboxypeptidase (ACE2), a member of the M2 family (Guy *et al.*, 2003; Towler *et al.*, 2004). Also, *Pyrococcus furiosus* carboxypeptidase (Arndt *et al.*, 2002) from the M32 family adopts the neurolysin/TOP fold.

## Crystal structures of the TOP 2 and neurolysin 2 mutants

The TOP 2 mutant and neurolysin 2 mutant proteins were crystallized under similar conditions to those used for wild type TOP and neurolysin, and the crystal structures were determined at 1.94 Å and 2.2 Å respectively by molecular replacement with the structures of the wild type enzymes (Figure 4.1 and 4.4). The structures have been fully refined. The crystal structure of TOP 2 mutant has 654 residues and 471 waters.  $R_{\text{work}}$  and  $R_{\text{free}}$  of TOP 2 mutant are 0.2022 and 0.2375, respectively. The neurolysin 2 mutant structure has 665 residues, 209 waters, and the values of  $R_{\text{work}}$  and  $R_{\text{free}}$  are 0.2189 and 0.2682, respectively (Table 4.1). Difference electron density maps show clearly the mutant side chains at positions Arg469/Glu470 and Thr498/Arg499 (Figure 4.2 and 4.5). In both enzymes, the side chains are well defined by phase improved  $F_o$  electron density.

Superimposing the wild type TOP structure on TOP 2 mutant demonstrates that the introduction of the two point mutations does not cause any change in either global or local backbone conformation (Figure 4.1). Similarly, no backbone changes in main chain conformation relative to the wild type enzyme are caused by introducing the two mutations in the neurolysin 2 mutant (Figure 4.4). The absence of any substantial conformational changes accompanying mutation indicates that the changes in specificity for NT cleavage sites are caused by the identities of the substituted side chains rather than any larger scale changes in structure.

In order to compare the conformations of side chains in the mutant enzymes with the wild type enzymes they are intended to mimic, the TOP wild type structure was superimposed on the neurolysin 2 mutant, and the neurolysin wild type structure was superimposed on the TOP 2 mutant. In the TOP 2 mutant, the side chain of introduced Arg469 had very similar conformations to the corresponding residues in wild type neurolysin (Figure 4.3A; Table 4.2). But, the side chain of Thr498 adopted a different Chi1 rotamer from Thr499 in wild type neurolysin (Figure 4.3B; Table 4.2). It seems likely that this difference in rotamer conformation is due to a structural difference in an adjacent loop segment between TOP and neurolysin (Figure 4.3C). The loops (residues 599-611 in TOP and residues 600-612 in neurolysin) differ in sequence in the two enzymes at a single position, Ala607 in TOP and Gly608 in neurolysin. In

neurolysin, the loop passes close to Thr499, and Tyr606 may be steric contact with the gamma methyl of that residue, influencing its conformation. In contrast, the loop in TOP 2 mutant, which has the same conformation found in wild type TOP, is shifted too far away from Thr498 to make any contacts. Instead, the side chain of Thr498 reorients, making hydrogen bond with Asn283 and Gln608.

For neurolysin 2 mutant, the comparison with the enzyme being mimicked follows the same pattern. The side chains of the substituted Glu470 in the neurolysin 2 mutant also showed similar conformations to Glu469 in wild type TOP (Figure 4.6A; Table 4.2). However, Arg499 adopted a different Chi2 rotamer from Arg498 in wild type TOP (Figure 4.6B; Table 4.2). Again, it seems likely that the differences at position 498/499 are due to differences in the adjacent loop segment (599-611/600-612) (Figure 4.6C; Table 4.2). In wild type TOP, the side chain of Arg498 is oriented toward the loop, and in fact makes a hydrogen bond contact with the main chain carbonyl oxygen at Gly604. This orientation of the arginine side chain would clash with the side chain of Tyr606 in the shifted loop of neurolysin 2 mutant, which adopts the same conformation as wild type neurolysin.

**Table 4. 1: Summary of crystallographic data and refinement for TOP 2 and neurolysin 2 mutants**

	TOP 2 mutant	Neurolysin 2 mutant
<b>Crystallographic data</b>		
Wavelength (Å)	0.9997	0.9997
Resolution (Å)	30-1.94	50-2.2
Last shell (Å)	2.01-1.94	2.28-2.2
Average redundancy (last shell) (%)	4.8 (4.4)	4.3 (4.2)
$R_{\text{sym}}^{\dagger}$ (last shell) (%)	0.075 (0.299)	0.088 (0.412)
$I/\sigma I$ (last shell) (%)	20.06 (4.68)	14.96 (3.98)
Completeness (last shell) (%)	98.2 (90.5)	98.7 (99.6)
<b>Refinement</b>		
Resolution (Å)	30-1.94	50-2.2
Number of reflections included in refinement	59,387	41,630
$R_{\text{work}}/R_{\text{free}}^{\ddagger}$	0.2022/0.2375	0.2189/0.2682
r.m.s.d.* bond lengths (Å)	0.004963	0.006470
r.m.s.d. bond angles (°)	1.11288	1.20223
r.m.s.d. improper angles (°)	0.73355	0.78865
r.m.s.d. dihedral angles (°)	19.43866	20.20443
B§ r.m.s.d. bonded atoms (main/side)	1.35/2.341	1.311/2.215
Average B for all protein atoms (Å <sup>2</sup> )	25.19	39.10
Average B for ordered solvent (Å <sup>2</sup> )	30.77	38.18
Number of solvent molecules	471	209
Number of metal ions	1	2

$$\dagger R_{\text{sym}} = \frac{\sum \sum_j |I_j - \langle I \rangle|}{\sum I_j}$$

$$\ddagger R_{\text{work,free}} = \frac{\sum \| |F_{\text{obs}}| - |F_{\text{calc}}| \|}{\sum |F_{\text{obs}}|}$$

for the reflections used in refinement (work) and the 10% of reflections held aside (free)

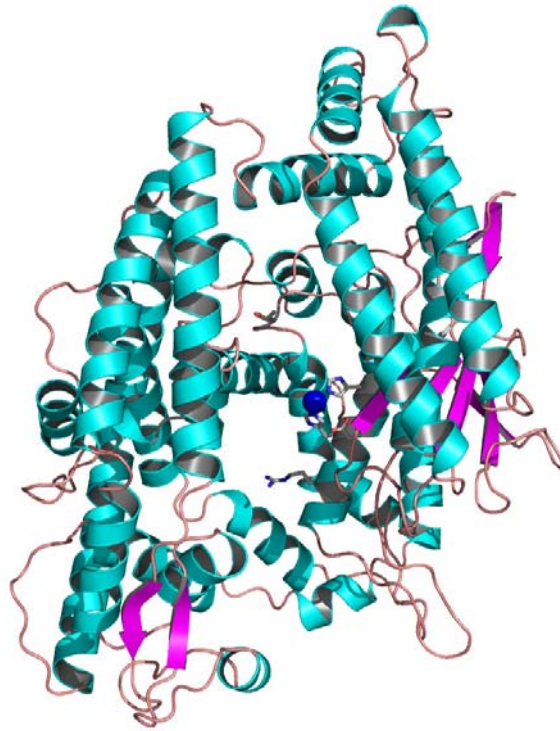
\* root mean square deviation

§ Isotropic thermal factor

**Table 4. 2: The main chain and side chain torsion angles (in degrees) for the wild type TOP , wild type neurolysin, TOP 2 mutant and neurolysin 2 mutant residues at the mutated positions**

	Main chain		Side chain			
	PSI	PHI	CHI1	CHI2	CHI3	CHI4
Wild type neurolysin (Arg470)	-33	-69	-173	157	60	77
TOP 2 mutant (Arg469)	-47	-62	-174	170	64	167
Wild type neurolysin (Thr499)	-38	-51	-55			
TOP 2 mutant (Thr498)	-30	-56	63			
Wild type TOP (Glu469)	-46	-63	-179	172	57	
Neurolysin 2 mutant (Glu470)	-41	-63	-174	175	58	
Wild type TOP (Arg498)	-29	-60	-81	-167	62	176
Neurolysin 2 mutant (Arg499)	-31	-59	-72	-52	82	179

A



B

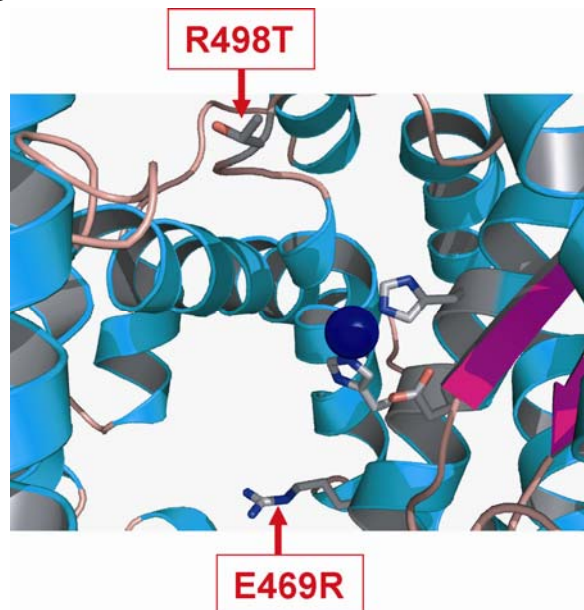
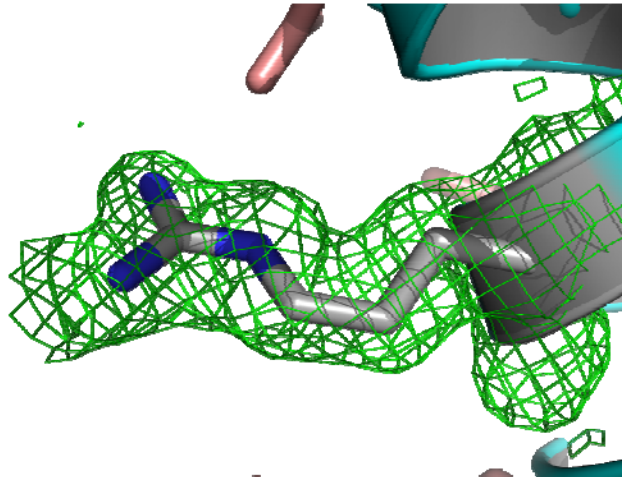


**Figure 4. 1. The TOP 2 mutant crystal structure.** A, Ribbons view of the structure. B, Active site and side chains at positions 469 and 498. Side chains are shown in a stick representation. Active site residue side chains are also shown. The zinc cofactor is shown as a blue sphere in both panels.

**A**



**B**

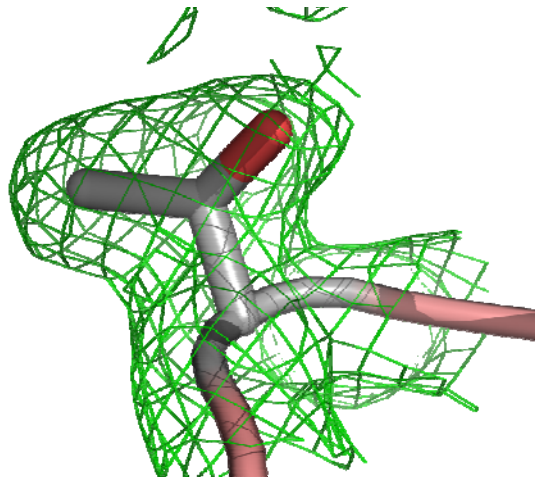


**Figure 4. 2. Electron density for side chains of Arg469 and Thr498 in the TOP 2 mutant crystal structure. A,** Electron density for Arg469. The 2Fo-Fc density is shown in a wireframe representation (green) along with a combined ribbons and stick representation of the protein. **B,** View as in panel A of Thr498 from the crystal structure. In both panels A and B, the electron density is shown with a cutoff contour of 1.0 times the r.m.s deviation of the maps.

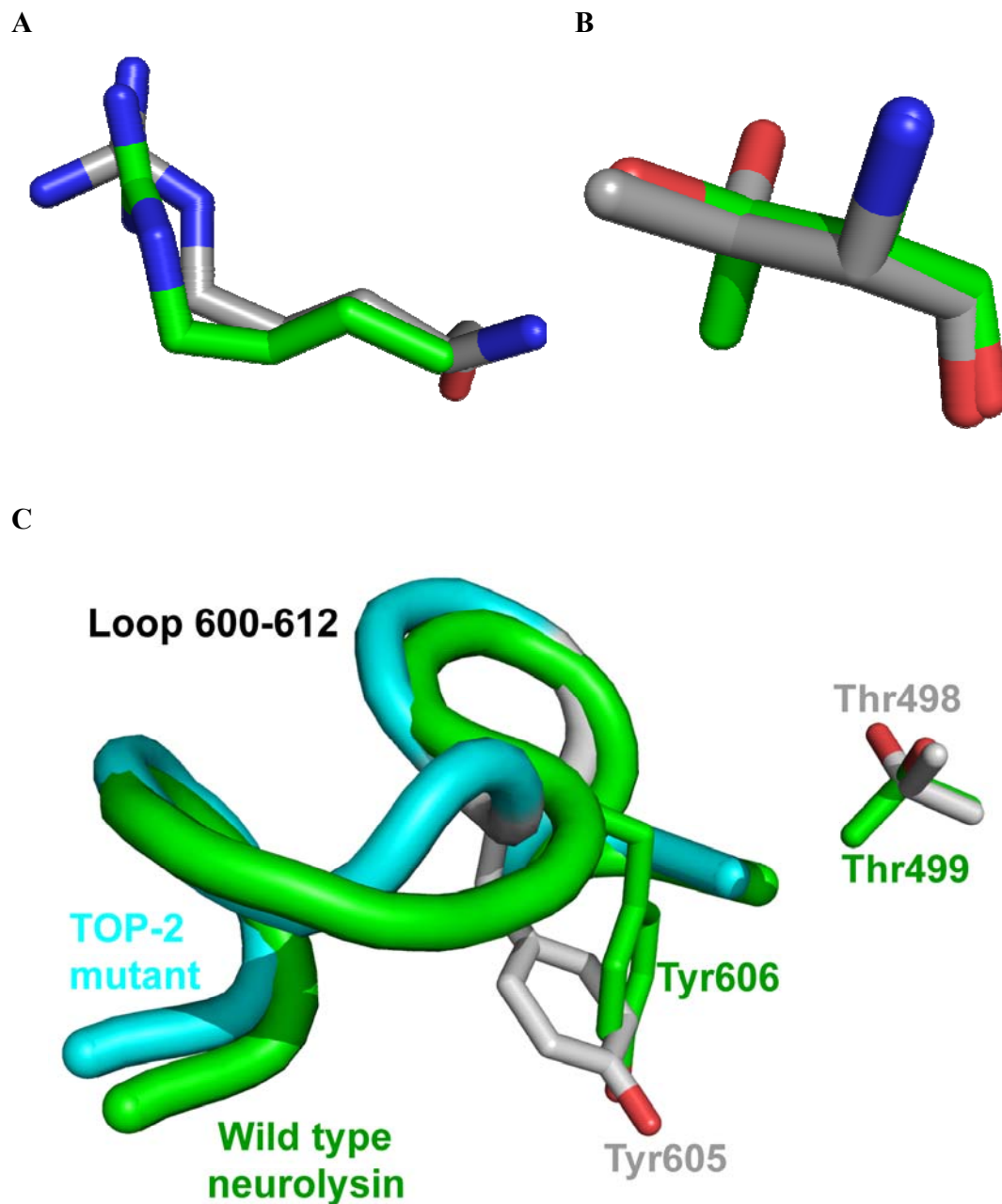
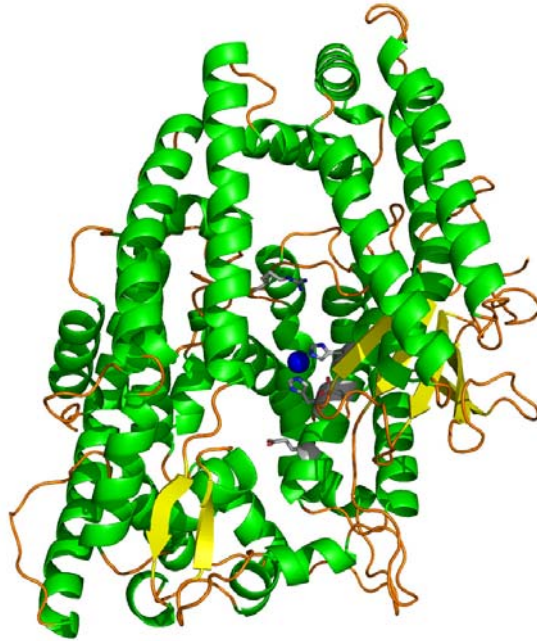


**Figure 4. 3. Superposition of Arg469 and Thr498 in TOP 2 mutant with the corresponding residues in wild type neurolysin. A,** Superposition of the side chain of Arg469 (gray) from the TOP 2 mutant structure with Arg470 (green) from wild type neurolysin. **B,** Superposition of the side chain of Thr498 (gray) from the TOP 2 mutant with Thr499 (green) from wild type neurolysin. **C,** The conformations of active site loop in TOP 2 mutant (599-611, cyan) and wild type neurolysin (600-612, green). The side chains of Tyr605/606 in active site loop and Thr498/499 are shown in a stick representation.



A



B

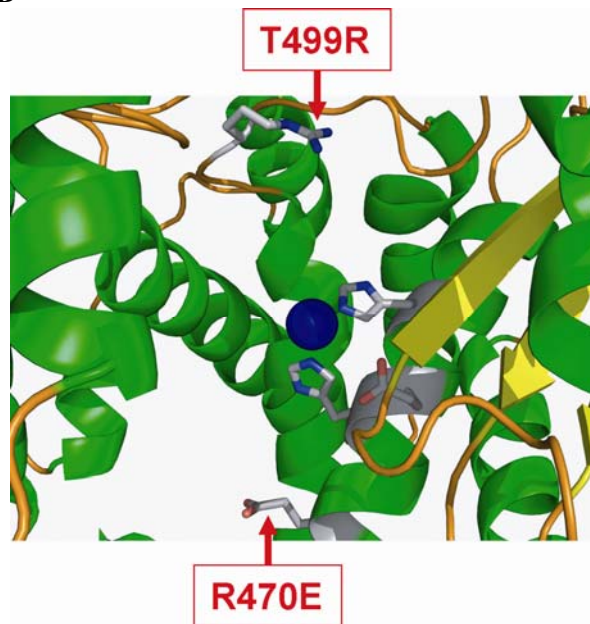
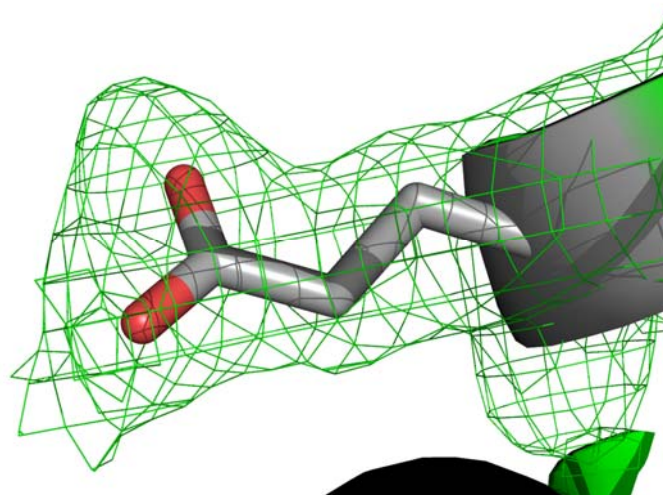


**Figure 4. 4. Crystal structure of the neurolysin 2 mutant. A,** Ribbons view of the structure. **B,** Active site and side chains at positions 470 and 499. Side chains are shown in a stick representation. Active site residue side chains are also shown. The zinc cofactor is shown as a blue sphere in both panels.

**A**



**B**

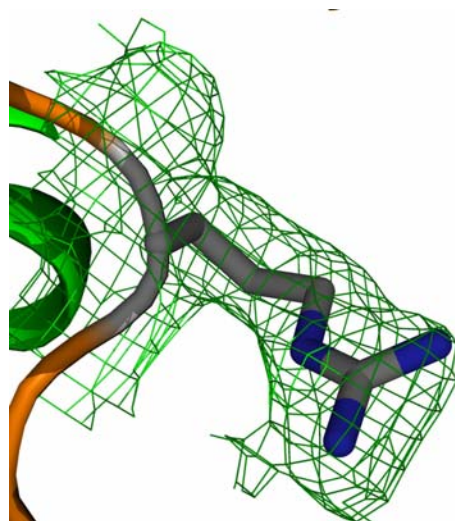


**Figure 4. 5. Electron density for the side chains of Glu470 and Arg499 in the neurolysin 2 mutant crystal structure. A,** Electron density for Glu470. The 2Fo-Fc density is shown in a wireframe representation (green) along with a combined ribbons and stick representation of the protein. **B,** View as in panel A of Arg499 from the crystal structure. In both panels A and B, the electron density is shown with a cutoff contour of 1.0 times the r.m.s deviation of the maps.

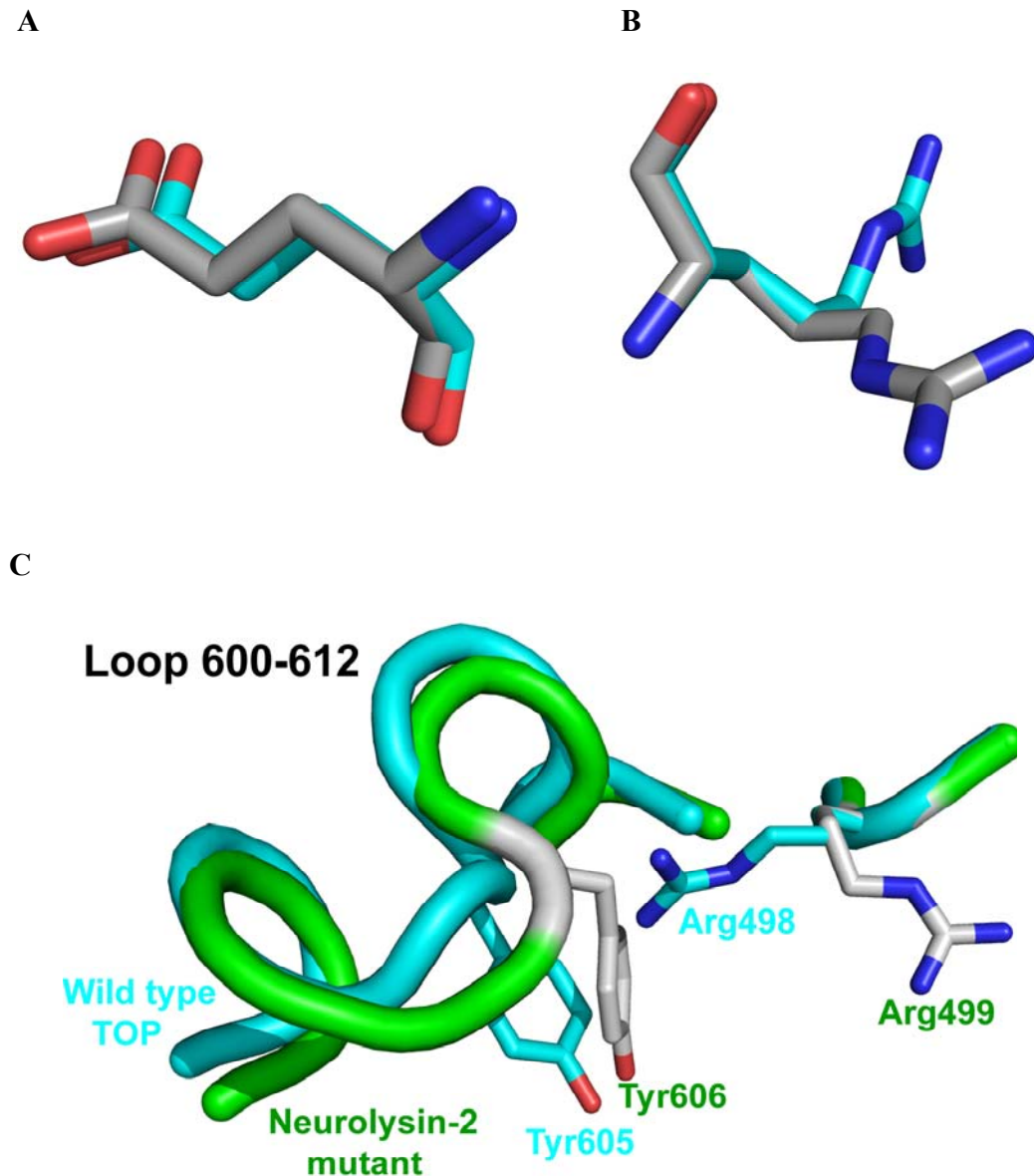


**Figure 4. 6. The superposition of Glu470 and Arg499 in the neurolysin 2 mutant with the corresponding residues in wild type TOP.** **A**, Superposition of the side chain of Glu470 (gray) from the neurolysin 2 mutant structure with Glu469 (cyan) from wild type TOP. **B**, Superposition of the side chain of Arg499 (gray) from the neurolysin 2 mutant with Arg498 (cyan) from wild type TOP. **C**, The conformations of active site loop in wild type TOP (599-611, cyan) and neurolysin 2 mutant (600-612, green). The side chains of Tyr605/606 in active site loop and Thr498/499 are shown in a stick representation.

## Chapter 5: Human neprilysin (hNEP)

### Introduction

Neprilysin, TOP, and neurolysin are zinc metallopeptidases within the MA clan, all having thermolysin-like active sites (Barrett *et al.*, 2003). The common features of substrate selectivity by these metallopeptidases are a restriction to small peptides and the ability to recognize a variety of cleavage-site sequences. TOP and neurolysin have active sites that are located in a deep substrate binding channel, which limits the access to unstructured peptides (Brown *et al.*, 2001; Ray *et al.*, 2004). NEP also has structural elements that limit access to the active site (Oefner *et al.*, 2000), but in this enzyme these elements create a bowl-shaped cavity with a narrow, roughly circular opening (Figure 1.6). The structural components of the shielding walls of the bowl have no resemblance to those in neurolysin and TOP, making NEP a good additional system to consider when testing the generality of recognition mechanisms. In this regard, NEP shows the same sort of fuzzy specificity found in TOP and neurolysin. It recognizes a wide variety of sequences, without any strong sequence preference at any particular position relative to the cleaved peptide bond.

Interestingly, NEP, like TOP and neurolysin, hydrolyzes the 13 residue neuropeptide NT, and it may even be partially responsible for metabolism of this peptide *in vivo* (Oliveira *et al.*, 2001). TOP hydrolyzes NT between Arg8 and Arg9, producing NT1-8 and NT9-13 fragments, while neurolysin cleaves the peptide between Pro10 and Tyr11, producing NT1-10 and NT11-13 fragments (Figure 1.2A). NEP also hydrolyzes NT at between Pro10 and Tyr11, the same position recognized by neurolysin. Thus, as with TOP and neurolysin, examining the determinants of recognition using the NT substrate will be especially informative.

## **Production of recombinant human neprilysin**

The pPICZ $\alpha$ -hNEP construct was overexpressed in *Pichia pastoris* GS115 cells roughly following the protocol established by the group that initially crystallized the enzyme (Dale *et al.*, 2000). The overexpression and purification steps were modified, resulting in a much shorter time required for purification of the enzyme. The other group used BMMY medium to overexpress the enzyme, which prevents degradation of the secreted enzyme, since the peptidases do not act at this low pH medium (EasySelect *Pichia* expression kit, version F from Invitrogen). But, to overexpress the enzyme in this medium, they needed a very large amount of pre-cultured cells expressing protein at 30°C for 3 days. We overexpressed the enzyme in rich YP medium, using pre-cultured cells at 30°C for only 1 day. And we also add a hexahistidine to the N terminus of the enzyme, resulting in rapid isolation of the secreted protein from the 7 liters of media. The other group concentrated their 10 liters of media to 300 ml by crossflow ultrafiltration using a 3 kDa microfiltration module (Skan AG), a time consuming approach (Dale *et al.*, 2000). The final yield of purified protein was about 1 mg / l, which compared favorably with that achieved by the other group.

## **Crystallization of neprilysin**

Initially, wild type, glycosylated human neprilysin was used for crystallization trials utilizing the hanging drop vapor diffusion method at room temperature. Crystal screening kits (Hampton Research, Molecular Dimensions, and Emerald Biosystems) were used as well as trials with gradients of different precipitants, particularly different sizes of PEG. Buffers and pH, salts, as well as the concentration of the protein (3-12 mg/ml) were also varied systematically. The material did not crystallize in these trials, however.

Since glycosylation hinders the crystallization (Kalisz *et al.*, 1990; Kalisz *et al.*, 1991), we mutated the known N-linked glycosylation sites N144, N324, and N627 to glutamine (hNEP 3 mutant) in order to prevent carbohydrate addition (Figure 1.6A). An approach where the sites are mutated to prevent glycosylation was attempted because of the prohibitive cost of purchasing sufficient glycosylase to remove the carbohydrate from the large quantities of enzyme required

for crystallographic work. The resulting protein retained full activity, and a high level of overexpression was achieved by careful selection of the best clone. Unfortunately, even hNEP 3 mutant did not crystallize despite extensive trials. Treatment of the hNEP 3 mutant with Endo F1 glycosylase (QAbio), increased its mobility on SDS PAGE gels, suggesting that there are additional glycosylation sites in hNEP. Using sequence analysis software (ExpASy proteomics tools, NetNGlyc 1.0 server; <http://www.cbs.dtu.dk/services/NetNGlyc/>), we found three more predicted glycosylation sites in hNEP (N284, N310, and N334), and future work should focus on preventing modification at these sites as well in efforts to reproduce the crystals reported in the literature.

## Chapter 6: Human choline acetyltransferase

### Introduction

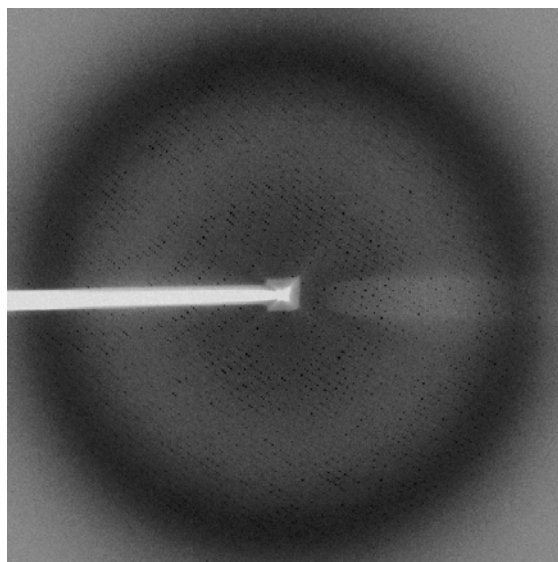
Cholinergic neurons communicate with target cells using the neurotransmitter acetylcholine (ACh) that is synthesized by choline acetyltransferase (Loewi, 1921). ACh has been shown to play critical roles in skeletal muscle contraction, learning, and short-term memory formation (Karczmar, 1993). But in several studies, decreases in ChAT activity are implicated in the pathology of the number of neurologic and psychiatric disorders, including Alzheimer's disease, Huntington's disease, and schizophrenia (Oda, 1999; Dunn and MacLeod, 2001). A motor disorder known as congenital myasthenic syndrome associated with episodic apnea (CMS-EA) is affected by recessive loss of function mutations in ChAT (Ohno *et al.*, 2001; Kraner *et al.*, 2003; Maselli *et al.*, 2003; Schmidt *et al.*, 2003) (Figure 1.7B). Unexpectedly, many of these mutations occur at considerable distances from the catalytic residue histidine, even though some mutations are close to active site. We need to understand why these mutations can affect ChAT activity. Our group has determined the crystal structure of rat ChAT (Cai *et al.*, 2004), but we would prefer to work with human ChAT, since it is more relevant to the congenital disease caused by ChAT mutations. Therefore, detailed understanding about the structural effects of human ChAT mutations will help us design therapies for this disorder.

## Data collection and structure determination of hChAT

Expression of recombinant hChAT and crystallization are described in Chapter 2. X-ray data from the hChAT crystals were collected at the Advanced Photon Source beamline 22-ID (Southeast Regional Collaborative Access Team), Argonne National Laboratory (Figure 6.1A and B). Data were processed with HKL2000, yielding a data set to a resolution of 3.2 Å and two space group. One of two space groups of hChAT crystal was  $P2_1$  and cell dimension was  $a=285.71$  Å,  $b=136.66$  Å,  $c=534.98$  Å. Another was C222 with unit cell dimensions of  $a=316.55$  Å,  $b=475.38$  Å,  $c=136.56$  Å. Extensive attempts to find a molecular replacement solution using the coordinates of rat ChAT (Protein Data Bank code 1Q6X) as a search object failed. The large unit cell of the hChAT crystal suggests that over 20 ChAT molecules are present in the asymmetric unit, making structure determination difficult. Ultimately, even if a molecular replacement solution could be found, it is unlikely that this form would be suitable for continued studies of ChAT because of the difficulties of working such a large number of molecules in the asymmetric unit. Future work should focus on finding a different crystal form using modified constructs of hChAT.



**A**



**B**

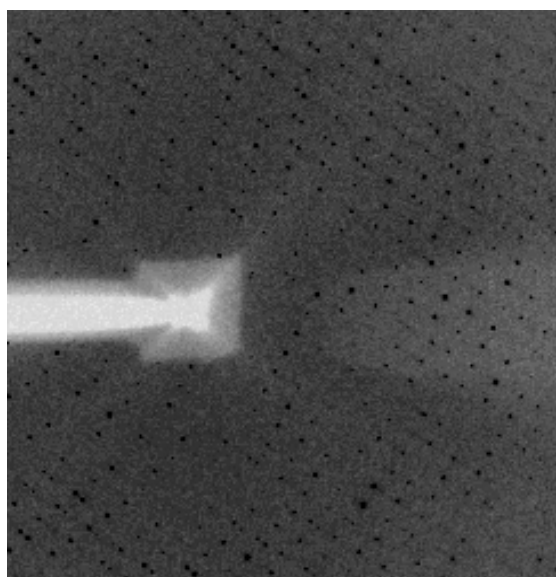


**Figure 6. 1. Diffraction pattern from a hChAT crystal.** **A**, Pattern from a  $1^\circ$  oscillation exposure taken at the 22ID beamline of the Advanced Photon Source, Argonne National Laboratory. The exposure time was 3 seconds. **B**, Close up of the diffraction lattice from the pattern in panel A.

Copyright © Eun Jeong Lim, 2006

## Chapter 7: Discussion and Conclusions

### Specificity in TOP and neurolysin

Our study is one of a relatively few examples of reengineering of substrate specificity in peptidases (DeSantis *et al.*, 1999; Varadarajan *et al.*, 2005). Mapping sequence differences between enzymes on their structural models (Brown *et al.*, 2001; Ray *et al.*, 2002) proved a relatively successful way of identifying residues that determine differences in specificity between these two closely related enzymes.

Other examples of reengineering substrate specificity in peptidases include alteration of subtilisin by site-directed mutagenesis and chemical modification (DeSantis *et al.*, 1999). A serine residue in the S1 subsite of the enzyme (interaction site for the P1 residue) was replaced with a cysteine, allowing covalent linking of branching or charged chemical groups. In this way, the original preference of the enzyme for large hydrophobic residues at P1 could be altered to favor either small nonpolar or charged residues. In another example, *in vitro* selection techniques were used to alter the specificity of the *Escherichia coli* endopeptidase OmpT (Varadarajan *et al.*, 2005). A variant with a single change from arginine to serine near the active site cleaved substrate at a Ala-Arg bond instead of the Arg-Arg bond preferred by the wild type enzyme. The change in catalytic efficiency at the two sites between the wild type and mutant enzyme was over a million fold as a result of the single amino acid change.

In some cases, however, it has not been possible to completely swap specificities between related enzymes despite extensive structural knowledge and considerable effort (Perona *et al.*, 1995). Several studies have demonstrated that converting the specificity between trypsin and chymotrypsin requires substitutions of amino acids in multiple positions of the protein, including exchange of four residues in the S1 site and six residues mutations in two surface loops which do not directly contact the substrate (Graf *et al.*, 1988; Hedstrom *et al.*, 1992; Perona *et al.*, 1995). The best reengineered trypsin mutant hydrolyzes substrates containing large hydrophobic residues at P1 position, like chymotrypsin, but its substrate affinity is highly impaired (Hedstrom *et al.*, 1992).

Only two of the four identified residue differences between TOP and neurolysin proved to actually mediate differential specificity with respect to NT. The two residue positions that did not affect specificity (Met490/Arg491 and His495/Asn496) are located at one end of the channel far from the active site (Figure 1.5). Models of NT binding (Brown *et al.*, 2001; Ray *et al.*, 2004) suggested that the N terminus of the peptide would bind at this end of the channel. The results of this study suggest that either this model is incorrect, or that the peptide does not interact strongly with these residues despite binding nearby.

The two residue positions that were shown to mediate substrate specificity (Glu469/Arg470 and Arg498/Thr499) may exert their effects through their influence on the surface electrostatic potential in the binding site. Clearly, NT has two sites that make good cleavage sequences (unlike many other peptides that only have one). TOP selects one of these sites and neurolysin the other. NT has three basic residues (Lys6, Arg8, and Arg9) in the middle of its sequence, creating a strongly electropositive region. In neurolysin, Arg470 helps to create a slightly electropositive region in the open end of the substrate binding channel, and the electropositive region of NT shifts away giving preferential cleavage site at Pro10-Tyr11 (Figure 7.1A). In contrast, substitution with Glu469 in TOP results in a strongly electronegative region at the open end of its binding channel. The electropositive portion of NT shifts toward this region, giving cleavage at the Arg8-Arg9 site (Figure 7.1A). Mutating Arg9 to Glu9 in NT, making the NT(R9E) substrate, reduces the magnitude the charge on the central region and effectively shifts it toward the N-terminus. The loss of the charge concentration on NT means that the gradients in the binding site no longer strongly influence which of the two sites is chosen, and cleavage occur at both sites (Figure 7.1B). In the same way, decreasing the charge gradient in the binding site, in this case with the TOP E469R mutant, also causes loss of site preference. Thus, the TOP E469R mutant cleaves NT at both sites (Figure 7.1C). The distribution of cleavage sites doesn't change when both the NT(R9E) and the TOP E469R mutant are combined, indicating that losing the charge on either the substrate or enzyme is sufficient to remove specificity for one site. The surface electrostatic potential for the floor of the binding channel is shown for both enzymes in Figure 7.2.

Interestingly, recent work by others in our group suggests that initial recognition of peptide substrates by TOP and neurolysin is mediated by an unusual surface located across the channel from the active site (Figure 7.3A). The surface interacts with residues C terminal to the scissile bond in a number of crystal structures with TOP that have been determined using enzyme variants with no or greatly reduced activity. In the TOP-NT complex crystal structure, the residues from P2 to the N terminus are disordered, suggesting that they do not play a significant role in initial binding of the peptide. This possibility is consistent with the lack of a role for the distant residues in differential specificity. The surface that interacts with the C terminal peptide residues is unusual in the sense that it is relatively flat, not having the usual specificity pockets of peptidases/proteases, and it is highly enriched in aromatic and hydrophobic residues. Overall, it is similar to protein-protein interaction surfaces, and the different peptides interact with it in very different ways, accounting, we believe, for the fuzzy specificity shown by the enzymes.

The qualification of “initial” binding is important. There is evidence that enzymes with the neurolysin/TOP fold undergo a hinge-like conformational change upon binding substrate or transition state analog inhibitors. The two large domains rotate to substantially narrow the central channel, closing down on the bound ligands. This motion has been shown directly for the structurally related enzyme ACE2 from crystal structures determined in both the unliganded and inhibitor bound states (Towler *et al.*, 2004). In this case the relative rotation of the two domains is approximately  $16^\circ$  with a maximum shift in  $C\alpha$  positions of over 20 Å when the two structures are aligned on their catalytic domains. The inhibitor-bound dipeptidyl carboxypeptidase, which belongs to the same metallopeptidase family as TOP and neurolysin, also is in a closed conformation relative to unliganded TOP and neurolysin in the recently determined crystal structure (Comellas-Bigler *et al.*, 2005). In the TOP and neurolysin crystal structures, however, packing contacts prevent this hinge motion when peptides are soaked into preexisting crystals (although very tightly binding inhibitors disorder the crystals, suggesting that their binding energy is sufficient to overcome the lattice packing forces). Therefore, what is seen in the TOP-peptide complexes is likely a snapshot of the peptide binding process prior to the hinge-like conformational change in the enzyme. This view is consistent with the positions of the bound peptides themselves, which are placed 4-5 Å too far from the zinc ion cofactor to adopt the

correct coordination geometry for hydrolysis. Modeling the expected hinge motion brings the peptides, as well as a tyrosine residue from the enzyme shown to be involved in catalysis (Oliveira *et al.*, 2003), into correct alignment.

The hinge-like motion of the enzymes also has implications for interpretation of the results of this study. Based on the peptide positions in the TOP complexes, Arg498, one of the two residues mediating differential specificity, is in a position to interact with NT around the P1 position as it binds in the open enzyme conformation. The other determining residue, however, Glu469/Arg470, is not in a position to interact with the peptide in the initial binding conformation. The distance to the nearest atom of bound NT is about 10 Å in the case of Glu469 from the TOP-NT complex. Thus, as an alternative to the electrostatic model described, position 469/470 may play a role in determining specificity in the closed conformation of the enzyme-substrate complex (Figure 7.3B). The hinge motion would place the C-terminal residues of bound NT much closer to the 469/470 position.

At the other residue position that affects specificity, Arg498 from TOP would be close to Arg8 or Pro7 of the peptide, unlikely to make a specificity increasing interaction with the side chains of these residues (Figure 7.4). A geometry dependent interaction with the main chain is a possibility, however. In contrast, Thr499 from neurolysin would be near Arg9 of NT, and hydrogen bond interaction between the two side chains is possible. In terms of fuzzy specificity, this model would suggest that the two positions that mediate differential specificity on NT do not play a significant role in maintaining the broad specificity characteristic of neuropeptidases. Instead, as noted above, we believe fuzzy specificity is largely to the surface that binds the C-terminal peptide residues. The two residue positions identified here, likely only modulate the specificity to result in the occasional differences seen in TOP and neurolysin cleavage sites.

## **Neprilysin**

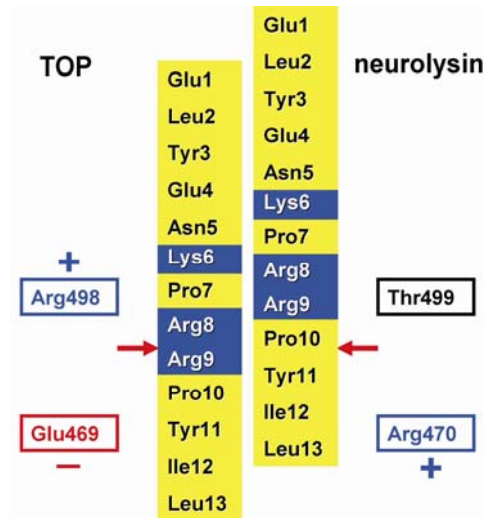
We believe that neprilysin is another good model system in which to study cleavage site recognition in metallopeptidases, since it shows the same sort of fuzzy specificity found in TOP and neurolysin. It recognizes a wide variety of sequences, without any strong sequence preference at any particular position close to the scissile bond. Since the crystal structure has already been determined (Oefner *et al.*, 2000), NEP is also attractive because we know it can form well ordered crystals.

Despite the published protocols for crystallizing hNEP, initial trials with the recombinant protein we produced were not successful. One possible reason for the lack of crystals is the carbohydrate still present on our hNEP despite mutation of three known glycosylation positions. The group that determined the original crystal structure was able to crystallize the enzyme despite extensive glycosylation, but the crystals were not well ordered (Dale *et al.*, 2000). Our construct differed from the one employed by the other group in that it contained a polyhistidine affinity purification tag, which may make it behave somewhat differently. Thus future work should focus on eliminating remaining potential modification sites (N284, N310, and N334) and in creating a construct as close as possible to the one that was successfully crystallized. We are encouraged by the successful overexpression of the construct mutated at three positions, which clearly prevents most of the carbohydrate addition. It is important to know that this modified enzyme still folds correctly and is active, encouraging us to pursue the approach of mutating the modification sites.

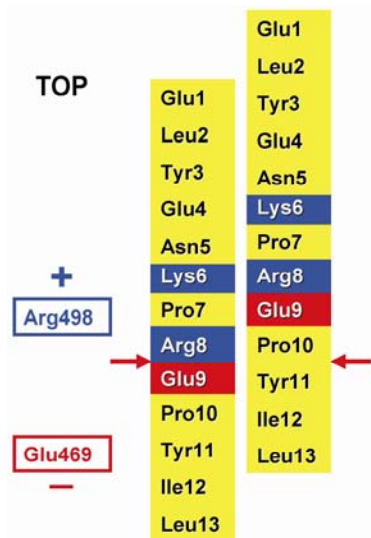
## Human ChAT

The crystal structure of rat ChAT was determined by our group (Cai *et al.*, 2004), but we would prefer to switch to the human ortholog, which is more relevant to our studies of the disease caused by mutations in the enzyme. We were able to overexpress and purify hChAT protein. A similar protocol has been published recently by another group (Kim *et al.*, 2005). The N-terminal 10 residues and the C-terminal 23 residues of the rat enzyme are disordered, so we made both a full length construct and a truncated at both ends. Both constructs crystallized in the same conditions and gave the same crystal form, but this form is not suitable for analysis because of the large number of molecules in the asymmetric unit. It is possible that further truncations at the N or C terminus will give a different crystal form, and the approach should be pursued. It may be possible using new software that has become available to attempt molecular replacement with the existing data set. Determining the packing in these crystals should allow the construct to be altered by mutagenesis to prevent formation of this lattice, increasing the probability of obtaining a new form in screens.

A



B



C

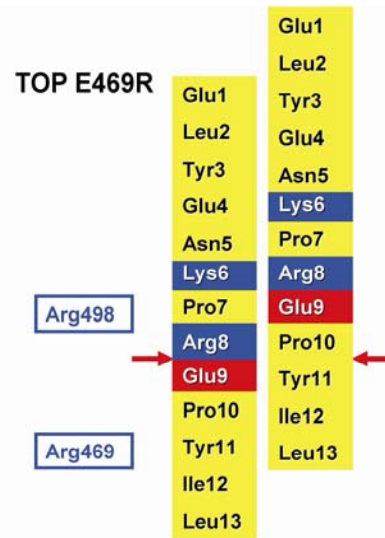


**Figure 7. 1. Model for differential specificity of TOP and neurolysin with respect to primary NT cleavage sites.** A, Schematic NT representations with the key residues mediating differential specificity shown along with their contribution to surface electrostatic potential in the substrate binding site. B and C, Similar representation of the NT(R9E) peptide with the key residues in wild type TOP (B) and the TOP E469R mutant (C).



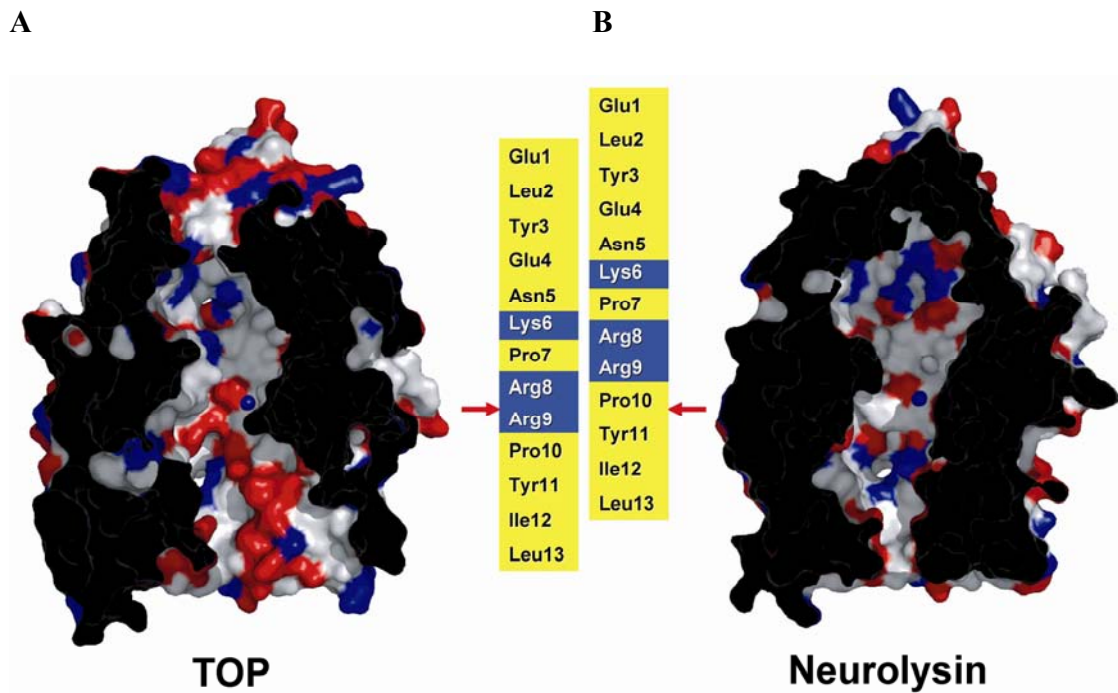
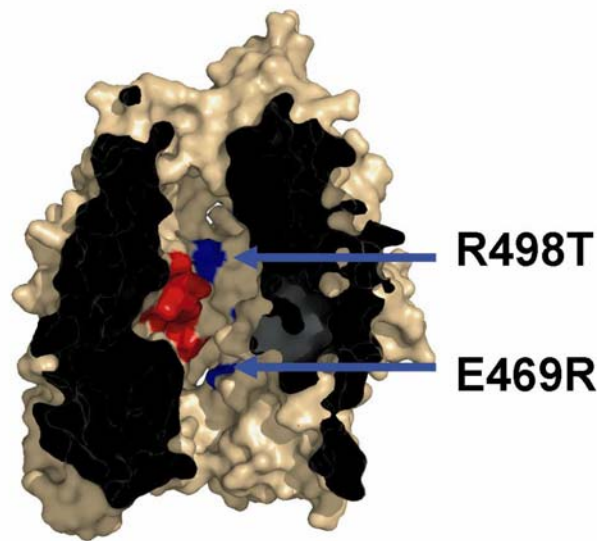


**Figure 7. 2. Surface electrostatic potential in the substrate binding channels of TOP and neurolysin.** Cut away molecular surface views of the TOP (**A**) and neurolysin (**B**) binding sites colored according to surface electrostatic potential (red, negative; blue, positive). The active site zinc ion is shown as a blue sphere. Schematic representations of the NT peptide in two binding registrations emphasizing the positively charged region in the center of the peptide are also shown.

A



B

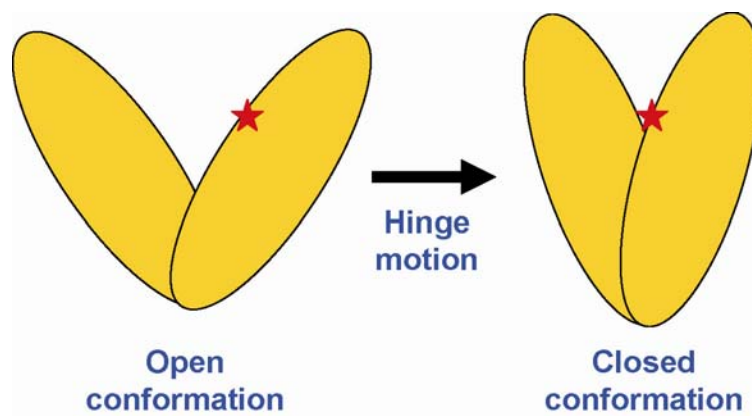


**Figure 7. 3. Initial binding sites of substrates and mutation residues in TOP.** **A**, Two mutation residues are colored by blue and the red color represents the initial binding site for the C-terminal residues of substrates. **B**, Model for hinge motion of TOP. Red star indicates E469 residue.

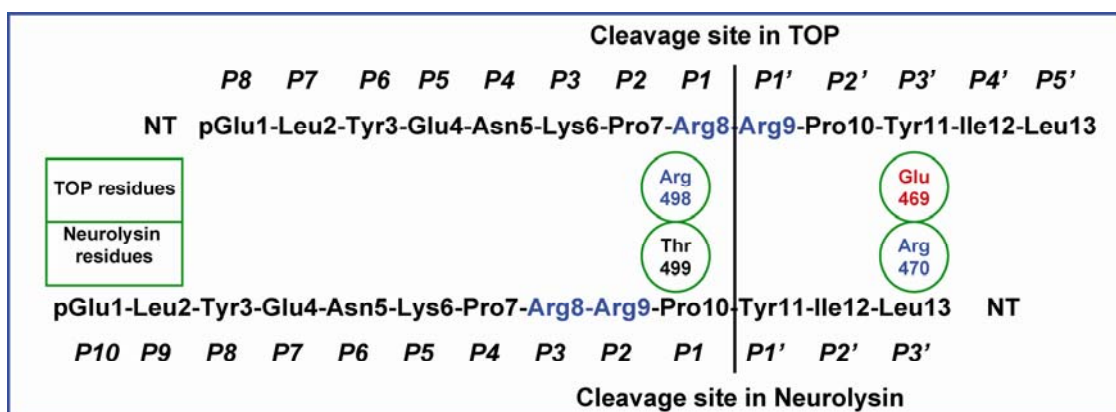


**Figure 7. 4. Model for NT binding in TOP and neurolysin.** The sequence of NT is shown twice, top and bottom, with the two representations shifted to represent the relative positions when bound to TOP and neurolysin, respectively. The positions of the two sites mediating differential specificity are shown in the center along with a vertical bar representing the position of the hydrolyzed peptide bond.

## Bibliography:

Acker, G. R., Molineaux, C., and Orłowski, M. (1987). Synaptosomal membrane-bound form of endopeptidase-24.15 generates Leu-enkephalin from dynorphin 1-8, alpha- and beta-neoendorphin, and Met-enkephalin from Met-enkephalin-Arg6-Gly7-Leu8. *J. Neurochem.* **48**, 284-292.

Arndt, J. W., Hao, B., Ramakrishnan, V., Cheng, T., Chan, S. I., and Chan, M. K. (2002). Crystal structure of a novel carboxypeptidase from the hyperthermophilic archaeon *Pyrococcus furiosus*. *Structure (Camb)* **10**, 215-224.

Authier, F., Posner, B. I., and Bergeron, J. J. (1996). Insulin-degrading enzyme. *Clin. Invest. Med.* **19**, 149-160.

Barelli, H., Dive, V., Yiotakis, A., Vincent, J. P., and Checler, F. (1992). Potent inhibition of endopeptidase 24.16 and endopeptidase 24.15 by the phosphonamide peptide N-(phenylethylphosphonyl)-Gly-L-Pro-L-aminohexanoic acid. *Biochem. J.* **287 ( Pt 2)**, 621-625.

Barelli, H., Fox-Threlkeld, J. E. T., Dive, V., Daniel, E. E., Vincent, J. P., and Checler, F. (1994). Role of endopeptidase 3.4.24.16 in the catabolism of neurotensin, in vivo, in the vascularly perfused dog ileum. *Br. J. Pharmacol.* **112**, 127-132.

Barnes, K., Turner, A. J., and Kenny, A. J. (1992). Membrane localization of endopeptidase-24.11 and peptidyl dipeptidase A (angiotensin converting enzyme) in the pig brain: a study using subcellular fractionation and electron microscopic immunocytochemistry. *J. Neurochem.* **58**, 2088-2096.

Barrett, A. J., and Brown, M. A. (1990). Chicken liver Pz-peptidase, a thiol-dependent metallo-endopeptidase. *Biochem. J.* **271**, 701-706.

Barrett, A. J., Brown, M. A., Dando, P. M., Knight, C. G., McKie, N., Rawlings, N. D., and Serizawa, A. (1995). Thimet oligopeptidase and oligopeptidase M or neurolysin. *Meth. Enzymol.* **248**, 529-556.

Barrett, A. J., and Rawlings, N. D. (1992). Oligopeptidases and the emergence of the prolyl oligopeptidase family. *Biol. Chem. Hoppe Seyler* **373**, 353-360.

Barrett, A. J., Tolle, D. P., and Rawlings, N. D. (2003). Managing peptidases in the genomic era. *Biol. Chem.* **384**, 873-882.

Bauer, J. H. (1990). Angiotensin converting enzyme inhibitors. *Am. J. Hypertens.* **3**, 331-337.

Boules, M., Fredrickson, P., and Richelson, E. (2005). Neurotensin agonists as an alternative to antipsychotics. *Expert. Opin. Investig. Drugs* **14**, 359-369.

- Brown, C. K., Madauss, K., Lian, W., Beck, M. R., Tolbert, W. D., and Rodgers, D. W. (2001). Structure of neurolysin reveals a deep channel that limits substrate access. *Proc. Natl. Acad. Sci. USA* **98**, 3127-3132.
- Burnett, J. C., Jr. (1999). Vasopeptidase inhibition: a new concept in blood pressure management. *J. Hypertens.* **17**, S37-43.
- Cai, Y., Cronin, C. N., Engel, A. G., Ohno, K., Hersh, L. B., and Rodgers, D. W. (2004). Choline acetyltransferase structure reveals distribution of mutations that cause motor disorders. *Embo J.* **23**, 2047-2058.
- Camargo, A. C., Gomes, M. D., Toffoletto, O., Ribeiro, M. J., Ferro, E. S., Fernandes, B. L., Suzuki, K., Sasaki, Y., and Juliano, L. (1994). Structural requirements of bioactive peptides for interaction with endopeptidase 22.19. *Neuropeptides* **26**, 281-287.
- Carraway, R., and Leeman, S. E. (1973). The isolation of a new hypotensive peptide, neurotensin, from bovine hypothalami. *J. Biol. Chem.* **248**, 6854-6861.
- Carroll, P. T. (1994). Membrane-bound choline-O-acetyltransferase in rat hippocampal tissue is associated with synaptic vesicles. *Brain Res.* **633**, 112-118.
- Carson, J. A., and Turner, A. J. (2002). Beta-amyloid catabolism: roles for neprilysin (NEP) and other metallopeptidases? *J. Neurochem.* **81**, 1-8.
- Chalon, P., Vita, N., Kaghad, M., Guillemot, M., Bonnin, J., Delpech, B., Le Fur, G., Ferrara, P., and Caput, D. (1996). Molecular cloning of a levocabastine-sensitive neurotensin binding site. *FEBS Lett.* **386**, 91-94.
- Chappell, M. C., Iyer, S. N., Diz, D. I., and Ferrario, C. M. (1998). Antihypertensive effects of angiotensin-(1-7). *Braz. J. Med. Biol. Res.* **31**, 1205-12.
- Charli, J. L., Mendez, M., Vargas, M. A., Cisneros, M., Assai, M., Joseph-Bravo, P., and Wilk, S. (1989). Pyroglutamyl peptidase II inhibition specifically increases recovery of TRH released from rat brain slices. *Neuropeptides* **14**, 191-196.
- Charli, J. L., Vargas, M. A., Cisneros, M., de Gortari, P., Baeza, M. A., Jasso, P., Bourdais, J., Perez, L., Uribe, R. M., and Joseph-Bravo, P. (1998). TRH inactivation in the extracellular compartment: role of pyroglutamyl peptidase II. *Neurobiology* **6**, 45-57.
- Checler, F. (1993). *Methods in Neurotransmitter and Neuropeptide Research*. Nagatsu, T., Parvez, H., Naoi, M., and Parvez, S., Amsterdam, Elsevier, 375-418.
- Checler, F., Barelli, H., Dauch, P., Dive, V., Vincent, B., and Vincent, J. P. (1995). Neurolysin: purification and assays. *Meth. Enzymol.* **248**, 593-614.

- Checler, F., Barelli, H., Dauch, P., Vincent, B., Dive, V., Beaudet, A., Daniel, E. E., Fox-Threlkeld, J. E., Masuo, Y., and Vincent, J. P. (1993). Recent advances on endopeptidase-3.4.24.16. *Biochem. Soc. Trans.* **21**, 692-697.
- Checler, F., Vincent, J. P., and Kitabgi, P. (1983). Degradation of neurotensin by rat brain synaptic membranes: involvement of a thermolysin-like metalloendopeptidase (enkephalinase), angiotensin-converting enzyme, and other unidentified peptidases. *J. Neurochem.* **41**, 375-384.
- Checler, F., Vincent, J. P., and Kitabgi, P. (1985). Inactivation of neurotensin by rat brain synaptic membranes partly occurs through cleavage at the Arg8-Arg9 peptide bond by a metalloendopeptidase. *J. Neurochem.* **45**, 1509-1513.
- Checler, F., Vincent, J. P., and Kitabgi, P. (1986). Purification and characterization of a novel neurotensin-degrading peptidase from rat brain synaptic membranes. *J Biol Chem* **261**, 11274-81.
- Chen, H., Noble, F., Coric, P., Fournie-Zaluski, M. C., and Roques, B. P. (1998). Aminophosphinic inhibitors as transition state analogues of enkephalin-degrading enzymes: a class of central analgesics. *Proc. Natl. Acad. Sci. U S A* **95**, 12028-12033.
- Chu, T. G., and Orłowski, M. (1985). Soluble metalloendopeptidase from rat brain: action on enkephalin-containing peptides and other bioactive peptides. *Endocrinology* **116**, 1418-1425.
- Cohen, A. J., Bunn, P. A., Franklin, W., Magill-Solc, C., Hartmann, C., Helfrich, B., Gilman, L., Folkvord, J., Helm, K., and Miller, Y. E. (1996). Neutral endopeptidase: variable expression in human lung, inactivation in lung cancer, and modulation of peptide-induced calcium flux. *Cancer Res.* **56**, 831-839.
- Comellas-Bigler, M., Lang, R., Bode, W., and Maskos, K. (2005). Crystal structure of the E. coli dipeptidyl carboxypeptidase Dcp: further indication of a ligand-dependent hinge movement mechanism. *J. Mol. Biol.* **349**, 99-112.
- Csuhai, E., Safavi, A., Thompson, M. W., and Hersh, L. B. (1998). *Proteolytic and Cellular Mechanisms in Prohormone and Neuropeptide Precursor Processing*. Hook, V., Heidelberg, Springer-Verlag, 173-182.
- Cummins, P. M., Pabon, A., Margulies, E. H., and Glucksman, M. J. (1999). Zinc coordination and substrate catalysis within the neuropeptide processing enzyme endopeptidase EC 3.4.24.15. Identification of active site histidine and glutamate residues. *J. Biol. Chem.* **274**, 16003-16009.
- Czyzyk, T. A., Morgan, D. J., Peng, B., Zhang, J., Karantzas, A., Arai, M., and Pintar, J. E. (2003). Targeted mutagenesis of processing enzymes and regulators: implications for development and physiology. *J. Neurosci. Res.* **74**, 446-55.
- Dahms, P., and Mentlein, R. (1992). Purification of the main somatostatin-degrading proteases from rat and pig brains, their action on other neuropeptides, and their identification as endopeptidases 24.15 and 24.16. *Eur. J. Biochem.* **208**, 145-154.

- Dale, G. E., D'Arcy, B., Yuwaniyama, C., Wipf, B., Oefner, C., and D'Arcy, A. (2000). Purification and crystallization of the extracellular domain of human neutral endopeptidase (neprilysin) expressed in *Pichia pastoris*. *Acta Crystallogr. D Biol. Crystallogr.* **56** ( Pt 7), 894-897.
- Dando, P. M., Brown, M. A., and Barrett, A. J. (1993). Human thimet oligopeptidase. *Biochem. J.* **294**, 451-457.
- Dauch, P., Vincent, J. P., and Checler, F. (1995). Molecular cloning and expression of rat brain endopeptidase 3.4.24.16. *J. Biol. Chem.* **270**, 27266-27271.
- Dendorfer, A., Vordermark, D., and Dominiak, P. (1997). Degradation of bradykinin by bovine tracheal epithelium and isolated epithelial cells. *Br. J. Pharmacol.* **120**, 121-129.
- DeSantis, G., Shang, X., and Jones, J. B. (1999). Toward tailoring the specificity of the S1 pocket of subtilisin B. *lentus*: chemical modification of mutant enzymes as a strategy for removing specificity limitations. *Biochemistry* **38**, 13391-13397.
- Devault, A., Lazure, C., Nault, C., Le Moual, H., Seidah, N. G., Chretien, M., Kahn, P., Powell, J., Mallet, J., Beaumont, A., and et al. (1987). Amino acid sequence of rabbit kidney neutral endopeptidase 24.11 (enkephalinase) deduced from a complementary DNA. *Embo J.* **6**, 1317-1322.
- Dobner, P. R., Deutch, A. Y., and Fadel, J. (2003). Neurotensin: dual roles in psychostimulant and antipsychotic drug responses. *Life Sci.* **73**, 801-11.
- Dobransky, T., Brewer, D., Lajoie, G., and Rylett, R. J. (2003). Phosphorylation of 69-kDa choline acetyltransferase at threonine 456 in response to amyloid-beta peptide 1-42. *J. Biol. Chem.* **278**, 5883-5893.
- Dobransky, T., Davis, W. L., and Rylett, R. J. (2001). Functional characterization of phosphorylation of 69-kDa human choline acetyltransferase at serine 440 by protein kinase C. *J. Biol. Chem.* **276**, 22244-22250.
- Dobransky, T., Doherty-Kirby, A., Kim, A. R., Brewer, D., Lajoie, G., and Rylett, R. J. (2004). Protein kinase C isoforms differentially phosphorylate human choline acetyltransferase regulating its catalytic activity. *J. Biol. Chem.* **279**, 52059-52068.
- Dobransky, T., and Rylett, R. J. (2003). Functional regulation of choline acetyltransferase by phosphorylation. *Neurochem. Res.* **28**, 537-542.
- Dobransky, T., and Rylett, R. J. (2005). A model for dynamic regulation of choline acetyltransferase by phosphorylation. *J. Neurochem.* **95**, 305-313.

- Dunn, H. G., and MacLeod, P. M. (2001). Rett syndrome: review of biological abnormalities. *Can. J. Neurol. Sci.* **28**, 16-29.
- Endoh, T. (2004). Modulation of voltage-dependent calcium channels by neurotransmitters and neuropeptides in parasympathetic submandibular ganglion neurons. *Arch. Oral. Biol.* **49**, 539-557.
- Engel, A. G., Ohno, K., and Sine, S. M. (2003). Congenital myasthenic syndromes: progress over the past decade. *Muscle Nerve* **27**, 4-25.
- Erickson, J. D., and Varoqui, H. (2000). Molecular analysis of vesicular amine transporter function and targeting to secretory organelles. *Faseb J.* **14**, 2450-2458.
- Ferro, E. S., Tambourgy, D. V., Abreu, P. A., Camargo, A. C., Raw, I., and Ho, P. L. (1995). Characterization of an endooligopeptidase A-like protein in PC12 cells: activity modulation by cAMP but not by basic fibroblast growth factor. *J. Cell. Biochem.* **57**, 311-320.
- Ferro, E. S., Tullai, J. W., Glucksman, M. J., and Roberts, J. L. (1999). Secretion of metalloendopeptidase 24.15 (EC 3.4.24.15). *DNA Cell Biol.* **18**, 781-9.
- Fontenele-Neto, J. D., Massarelli, E. E., Gurgel Garrido, P. A., Beaudet, A., and Ferro, E. S. (2001). Comparative fine structural distribution of endopeptidase 24.15 (EC3.4.24.15) and 24.16 (EC3.4.24.16) in rat brain. *J. Comp. Neurol.* **438**, 399-410.
- Fredrickson, P., Boules, M., Lin, S. C., and Richelson, E. (2005). Neurobiologic basis of nicotine addiction and psychostimulant abuse: a role for neurotensin? *Psychiatr. Clin. North. Am.* **28**, 737-751.
- Fülöp, V., Böcskei, Z., and Polgár, L. (1998). Prolyl oligopeptidase: an unusual  $\beta$ -propeller domain regulates proteolysis. *Cell* **94**, 161-170.
- Gabrielle, P., Jeana, M., and Lorenza, E. C. (2003). Cytosolic choline acetyltransferase binds specifically to cholinergic plasma membrane of rat brain synaptosomes to generate membrane-bound enzyme. *Neurochem. Res.* **28**, 543-549.
- Garrido, P. A., Vandenbulcke, F., Ramjaun, A. R., Vincent, B., Checler, F., Ferro, E., and Beaudet, A. (1999). Confocal microscopy reveals thimet oligopeptidase (EC 3.4.24.15) and neurolysin (EC 3.4.24.16) in the classical secretory pathway. *DNA Cell Biol.* **18**, 323-331.
- Genden, E. M., and Molineaux, C. J. (1991). Inhibition of endopeptidase-24.15 decreases blood pressure in normotensive rats. *Hypertension* **18**, 360-365.
- Gill, S. K., Bhattacharya, M., Ferguson, S. S., and Rylett, R. J. (2003). Identification of a novel nuclear localization signal common to 69- and 82-kDa human choline acetyltransferase. *J. Biol. Chem.* **278**, 20217-20224.



- Gohring, B., Holzhausen, H. J., Meye, A., Heynemann, H., Rebmann, U., Langner, J., and Riemann, D. (1998). Endopeptidase 24.11/CD10 is down-regulated in renal cell cancer. *Int. J. Mol. Med.* **2**, 409-414.
- Gomes, M. D., Juliano, L., Ferro, E. S., Matsueda, R., and Camargo, A. C. (1993). Dynorphin-derived peptides reveal the presence of a critical cysteine for the activity of brain endo-oligopeptidase A. *Biochem. Biophys. Res. Commun.* **197**, 501-7.
- Graf, L., Jancso, A., Szilagyi, L., Hegyi, G., Pinter, K., Naray-Szabo, G., Hepp, J., Medzihradsky, K., and Rutter, W. J. (1988). Electrostatic complementarity within the substrate-binding pocket of trypsin. *Proc. Natl. Acad. Sci. U S A* **85**, 4961-4965.
- Guy, J. L., Jackson, R. M., Acharya, K. R., Sturrock, E. D., Hooper, N. M., and Turner, A. J. (2003). Angiotensin-converting enzyme-2 (ACE2): comparative modeling of the active site, specificity requirements, and chloride dependence. *Biochemistry* **42**, 13185-13192.
- Guyenet, P., Lefresne, P., Rossier, J., Beaujouan, J. C., and Glowinski, J. (1973). Inhibition by hemicholinium-3 of (14C)acetylcholine synthesis and (3H)choline high-affinity uptake in rat striatal synaptosomes. *Mol. Pharmacol.* **9**, 630-639.
- Hanson, G. R., Singh, N., Merchant, K., Johnson, M., Bush, L., and Gibb, J. W. (1992). Responses of limbic and extrapyramidal neurotensin systems to stimulants of abuse. Involvement of dopaminergic mechanisms. *Ann. N. Y. Acad. Sci.* **668**, 165-172.
- Harding, M. M. (2001). Geometry of metal-ligand interactions in proteins. *Acta Crystallogr. D Biol. Crystallogr.* **57**, 401-411.
- Healy, D. P., and Orlowski, M. (1992). Immunocytochemical localization of endopeptidase 24.15 in rat brain. *Brain Res.* **571**, 121-128.
- Hedstrom, L., Szilagyi, L., and Rutter, W. J. (1992). Converting trypsin to chymotrypsin: the role of surface loops. *Science* **255**, 1249-1253.
- Hersh, L. B., Coe, B., and Casey, L. (1978). A fluorometric assay for choline acetyltransferase and its use in the purification of the enzyme from human placenta. *J. Neurochem.* **30**, 1077-1085.
- Ishimaru, F., Mari, B., and Shipp, M. A. (1997). The type 2 CD10/neutral endopeptidase 24.11 promoter: functional characterization and tissue-specific regulation by CBF/NF-Y isoforms. *Blood* **89**, 4136-4145.
- Jacchieri, S. G., Gomes, M. D., Juliano, L., and Carmago, A. C. M. (1998). A comparative conformational analysis of thimet oligopeptidase (EC 3.4.24.15) substrates. *J. Pept. Res.* **51**, 452-459.
- Jogl, G., and Tong, L. (2003). Crystal structure of carnitine acetyltransferase and implications for the catalytic mechanism and fatty acid transport. *Cell* **112**, 113-122.

- Juers, D. H., Kim, J., Matthews, B. W., and Sieburth, S. M. (2005). Structural analysis of silanediols as transition-state-analogue inhibitors of the benchmark metalloprotease thermolysin. *Biochemistry* **44**, 16524-16528.
- Kalisz, H. M., Hecht, H. J., Schomburg, D., and Schmid, R. D. (1990). Crystallization and preliminary X-ray diffraction studies of a deglycosylated glucose oxidase from *Aspergillus niger*. *J. Mol. Biol.* **213**, 207-209.
- Kalisz, H. M., Hecht, H. J., Schomburg, D., and Schmid, R. D. (1991). Effects of carbohydrate depletion on the structure, stability and activity of glucose oxidase from *Aspergillus niger*. *Biochim. Biophys. Acta.* **1080**, 138-142.
- Karczmar, A. G. (1993). Brief presentation of the story and present status of studies of the vertebrate cholinergic system. *Neuropsychopharmacology* **9**, 181-199.
- Kato, A., Sugiura, N., Saruta, Y., Hosoiri, T., Yasue, H., and Hirose, S. (1997). Targeting of endopeptidase 24.16 to different subcellular compartments by alternative promoter usage. *J. Biol. Chem.* **272**, 15313-15322.
- Kenny, A. J., and Stephenson, S. L. (1988). Role of endopeptidase-24.11 in the inactivation of atrial natriuretic peptide. *FEBS Lett.* **232**, 1-8.
- Kerr, M. A., and Kenny, A. J. (1974). The purification and specificity of a neutral endopeptidase from rabbit kidney brush border. *Biochem. J.* **137**, 477-488.
- Kim, A. R., Doherty-Kirby, A., Lajoie, G., Rylett, R. J., and Shilton, B. H. (2005). Two methods for large-scale purification of recombinant human choline acetyltransferase. *Protein Expr. Purif.* **40**, 107-117.
- Kim, H. M., Shin, D. R., Yoo, O. J., Lee, H., and Lee, J. O. (2003). Crystal structure of *Drosophila* angiotensin I-converting enzyme bound to captopril and lisinopril. *FEBS Lett.* **538**, 65-70.
- Kim, S. I., Grum-Tokars, V., Swanson, T. A., Cotter, E. J., Cahill, P. A., Roberts, J. L., Cummins, P. M., and Glucksman, M. J. (2003). Novel roles of neuropeptide processing enzymes: EC3.4.24.15 in the neurome. *J. Neurosci. Res.* **74**, 456-467.
- Kim, S. I., Pabon, A., Swanson, T. A., and Glucksman, M. J. (2003). Regulation of cell-surface major histocompatibility complex class I expression by the endopeptidase EC3.4.24.15 (thimet oligopeptidase). *Biochem. J.* **375**, 111-120.
- Koike, H., Seki, H., Kouchi, Z., Ito, M., Kinouchi, T., Tomioka, S., Sorimachi, H., Saido, T. C., Maruyama, K., Suzuki, K., and Ishiura, S. (1999). Thimet oligopeptidase cleaves the full-length Alzheimer amyloid precursor protein at a beta-secretase cleavage site in COS cells. *J. Biochem. (Tokyo)* **126**, 235-242.

Koiso, K., Akaza, H., Ohtani, M., Miyanaga, N., and Aoyagi, K. (1994). A new tumor marker for bladder cancer. *Int. J. Urol.* **1**, 33-36.

Kong, C. F., Hilt, D., and Hersh, L. B. (1989). Isolation of a Genomic Clone of Human Choline Acetyltransferase. Proc. Intern. Symp "Pharmacological Interventions on Central Cholinergic Mechanisms in Senile Dementia (Alzheimer's Disease)", Berlin, Zuckschwerdt-Verl.; Klin. Pharmakol.

Konkoy, C. S., and Davis, T. P. (1995). Regional metabolism of Met-enkephalin and cholecystokinin on intact ratbrain slices: characterization of specific peptidases. *J. Neurochem.* **65**, 2773-2782.

Konkoy, C. S., and Davis, T. P. (1996). Ectoenzymes as sites of peptide regulation. *Trends in Pharm. Sci.* **17**, 288-294.

Konkoy, C. S., Waters, S. M., and Davis, T. P. (1996). Subchronic haloperidol administration decreases aminopeptidase N activity and [Met5]enkephalin metabolism in rat striatum and cortex. *Eur. J. Pharmacol.* **297**, 47-51.

Kraner, S., Laufenberg, I., Strassburg, H. M., Sieb, J. P., and Steinlein, O. K. (2003). Congenital myasthenic syndrome with episodic apnea in patients homozygous for a CHAT missense mutation. *Arch. Neurol.* **60**, 761-763.

Lasdun, A., and Orłowski, M. (1990). Inhibition of endopeptidase 24.15 greatly increases the release of luteinizing hormone and follicle stimulating hormone in response to luteinizing hormone/releasing hormone. *J. Pharmacol. Exp. Ther.* **253**, 1265-1271.

Lasdun, A., Reznik, S., Molineaux, C. J., and Orłowski, M. (1989). Inhibition of endopeptidase 24.15 slows the in vivo degradation of luteinizing hormone-releasing hormone. *J. Pharmacol. Exp. Ther.* **251**, 439-447.

Le, F., Cusack, B., and Richelson, E. (1996). The neurotensin receptor: is there more than one subtype? *Trends Pharmacol. Sci.* **17**, 1-3.

Lew, R. A. (2004). The zinc metallopeptidase family: new faces, new functions. *Protein Pept. Lett.* **11**, 407-414.

Lew, R. A., Cowley, M., Clarke, I. J., and Smith, A. I. (1997). Peptidases that degrade gonadotropin-releasing hormone: influence on LH secretion in the ewe. *J. Neuroendocrinol.* **9**, 707-712.

Lew, R. A., Hey, N. J., Tetaz, T. J., Glucksman, M. J., Roberts, J. L., and Smith, A. I. (1995). Substrate specificity differences between recombinant rat testes endopeptidase EC 3.4.24.15 and the native brain enzyme. *Biochem. Biophys. Res. Commun.* **209**, 788-795.

Li, C., and Hersh, L. B. (1995). Neprilysin: assay methods, purification, and characterization. *Methods Enzymol.* **248**, 253-263.

Loewi, O. (1921). Uber humorale ubertragbarkeit der hirzenwicklung. *Pflugers Arch.* **189**, 239-242.

Malfroy, B., Swerts, J. P., Guyon, A., Roques, B. P., and Schwartz, J. C. (1978). High-affinity enkephalin-degrading peptidase in brain is increased after morphine. *Nature* **276**, 523-526.

Marr, R. A., Guan, H., Rockenstein, E., Kindy, M., Gage, F. H., Verma, I., Masliah, E., and Hersh, L. B. (2004). Neprilysin regulates amyloid Beta peptide levels. *J. Mol. Neurosci.* **22**, 5-11.

Martinez-Murillo, R., Villalba, R. M., and Rodrigo, J. (1989). Electron microscopic localization of cholinergic terminals in the rat substantia nigra: an immunocytochemical study. *Neurosci. Lett.* **96**, 121-126.

Maselli, R. A., Chen, D., Mo, D., Bowe, C., Fenton, G., and Wollmann, R. L. (2003). Choline acetyltransferase mutations in myasthenic syndrome due to deficient acetylcholine resynthesis. *Muscle Nerve* **27**, 180-187.

Massarelli, E. E., Casatti, C. A., Kato, A., Camargo, A. C., Bauer, J. A., Glucksman, M. J., Roberts, J. L., Hirose, S., and Ferro, E. S. (1999). Differential subcellular distribution of neurolysin (EC 3.4.24.16) and thimet oligopeptidase (EC 3.4.24.15) in the rat brain. *Brain Res.* **851**, 261-265.

Matsas, R., Fulcher, I. S., Kenny, A. J., and Turner, A. J. (1983). Substance P and [Leu]enkephalin are hydrolyzed by an enzyme in pig caudate synaptic membranes that is identical with the endopeptidase of kidney microvilli. *Proc. Natl. Acad. Sci. U S A* **80**, 3111-3115.

Matthews, B. W., Weaver, L. H., and Kester, W. R. (1974). The conformation of thermolysin. *J. Biol. Chem.* **249**, 8030-8044.

Mazella, J., Zsurger, N., Navarro, V., Chabry, J., Kaghad, M., Caput, D., Ferrara, P., Vita, N., Gully, D., Maffrand, J. P., and Vincent, J. P. (1998). The 100-kDa neurotensin receptor is gp95/sortilin, a non-G-protein-coupled receptor. *J. Biol. Chem.* **273**, 26273-26276.

McCool, S., and Pierotti, A. R. (2000). Expression of the thimet oligopeptidase gene is regulated by positively and negatively acting elements. *DNA Cell Biol.* **19**, 729-738.

Mentlein, R., and Dahms, P. (1994). Endopeptidases 24.16 and 24.15 are responsible for the degradation of somatostatin, neurotensin, and other neuropeptides by cultivated rat cortical astrocytes. *J. Neurochem.* **64**, 27-37.

- Misawa, H., Ishii, K., and Deguchi, T. (1992). Gene expression of mouse choline acetyltransferase. Alternative splicing and identification of a highly active promoter region. *J. Biol. Chem.* **267**, 20392-20399.
- Misawa, H., Matsuura, J., Oda, Y., Takahashi, R., and Deguchi, T. (1997). Human choline acetyltransferase mRNAs with different 5'-region produce a 69-kDa major translation product. *Brain Res. Mol. Brain Res.* **44**, 323-333.
- Mohajeri, M. H., Kuehnle, K., Li, H., Poirier, R., Tracy, J., and Nitsch, R. M. (2004). Anti-amyloid activity of neprilysin in plaque-bearing mouse models of Alzheimer's disease. *FEBS Lett.* **562**, 16-21.
- Molineaux, C. J., and Ayala, J. M. (1990). An inhibitor of endopeptidase 24.15 blocks the degradation of intraventricularly administered dynorphins. *J. Neurochem.* **55**, 611-618.
- Moodie, S. L., Mitchell, J. B., and Thornton, J. M. (1996). Protein recognition of adenylate: an example of a fuzzy recognition template. *J. Mol. Biol.* **263**, 486-500.
- Moody, T. W., Chan, D., Fahrenkrug, J., and Jensen, R. T. (2003). Neuropeptides as autocrine growth factors in cancer cells. *Curr. Pharm. Des.* **9**, 495-509.
- Moody, T. W., Mayr, C. A., Gillespie, T. J., and Davis, T. P. (1998). Neurotensin is metabolized by endogenous proteases in prostate cancer cell lines. *Peptides* **19**, 253-258.
- Nachmansohn, D., and Machado, A. L. (1943). The formation of acetylcholine. A new enzyme choline acetylase. *J. Neurophysiol.* **6**, 397-403.
- Natesh, R., Schwager, S. L., Evans, H. R., Sturrock, E. D., and Acharya, K. R. (2004). Structural details on the binding of antihypertensive drugs captopril and enalaprilat to human testicular angiotensin I-converting enzyme. *Biochemistry* **43**, 8718-8724.
- Natesh, R., Schwager, S. L., Sturrock, E. D., and Acharya, K. R. (2003). Crystal structure of the human angiotensin-converting enzyme-lisinopril complex. *Nature* **421**, 551-554.
- Nemeroff, C. B., Hernandez, D. E., Luttinger, D., Kalivas, P. W., and Prange, A. J., Jr. (1982). Interactions of neurotensin with brain dopamine systems. *Ann. N Y Acad. Sci.* **400**, 330-344.
- Nykjaer, A., Lee, R., Teng, K. K., Jansen, P., Madsen, P., Nielsen, M. S., Jacobsen, C., Kliemannel, M., Schwarz, E., Willnow, T. E., Hempstead, B. L., and Petersen, C. M. (2004). Sortilin is essential for proNGF-induced neuronal cell death. *Nature* **427**, 843-848.
- Oda, Y. (1999). Choline acetyltransferase: the structure, distribution and pathologic changes in the central nervous system. *Pathol. Int.* **49**, 921-937.

Oda, Y., Imai, S., Nakanishi, I., Ichikawa, T., and Deguchi, T. (1995). Immunohistochemical study on choline acetyltransferase in the spinal cord of patients with amyotrophic lateral sclerosis. *Pathol. Int.* **45**, 933-939.

Oda, Y., Nakanishi, I., and Deguchi, T. (1992). A complementary DNA for human choline acetyltransferase induces two forms of enzyme with different molecular weights in cultured cells. *Brain Res. Mol. Brain Res.* **16**, 287-294.

Oefner, C., D'Arcy, A., Hennig, M., Winkler, F. K., and Dale, G. E. (2000). Structure of human neutral endopeptidase (neprilysin) complexed with phosphoramidon. *J. Mol. Biol.* **296**, 341-349.

Oefner, C., Roques, B. P., Fournie-Zaluski, M. C., and Dale, G. E. (2004). Structural analysis of neprilysin with various specific and potent inhibitors. *Acta Crystallogr. D Biol. Crystallogr.* **60**, 392-396.

Ohno, K., Tsujino, A., Brengman, J. M., Harper, C. M., Bajzer, Z., Udd, B., Beyring, R., Robb, S., Kirkham, F. J., and Engel, A. G. (2001). Choline acetyltransferase mutations cause myasthenic syndrome associated with episodic apnea in humans. *Proc. Natl. Acad. Sci. U S A* **98**, 2017-2022.

Okuda, T., Haga, T., Kanai, Y., Endou, H., Ishihara, T., and Katsura, I. (2000). Identification and characterization of the high-affinity choline transporter. *Nat. Neurosci.* **3**, 120-125.

Oliveira, V., Araujo, M. C., Rioli, V., de Camargo, A. C., Tersariol, I. L., Juliano, M. A., Juliano, L., and Ferro, E. S. (2003). A structure-based site-directed mutagenesis study on the neurolysin (EC 3.4.24.16) and thimet oligopeptidase (EC 3.4.24.15) catalysis. *FEBS Lett* **541**, 89-92.

Oliveira, V., Campos, M., Hemerly, J. P., Ferro, E. S., Camargo, A. C., Juliano, M. A., and Juliano, L. (2001). Selective neurotensin-derived internally quenched fluorogenic substrates for neurolysin (EC 3.4.24.16): comparison with thimet oligopeptidase (EC 3.4.24.15) and neprilysin (EC 3.4.24.11). *Anal Biochem* **292**, 257-65.

Oliveira, V., Campos, M., Melo, R. L., Ferro, E. S., Carmago, A. C. M., Juliano, M. A., and Julinan, L. (2001). Substrate specificity characterization of recombinant metallo oligo-peptidases thimet oligopeptidase and neurolysin. *Biochemistry* **40**, 4417-4425.

Oliveira, V., Ferro, E. S., Gomes, M. D., Oshiro, M. E., Almeida, P. C., Juliano, M. A., and Juliano, L. (2000). Characterization of thiol-, aspartyl-, and thiol-metallo-peptidase activities in Madin-Darby canine kidney cells. *J. Cell Biochem.* **76**, 478-488.

Orawski, A. T., Susz, J. P., and Simmons, W. H. (1987). Aminopeptidase P from bovine lung: solubilization, properties, and potential role in bradykinin degradation. *Mol. Cell. Biochem.* **75**, 123-132.

- Orlowski, M., Michaud, C., and Chu, T. G. (1983). A soluble metalloendopeptidase from rat brain. Purification of the enzyme and determination of specificity with synthetic and natural peptides. *Eur. J. Biochem.* **135**, 81-88.
- Orlowski, M., Reznik, S., Ayala, J., and Pierotti, A. R. (1989). Endopeptidase 24.15 from rat testes. Isolation of the enzyme and its specificity toward synthetic and natural peptides, including enkephalin-containing peptides. *Biochem. J.* **261**, 951-958.
- Otwinowski, Z., and Minor, W. (1997). Processing of X-ray diffraction data collected in oscillation mode. *Methods Enzymol.* **276**, 307-326.
- Papandreou, C. N., Usmani, B., Geng, Y., Bogenrieder, T., Freeman, R., Wilk, S., Finstad, C. L., Reuter, V. E., Powell, C. T., Scheinberg, D., Magill, C., Scher, H. I., Albino, A. P., and Nanus, D. M. (1998). Neutral endopeptidase 24.11 loss in metastatic human prostate cancer contributes to androgen-independent progression. *Nat. Med.* **4**, 50-57.
- Parsons, S. M., Prior, C., and Marshall, I. G. (1993). Acetylcholine transport, storage, and release. *Int. Rev. Neurobiol.* **35**, 279-390.
- Perona, J. J., Hedstrom, L., Rutter, W. J., and Fletterick, R. J. (1995). Structural origins of substrate discrimination in trypsin and chymotrypsin. *Biochemistry* **34**, 1489-1499.
- Peterson, J. T. (2006). The importance of estimating the therapeutic index in the development of matrix metalloproteinase inhibitors. *Cardiovasc. Res.* **69**, 677-687.
- Pierotti, A., Dong, K. W., Glucksman, M. J., Orlowski, M., and Roberts, J. L. (1990). Molecular cloning and primary structure of rat testes metalloendopeptidase EC 3.4.24.15. *Biochemistry* **29**, 10323-10329.
- Portaro, F. C., Hayashi, M. A., Silva, C. L., and de Camargo, A. C. (2001). Free ATP inhibits thimet oligopeptidase (EC 3.4.24.15) activity, induces autophosphorylation in vitro, and controls oligopeptide degradation in macrophage. *Eur. J. Biochem.* **268**, 887-894.
- Rawlings, N. D., and Barrett, A. J. (1995). Evolutionary families of metallopeptidases. *Meth. Enzymol.* **248**, 183-228.
- Ray, K., Hines, C. S., Coll-Rodriguez, J., and Rodgers, D. W. (2004). Crystal structure of human thimet oligopeptidase provides insight into substrate recognition, regulation, and localization. *J. Biol. Chem.* **279**, 20480-20489.
- Ray, K., Hines, C. S., and Rodgers, D. W. (2002). Mapping sequence differences between thimet oligopeptidase and neurolysin implicates key residues in substrate recognition. *Protein Sci* **11**, 2237-46.
- Resendes, M. C., Dobransky, T., Ferguson, S. S., and Rylett, R. J. (1999). Nuclear localization of the 82-kDa form of human choline acetyltransferase. *J. Biol. Chem.* **274**, 19417-19421.

Richelson, E., Fredrickson, P. A., and Boules, M. M. (2005). Neurotensin receptor agonists and antagonists for schizophrenia. *Am. J. Psychiatry* **162**, 633-634.

Rioli, V., Kato, A., Portaro, F. C., Cury, G. K., te Kaat, K., Vincent, B., Checler, F., Camargo, A. C., Glucksman, M. J., Roberts, J. L., Hirose, S., and Ferro, E. S. (1998). Neuropeptide specificity and inhibition of recombinant isoforms of the endopeptidase 3.4.24.16 family: comparison with the related recombinant endopeptidase 3.4.24.15. *Biochem. Biophys. Res. Commun.* **250**, 5-11.

Robert, I., and Quirin-Stricker, C. (2001). A novel untranslated 'exon H' of the human choline acetyltransferase gene in placenta. *J. Neurochem.* **79**, 9-16.

Robl, J. A., Sulsky, R., Sieber-McMaster, E., Ryono, D. E., Cimarusti, M. P., Simpkins, L. M., Karanewsky, D. S., Chao, S., Asaad, M. M., Seymour, A. A., Fox, M., Smith, P. L., and Trippodo, N. C. (1999). Vasopeptidase inhibitors: incorporation of geminal and spirocyclic substituted azepinones in mercaptoacyl dipeptides. *J. Med. Chem.* **42**, 305-311.

Robl, J. A., Sun, C. Q., Stevenson, J., Ryono, D. E., Simpkins, L. M., Cimarusti, M. P., Dejneka, T., Slusarchyk, W. A., Chao, S., Stratton, L., Misra, R. N., Bednarz, M. S., Asaad, M. M., Cheung, H. S., Abboa-Offei, B. E., Smith, P. L., Mathers, P. D., Fox, M., Schaeffer, T. R., Seymour, A. A., and Trippodo, N. C. (1997). Dual metalloprotease inhibitors: mercaptoacetyl-based fused heterocyclic dipeptide mimetics as inhibitors of angiotensin-converting enzyme and neutral endopeptidase. *J. Med. Chem.* **40**, 1570-1577.

Rodgers, D. W. (1997). Practical Cryocrystallography. *Methods Enzymol.* **276**, 183-203.

Roques, B. P., and Beaumont, A. (1990). Neutral endopeptidase-24.11 inhibitors: from analgesics to antihypertensives? *Trends Pharmacol. Sci.* **11**, 245-249.

Roques, B. P., Noble, F., Dauge, V., Fournie-Zaluski, M. C., and Beaumont, A. (1993). Neutral endopeptidase 24.11: structure, inhibition, and experimental and clinical pharmacology. *Pharmacol. Rev.* **45**, 87-146.

Saito, T., Takaki, Y., Iwata, N., Trojanowski, J., and Saido, T. C. (2003). Alzheimer's disease, neuropeptides, neuropeptidase, and amyloid-beta peptide metabolism. *Sci. Aging Knowledge Environ.* **2003**, PE1.

Saric, T., Beninga, J., Graef, C. I., Akopian, T. N., Rock, K. L., and Goldberg, A. L. (2001). Major histocompatibility complex class I-presented antigenic peptides are degraded in cytosolic extracts primarily by thimet oligopeptidase. *J. Biol. Chem.* **276**, 36474-36481.

Sato, Y., Itoh, F., Hinoda, Y., Ohe, Y., Nakagawa, N., Ueda, R., Yachi, A., and Imai, K. (1996). Expression of CD10/neutral endopeptidase in normal and malignant tissues of the human stomach and colon. *J. Gastroenterol.* **31**, 12-17.



- Schechter, I., and Berger, A. (1967). On the size of the active site in proteases. I. Papain. *Biochem. Biophys. Res. Commun.* **27**, 157-162.
- Schmidt, C., Abicht, A., Krampfl, K., Voss, W., Stucka, R., Mildner, G., Petrova, S., Schara, U., Mortier, W., Bufler, J., Huebner, A., and Lochmuller, H. (2003). Congenital myasthenic syndrome due to a novel missense mutation in the gene encoding choline acetyltransferase. *Neuromuscul. Disord.* **13**, 245-251.
- Serizawa, A., Dando, P. M., and Barrett, A. J. (1995). Characterization of a mitochondrial metallopeptidase reveals neurolysin as a homolog of thimet oligopeptidase. *J. Biol. Chem.* **270**, 2092-2098.
- Seufferlein, T., and Rozengurt, E. (1996). Galanin, neurotensin, and phorbol esters rapidly stimulate activation of mitogen-activated protein kinase in small cell lung cancer cells. *Cancer Res.* **56**, 5758-5764.
- Sha, D., Jin, H., Kopke, R. D., and Wu, J. Y. (2004). Choline acetyltransferase: regulation and coupling with protein kinase and vesicular acetylcholine transporter on synaptic vesicles. *Neurochem Res.* **29**, 199-207.
- Shen, R., Sumitomo, M., Dai, J., Hardy, D. O., Navarro, D., Usmani, B., Papandreou, C. N., Hersh, L. B., Shipp, M. A., Freedman, L. P., and Nanus, D. M. (2000). Identification and characterization of two androgen response regions in the human neutral endopeptidase gene. *Mol. Cell. Endocrinol.* **170**, 131-142.
- Shrimpton, C. N., Abbenante, G., Lew, R. A., and Smith, I. (2000). Development and characterization of novel potent and stable inhibitors of endopeptidase EC 3.4.24.15. *Biochem. J.* **345 Pt 2**, 351-356.
- Shrimpton, C. N., Glucksman, M. J., Lew, R. A., Tullai, J. W., Margulies, E. H., Roberts, J. L., and Smith, A. I. (1997). Thiol Activation of Endopeptidase EC 3.4.24.15: A novel mechanism for the regulation of catalytic activity. *J. Biol. Chem.* **272**, 17395-17399.
- Shrimpton, C. N., Smith, A. I., and Lew, R. A. (2002). Soluble metalloendopeptidases and neuroendocrine signaling. *Endocr. Rev.* **23**, 647-664.
- Shrimpton, C. N., Wolfson, A. J., Smith, A. I., and Lew, R. A. (2003). Regulators of the neuropeptide-degrading enzyme, EC 3.4.24.15 (thimet oligopeptidase), in cerebrospinal fluid. *J. Neurosci. Res.* **74**, 474-478.
- Skidgel, R. A., Davis, R. M., and Tan, F. (1989). Human carboxypeptidase M. Purification and characterization of a membrane-bound carboxypeptidase that cleaves peptide hormones. *J. Biol. Chem.* **264**, 2236-2241.

Smith, A. I., Lew, R. A., Shrimpton, C. N., Evans, R. G., and Abbenante, G. (2000). A novel stable inhibitor of endopeptidases EC 3.4.24.15 and 3.4.24.16 potentiates bradykinin-induced hypotension. *Hypertension* **35**, 626-630.

St-Gelais, F., Jomphe, C., and Trudeau, L. E. (2006). The role of neurotensin in central nervous system pathophysiology: what is the evidence? *J Psychiatry. Neurosci.* **31**, 229-245.

Suzuki, T., Kikkawa, F., Ino, K., Nagasaka, T., Tamakoshi, K., and Mizutani, S. (2001). Imbalance between neutral endopeptidase 24.11 and endothelin-1 expression in human endometrial carcinoma. *Oncology* **60**, 258-267.

Takaki, Y., Iwata, N., Tsubuki, S., Taniguchi, S., Toyoshima, S., Lu, B., Gerard, N. P., Gerard, C., Lee, H. J., Shirotani, K., and Saido, T. C. (2000). Biochemical identification of the neutral endopeptidase family member responsible for the catabolism of amyloid beta peptide in the brain. *J. Biochem.* **128**, 897-902.

Towler, P., Staker, B., Prasad, S. G., Menon, S., Tang, J., Parsons, T., Ryan, D., Fisher, M., Williams, D., Dales, N. A., Patane, M. A., and Pantoliano, M. W. (2004). ACE2 X-ray structures reveal a large hinge-bending motion important for inhibitor binding and catalysis. *J. Biol. Chem.* **279**, 17996-18007.

Tullai, J. W., Cummins, P. M., Pabon, A., Roberts, J. L., Lopingco, M. C., Shrimpton, C. N., Smith, A. I., Martignetti, J. A., Ferro, E. S., and Glucksman, M. J. (2000). The neuropeptide processing enzyme EC 3.4.24.15 is modulated by protein kinase A phosphorylation. *J. Biol. Chem.* **275**, 36514-36522.

Turner, A. J., and Tanzawa, K. (1997). Mammalian membrane metallopeptidases: NEP, ECE, KELL, and PEX. *Faseb J.* **11**, 355-364.

Tyler-McMahon, B. M., Boules, M., and Richelson, E. (2000). Neurotensin: peptide for the next millennium. *Regul. Pept.* **93**, 125-36.

Vallee, B. L., and Auld, D. S. (1990). Zinc coordination, function, and structure of zinc enzymes and other proteins. *Biochemistry* **29**, 5647-5659.

Varadarajan, N., Gam, J., Olsen, M. J., Georgiou, G., and Iverson, B. L. (2005). Engineering of protease variants exhibiting high catalytic activity and exquisite substrate selectivity. *Proc. Natl. Acad. Sci. U S A* **102**, 6855-6860.

Vincent, B., Beaudet, A., Dauch, P., Vincent, J. P., and Checler, F. (1996). Distinct properties of neuronal and astrocytic endopeptidase 3.4.24.16: a study on differentiation, subcellular distribution, and secretion processes. *J. Neurosci.* **16**, 5049-5059.

Vincent, B., Jiracek, J., Nobel, F., Loog, M., Roques, B., Dive, V., Vincent, J.-P., and Checler, F. (1997a). Effect of a novel selective and potent phosphinic peptide inhibitor of endopeptidase

3.4.24.16 on neurotensin-induced analgesia and neuronal inactivation. *Br. J. Pharmacol.* **121**, 705-710.

Vincent, B., Jiracek, J., Noble, F., Loog, M., Roques, B., Dive, V., Vincent, J. P., and Checler, F. (1997b). Contribution of endopeptidase 3.4.24.15 to central neurotensin inactivation. *Eur. J. Pharmacol.* **334**, 49-53.

Vincent, J. P., Mazella, J., and Kitabgi, P. (1999). Neurotensin and neurotensin receptors. *Trends Pharmacol. Sci.* **20**, 302-309.

Waters, S. M., and Davis, T. P. (1997). Alterations of peptide metabolism and neuropeptidase activity in senile dementia of the Alzheimer's type. *Ann. N Y Acad. Sci.* **814**, 30-39.

Watson, M., Isackson, P. J., Makker, M., Yamada, M. S., Yamada, M., Cusack, B., and Richelson, E. (1993). Identification of a polymorphism in the human neurotensin receptor gene. *Mayo Clin. Proc.* **68**, 1043-1048.

Woulfe, J., Checler, F., and Beaudet, A. (1992). Light and Electron Microscopic Localization of the Neutral Metalloendopeptidase EC 3.4.24.16 in the Mesencephalon of the Rat. *Eur. J. Neurosci.* **4**, 1309-1319.

Wu, D., Ahmed, S. N., Lian, W., and Hersh, L. B. (1995). Activation of rat choline acetyltransferase by limited proteolysis. *J. Biol. Chem.* **270**, 19395-19401.

Wu, D., and Hersh, L. B. (1995). Identification of an active site arginine in rat choline acetyltransferase by alanine scanning mutagenesis. *J. Biol. Chem.* **270**, 29111-29116.

Wu, T. J., Pierotti, A. R., Jakubowski, M., Sheward, W. J., Glucksman, M. J., Smith, A. I., King, J. C., Fink, G., and Roberts, J. L. (1997). Endopeptidase EC 3.4.24.15 presence in the rat median eminence and hypophysial portal blood and its modulation of the luteinizing hormone surge. *J. Neuroendocrinol.* **9**, 813-822.

Yamamura, H. I., and Snyder, S. H. (1973). High affinity transport of choline into synaptosomes of rat brain. *J. Neurochem.* **21**, 1355-1374.

Yamin, R., Malgeri, E. G., Sloane, J. A., McGraw, W. T., and Abraham, C. R. (1999). Metalloendopeptidase EC 3.4.24.15 is necessary for Alzheimer's amyloid-beta peptide degradation. *J. Biol. Chem.* **274**, 18777-18784.

Yang, X. P., Saitoh, S., Scicli, A. G., Mascha, E., Orlowski, M., and Carretero, O. A. (1994). Effects of a metalloendopeptidase-24.15. Inhibitor on renal hemodynamics and function in rats. *Hypertension* **23**, 1235-1239.

York, I. A., Mo, A. X., Lemerise, K., Zeng, W., Shen, Y., Abraham, C. R., Saric, T., Goldberg, A. L., and Rock, K. L. (2003). The cytosolic endopeptidase, thimet oligopeptidase, destroys

antigenic peptides and limits the extent of MHC class I antigen presentation. *Immunity* **18**, 429-440.

Zhou, A., Webb, G., Zhu, X., and Steiner, D. (1999). Proteolytic processing in the secretory pathway. *J. Biol. Chem.* **274**, 20745-20748.

## Vita

Name: Eun Jeong Lim

Date of Birth: 8<sup>th</sup> April, 1972

Place of Birth: Ulsan, Republic of Korea

**Education:** M.S., 1998, Biochemistry, Hanyang University, Korea

Thesis: Mutational analysis of aspartate residues in the transmembrane regions and cytoplasmic loops of rat vesicular acetylcholine transporter

B.S., 1996, Biochemistry, Hanyang University, Korea

**Academic Awards:** Travel award for Gordon Research Conference on Diffraction methods in structural biology from University of Kentucky Graduate School, July, 2006

Graduate Student Incentive Award, University of Kentucky, 2002-2003

Excellent graduate, Hanyang University, 1996

Scholarship, Hanyang University, 1992-1995

**Professional positions:** Teaching assistant, University of Kentucky, 2002-2003

Intern researcher, Hanyang University, 1999-2000

Research assistant, Hanyang University, 1996-1999

**Publications:** Lim EJ, Sampath S, Coll-Rodriguez J, Schmidt J, Ray K, Rodgers DW. Swapping the specificities of the neuropeptidases

neurolysin and thimet oligopeptidase. (Submitted)

Kim MH, Lu M, Lim EJ, Chai YG, and Hersh LB. Mutational analysis of aspartate residues in the transmembrane regions and cytoplasmic loops of rat vesicular acetylcholine transporter. *Journal of Biological Chemistry*, 1999;274(2):673-80.

Lim EJ, Hong KJ, Yang BH, and Chai YG. Cell death induced by ethanol: Prevention of cell death by the bcl-2 proto-oncogene. *Journal of the Korean Society of Biological Psychiatry*, 1997;4(2):211-17

**Presentations and Abstracts:**

Reengineering substrate specificity in thimet oligopeptidase and neurolysin. Lim, E.J., Sampath, S., Ray, K., Coll-Rodriguez, J., and Rodgers, D.W. (Gordon Research Conference, Lewiston, ME, July 2006)

Reengineering substrate specificity in thimet oligopeptidase Lim, E.J., Sampath, S., Ray, K., Coll-Rodriguez, J., and Rodgers, D.W. (Department of Biochemistry Summer Research Conference, University of Kentucky, 2004)

Recombination Activating Gene (RAG) recombinases. Lim, E.J. and Rodgers, D.W. (Department of Biochemistry Summer Research Conference, University of Kentucky, 2003)

RAG 1 and RAG 2: Enzymes that mediate diversity generation in the immune system. Lim, E.J. and Rodgers, D.W. (Department of Biochemistry Summer Research Conference, University of Kentucky, 2002)